Study of Effective Use of Sugarcane Residue as Eco-friendly Construction Materials for Disaster Prevention Structures

RIBEIRO BRUNO

STUDY OF EFFECTIVE USE OF SUGARCANE RESIDUE AS ECO-FRIENDLY CONSTRUCTION MATERIALS FOR DISASTER PREVENTION STRUCTURES

by

RIBEIRO BRUNO

A Doctoral Thesis

Submitted to the
Division of Advanced Integrated Studies in Human Survivability
Graduate School of Advanced Integrated Studies in Human Survivability
In partial fulfillment of the requirement for the degree of
Doctor of Philosophy
At
Kyoto University
March 2021

Doctoral Thesis Chair: Prof. Dr. Yosuke Yamashiki
Doctoral Thesis Co-Chair: Prof. Dr. Takashi Yamamoto
Committee Members:
Prof. Dr. Kaoru Takara
Prof. Dr. Kei Saito

Dedico este trabalho aos meus pais,
José Osvaldo e Maria de Fátima,
exemplos de amor, carinho, honestidade e
perseverança, modelos a serem seguidos.
Orgulho de ser seu filho!

Acknowledgments

First of all, I am deeply grateful to our God Almighty for giving me the strength, knowledge, ability, and opportunity to undertake this research study and complete it satisfactorily. I praise God because, without his blessings, this achievement would not have been possible.

I dedicate this thesis to my Dad: José, Mom: Fátima and, my sister: Talita. I am always very grateful for your love, supporting, understanding, motivating, and courageous words that keep me focused on my dreams. This research thesis would not have been possible without your encouragement.

I want to thank the volunteers of the Nihongo Kyoushitsu in Kure, Hiroshima. I am thankful to you for believing in me.

I am also grateful to the Hiroshima Prefectural Kure Technical High School and all the teachers and employees who worked there. Thank you for putting your trust in me. I got here due to the opportunity you gave me.

I would like to express my sincere appreciation to Tokushima University and all teachers and staff working there who supported me when I was studying there.

I also want to thank Kyoto University and all teachers and employees who work there, which help me several times.

I would like to thank my supervisor Prof. Yosuke Yamashiki for his support and guidance during my research work. I am also heart-fully grateful to my co-supervisor, Prof. Takashi Yamamoto, who provided me an excellent source of help and unrelenting support for the present work. Without their invaluable guidance and support, this work would have never been accomplished.

I want to give my special thanks to Mr. Yuichi Hirano for his help and patience during my experiments. I would like to thank the Structural Materials Engineering Laboratory and Structural Dynamics Laboratory members, who gave me numerous supports and tutorials on experimental methods. In particular, I want to thank Team Satokibi (Maeda, Yin, Yang, Watanabe, and Urano) for their help with my experiments.

I would also like to thank the Nippon Foundation and the Association of Nikkei and Japanese Abroad for the great opportunity, which helped me concentrate on my studies and research.

I also thank Yasuhiro, David, Aisling, Nelly, Enoch, Joel, Gong, Kao, Juan, Malin, Alex, Sabrina, Ogunseye, Vera, Abraham, Botong, Zhewen, Fedor, Shoko, Zhe, Deng, Wenruo, Tatsuro, Xuwen, Natsuya, Hongfang, Ayaka, Sotaro, Rachael, Akiko, Thiago, Xueyan, Xuening, Lobsang, Lucas, Marcelo, and João for the collaboration, help, and companionship.

Finally, I would like to express my sincere gratitude to all who have supported this research directly or indirectly.

Abstract

For several countries in the world, sugarcane is the primary raw material used in the sugar industry. In some, it is also used for ethanol production. The sugar manufacturing process generates residues. Among them, the sugarcane bagasse is a fibrous residue made from the extraction of the mills' sugarcane broth. The bagasse is used as a primary fuel source in sugar/ethanol mills. After it is burned as fuel in the boilers, it generates residual products composed of unburned bagasse, sand, and ash. The latter is rich in silica and has a potential for pozzolanic reactivity, and can have a fill effect in concrete and mortar mixtures.

Since the sugarcane residues are renewable and sustainable resources, they are used in different ways in the construction industry that may reduce production costs, increase profits, and decrease environmental impacts of the sugar/ethanol industry. Moreover, this can reduce greenhouse gas emissions, which is a severe issue in the construction industry.

This research proposes a straightforward and worldwide accessible classification method for sugarcane resides. The residues were classified into three categories: bagasse fiber, sand, and ash. The classified residues were used as aggregates in cementitious composite materials, and different kinds of tests and surveys were applied to obtain the physical, mechanical properties of bagasse fiber; chemical components of the bagasse ash; mechanical behavior of the cementitious composite with the bagasse fiber and ash; the heat of hydration and thermal expansion behavior of the cementitious composite with the bagasse fiber and ash, assuming the availability for mass concrete; the resistance to the carbonation and chloride ion ingress in the cementitious composite with the bagasse fiber and ash; and environmental load associated with aggregate manufacturing and transportation.

In conclusion, the classified sugarcane residues can be used as mortar/concrete aggregates, depending on the composite application. The use of these residues decreases the load on the environment by replacing conventional aggregates and reducing the cost of the structures. Furthermore, it has been found that by adding sugarcane residues to the concrete, the heat of hydration was reduced, and the strain due to the thermal expansion was smaller than the control mixture.

Keywords: sugarcane bagasse fibers; sugarcane bagasse sand; sugarcane bagasse ash; new properties; heat of hydration; thermal strain; mechanical properties.

Contents

List of Figures

List of Tables

1 GENERAL INTRODUCTION

1.1 Research background

Recently, organizations and people's awareness about greenhouse gases has become increasingly important to global warming[1, 2]. Greenhouse gas emissions are now at the highest levels in history. If it continues at this rate, the world's average surface temperature will likely exceed 3 °C by the end of this century, aggravating the situation of our planet[3]. Lately, researchers have focused their studies on global warming and sustainable development, a concept that emerged in 1983. According to the Brundtland Report, "*sustainable development is development that meets the needs of the present without compromising the ability of future generations to meet their own needs*"[4].

Natural disasters can affect not only the economy but can also impact on human survival. In Japan, the heavy rains in July of 2018 in western Japan caused more than 200 deaths. Six thousand two hundred ninety-six buildings were destroyed, and 8929 houses were inundated above the floor level[5, 6]. In January of 2011, Brazil underwent one of the largest natural hazards in its history, which killed more than 900 people and affected more than 300000 people in the Mountainous Region of Rio de Janeiro[7]. The occurrence of climate-related disasters dominated between 1998 and 2017, accounting for 91% of all 7255 recorded events. Floods and landslides disasters sum together nearly 49% of all recorded events[8]. The annually worldwide natural disasters result in the necessity to prepare countermeasures[9] in some areas.

Structural countermeasures such as retaining structures, check dams, and sabo structures, for instance, are essential facilities for disaster prevention or mitigation against flash flooding and sediment-related hazards. However, at the same time, the construction industry is one of the main contributors to the greenhouse gases emitted in the world. Lizhen Huang et al. analyzed the CO_2 emission of the construction sector in 40 countries, considering 26 kinds of energy and non-energy use. Lizhen Huang's results showed that the total CO_2 emission of the global construction sector was 5.7 billion tons in 2009, contributing to 23% of the total CO_2 emissions produced by international economic activities that year[10]. As cited by Bas J. et al., the heavy industry sector, like cement and steel production, is a significant source of greenhouse gas emissions. Those industries accounted for 8% of global energy use and 15% of global anthropogenic CO_2 emissions

in 2012[11].

However, beyond the global-scale environmental issues such as greenhouse gases mentioned above, there are regional and local scale ecological issues related to noise and resource extractions. Aggregates, for example, make up about 70% of the volume of concrete[12]. This high demand for aggregates in concrete production directly impacts the ecological balance in several regions. Due to mining restrictions, the availability of suitable aggregates is limited at shorter haul distances. Consequently, the transportation of aggregates from longer distances to construction sites increases the total cost of construction[13].

Maintaining concrete structures is crucial to keep their performance for a more extended period, consequently decreasing the environmental load. Although this maintenance is beneficial in developed countries, such methods are challenging to replicate in developing countries. The reasons for this lack of maintenance may be linked with the costs and profits shortage. Besides, as a consequence of these countries' development levels, new structures are demanded, resulting in the constant establishment of new structures. Accordingly, there is a tendency to promote studies and design environmentally sustainable materials for application in those cases. Therefore, the incorporation of local materials in concrete should be an alternative to reduce CO_2 emissions and limit its environmental impact.

Several efforts have been made to reduce natural resource consumption, reuse industrial waste, and decrease CO_2 emissions. The use of fly ash and blast furnace slag as concrete additives are applicable in reconstruction projects, disaster prevention, green spaces, high ground relocation work, and other projects[14]. However, in countries with few coal-fired power plants and steel production plants, these materials' acquisition becomes problematic in most cases. Moreover, fibers such as steel fiber, synthetic fiber, and natural fiber have been mostly applied to reinforce cementitious composites. However, the health risks associated with asbestos and the need to replace synthetic fibers because of environmental concerns have made natural fibers gain popularity in the last few decades due to worldwide availability.

Among numerous additives and natural fibers, sugarcane residues have a high potential to replace conventional materials. Available in several countries globally, sugarcane is the primary raw material used in the sugar industry, and in some countries, it is also used for ethanol production[15].

The sugar manufacturing process generates several byproducts and production residues. Among those is sugarcane bagasse, a fibrous residue from the extraction of the broth of the sugarcane by milling[16, 17]. The main applications of bagasse are boiler fuel, pulp production, and feed to confined cattle. Also, the bagasse leftovers can be sold to other industries[17]. However, in several countries, these residues have been mainly discarded as soil fertilizer, which because of their environmental impact, is far from being the most suitable one[18, 19].

Different efforts to increase the standardization of sugarcane bagasse ash have been made. Nevertheless, the bagasse ash's re-burn process, one of the most common methods used for standardization, emits CO_2 and is not environmentally friendly. Also, the need for special equipment to re-burn the bagasse ash is a disadvantage since it is costly and inaccessible in some regions. In the bagasse fibers, similar to the bagasse ash, a complex process of classification and treatment is proposed, but it is difficult and inaccessible in most cases.

Since the sugarcane residues are renewable and sustainable resources, their easy classification and use in different construction industries can reduce production costs, increase the ethanol/sugar industry's profits, and decrease its environmental impacts. Moreover, it can reduce CO_2 emissions, which is a severe matter to the construction industry[20].

1.2 Originality and objective of work

Based on the previous research cited above, the development of new environmentally friendly mortar and concrete for preventive structures against natural disasters is urgently needed since this kind of structure consumes a high amount of aggregates. The use of local materials and natural materials can replace conventional ones, which sometimes are environmentally harmful. The usage of new building materials may help reduce greenhouse gas emissions and is a fundamental challenge to the construction industry. The exploitation of natural resources will drive the green building materials industry's growth once those materials are abundant. This research differs from other studies because this work focuses on:

1. An easy method of classification of sugarcane residues;
2. The mechanical properties of the cementitious composites with the addition of sugarcane residues in their original form;

3. The considerations of the thermal expansion due to the heat of hydration;
4. The factors linked to the corrosion of the steel in concrete, such as carbonation and chloride ions; and
5. An assessment of the environmental load of the composite.

This research proposes a classification method of sugarcane residues as aggregates and developing new environmentally friendly mortar and concrete for preventive structures against natural disasters. For these reasons, an easy and worldwide accessible classification method is proposed. Additionally, the classified residues were used as aggregates in cementitious composite materials, and different kinds of tests and surveys were applied in order to obtain the:

1. Physical and mechanical properties of bagasse fiber;
2. Chemical components of the bagasse ash;
3. Mechanical behavior of the cementitious composite with the bagasse fiber and ash;
4. Heat of hydration and thermal expansion behavior of the cementitious composite with the bagasse fiber and ash, assuming the availability for mass concrete;
5. Resistance to the carbonation and chloride ion ingress in the cementitious composite with the bagasse fiber and ash; and
6. Environmental load associated with aggregate manufacturing and transportation.

1.3 Contribution of Research

This research will contribute to civil engineering and materials science by developing and creating environmentally friendly construction materials for preventive structures against natural disasters. The straightforward classification of sugarcane residues and their incorporation with cement and conventional materials can be significant for developing cheap and ecological preventive structures against natural disasters.

Besides, the development of local materials can contribute to avoiding wastage and disposal problems of these residues. As a result, it can increase the value of the sugarcane production chain, accelerate the development of the green building materials industry, and promote the longer-term social economy.

1.4 Overview of Dissertation

This dissertation deals with the addition of sugarcane residues in concrete in order to develop environmentally-friendly cementitious composites. A brief description of each chapter is given below.

Chapter 1 is an introductory chapter that gives the reader an outline describing the background of the topic. Also, the most current issues about bagasse residues that need to be solved are listed. The next work described started based on those issues.

Chapter 2 aims to provide readers with general information about the use of bagasse residues on construction materials. A review of previous research of fiber reinforced cement-based materials was done. To conclude, this chapter reviews the issue of the environmental impacts of construction materials.

The proposal of a classification method of the sugarcane residues and their characteristics is presented in chapter 3. Preliminary trials applied to sugarcane bagasse residues are described. The classification and treatment of the bagasse and the classification of the burned residues are shown. In this chapter, bagasse fiber, bagasse sand, and bagasse ash are defined. The physical and mechanical properties and chemical composition of these materials are investigated and presented.

In the fourth chapter, a study on the mechanical properties of mortar with the addition of sugarcane bagasse fiber and bagasse ash was made, aiming to use sugarcane residues in mortar. In this chapter, the research methodology to achieve these research objectives is presented. It contains a flow chart of research and implementation of experiments on bagasse fibers, PVA fibers, bagasse sand, bagasse ash, and fly ash in cementitious composites. Then, the experimental devices and test standards used to obtain the physical and mechanical properties are presented.

Chapter 5 presents a study on the reduction in hydration heat and thermal strain of concrete with the addition of sugarcane bagasse fiber. This study investigates the possibility of using sugarcane residues in concrete and the sugarcane fiber's behavior in mass concrete structures, such as dams

and piers. The research methodology, devices, and test standards are presented.

In the sixth chapter, the application of mortar with sugarcane residues as shotcrete was investigated. This chapter aims to explore the potential of shotcrete with the addition of sugarcane residues to protect and stabilize slopes from erosion and possible slides. The methodologies and test results are showed and discussed.

Chapter 7 consists of the investigation of the durability of concrete with the addition of sugarcane residues. The description of the methodologies and the materials are shown. The durability was investigated by the resistance to the carbonation and chloride ion ingress velocity.

In chapters 8 and 9, the development of interlocking concrete blocks added with sugarcane residues and an environmental and cost assessment of the blocks was made. These chapters' results are products of work as a visiting researcher in the University of Ryukyus, Okinawa Prefecture, Japan, during the "Overseas Internship" and PBR (Project Based Research).

Finally, in chapter 10, general conclusions of the research and recommendations are presented. Also, future work perspectives are introduced.

1.5 References

[1] Sabbie A. Miller, Paulo J.M. Monteiro, Claudia P. Ostertag, Arpad Horvath, "Comparison indices for design and proportioning of concrete mixtures taking environmental impacts into account," *Cement and Concrete Composites,* vol. 68, pp. 131-143, 2016.

[2] Sabbie A Miller, Arpad Horvath, Paulo J M Monteiro, and Claudia P Ostertag, "Greenhouse gas emissions from concrete can be reduced by using mix proportions, geometric aspects, and age as design factors," *Environmental Research Letters,* vol. 10, no. 11, 2015.

[3] IPCC, "Global Warming of 1.5°C," 2018.

[4] U.N., "Our Common Future," *Report of the World Commission on Environment and Development,* 1987.

[5] Cabinet Office, Government of Japan, "Summary: the damage situations caused by the heavy rain in July, 2018 (in Japanese)," http://www.bousai.go.jp/updates/h30typhoon7/pdf/300905_, 2018.

[6] Hiroshige Tsuguti, Naoko Seino, Hiroaki Kawase, Yukiko Imada, Toshiyuki Nakaegawa & Izuru Takayabu, "Meteorological overview and mesoscale characteristics of the Heavy Rain Event of July 2018 in Japan," *Landslides,* vol. 16, p. 363–371, 2019.

[7] Marianna Rodrigues Gullo Cavalcante, Priscila da Cunha Luz Barcellos & Marcio Cataldi, "Flash flood in the mountainous region of Rio de Janeiro state (Brazil) in 2011: part I—calibration watershed through hydrological SMAP model," *Natural Hazards,* vol. 102, p. 1117–1134, 2020.

[8] Pascaline Wallemacq, Regina Below, Denis McClean, "UNISDR and CRED report: Economic Losses, Poverty & Disasters (1998 - 2017)," 2018.

[9] Ryota Hashimoto, Takashi Tsuchida, Takeo Moriwaki, Seiji Kano, "Hiroshima Prefecture geo-disasters due to Western Japan Torrential rainfall in July 2018," *Soils and Foundations,* vol. 60, no. 1, pp. 283-299, 2020.

[10] Lizhen Huang, Guri Krigsvoll, Fred Johansen, Yongping Liu, Xiaoling Zhang, "Carbon emission of global construction sector," *Renewable and Sustainable Energy Reviews,* vol. 81, no. 2, pp. 1906-1916, 2018.

[11] Bas J. van Ruijven, Detlef P. van Vuuren, Willem Boskaljon, Maarten L. Neelis, Deger Saygin, Martin K. Patel, "Long-term model-based projections of energy use and CO_2 emissions from the global steel and cement industries," *Resources, Conservation and Recycling,* vol. 112, pp. 15-36, 2012.

[12] K. Sakai, "Environmental design for concrete structures," *J. Adv. Concr. Technol.,* vol. 3, no. 1, pp. 17-28, 2003.

[13] Jayvant Choudhary, Brind Kumar, Ankit Gupta, "Utilization of solid waste materials as alternative fillers in asphalt mixes: A review," *Construction and Building Materials,* vol. 234, 2020.

[14] Sato, K., & Fujikawa, T., "Effective use of coal ash as ground materials in Japan," *Japanese Geotechnical Society Special Publication,* vol. 3, no. 2, pp. 65-70, 2015.

[15] Walter, Arnaldo & Galdos, Marcelo & Scarpare, Fabio & Leal, Manoel Regis & Seabra, Joaquim & Cunha, M.P. & Picoli, M.C.A. & Ortolan F. Oliveira, Camila, "Brazilian Sugarcane Ethanol: Developments so far and Challenges for the Future," *WIREs Energy and Environment,* pp. 70 - 92, 2014.

[16] F.A.O., "Sugar as feed," *F.A.O. animal production and health papers,* 1988.

[17] Yadav, R.L. & Solomon, S., "Potential of developing sugarcane byproduct based industries in India," *Sugar Tech,* vol. 8, pp. 104-111, 2006.

[18] K.C.P. Faria, R.F. Gurgel, J.N.F. Holanda, "Recycling of sugarcane bagasse ash waste in

the production of clay bricks," *Journal of Environmental Management,* vol. 101, pp. 7-12, 2012.

[19] Myrian Aparecida S. Schettino, José Nilson F. Holanda, "Characterization of Sugarcane Bagasse ash Waste for Its Use in Ceramic Floor Tile," *Procedia Materials Science,* vol. 8, pp. 190-196, 2015.

[20] E. CÂMARA; R. C. A. PINTO; J. C. ROCHA, "Setting process on mortars containing sugarcane bagasse ash," *Ibracon Structures and Materials Journal,* vol. 9, no. 4, pp. 617-642, 2016.

2 LITERATURE REVIEW

2.1 Introduction

This chapter's literature review aims to give a comprehensive and detailed overview of the theme argued by this dissertation. The current situation of the sugar/ethanol industry, as well as the sugarcane production, waste amount, and disposal process, are covered.

Besides, the results of previous studies on environmentally friendly construction materials are taken up in order to understand their behavior on the properties and performance characteristics of mortar and concrete with added sugarcane residues. Also, some methods and processes of treatment and classification of the sugarcane residues are presented.

2.2 Natural disasters

Annually, several natural disasters occur worldwide, often unexpected, seemingly unavoidable, and frequently catastrophic in their impact. These disasters result from natural processes of the Earth, such as geological, hydrological, and meteorological disasters. Figure 2.1 shows the classification of the major natural disasters in the world. Also, there are biological disasters that are not mentioned.

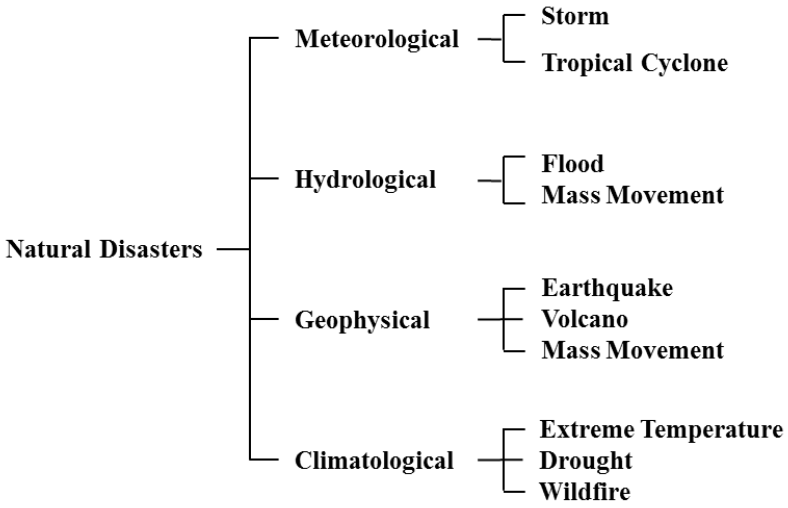

Figure 2.1 Natural disaster classification

In 2015 the 2030 Agenda for Sustainable Development was adopted by the United Nations General Assembly. It consists of 17 Sustainable Development Goals (SDGs). Goal number 11 targets are making cities and human settlements inclusive, safe, resilient, and sustainable[1].

According to a United Nations report, damages to housing attributed to disasters have statically and significantly risen from 1990 onwards[2], as shown in Figure 2.2.

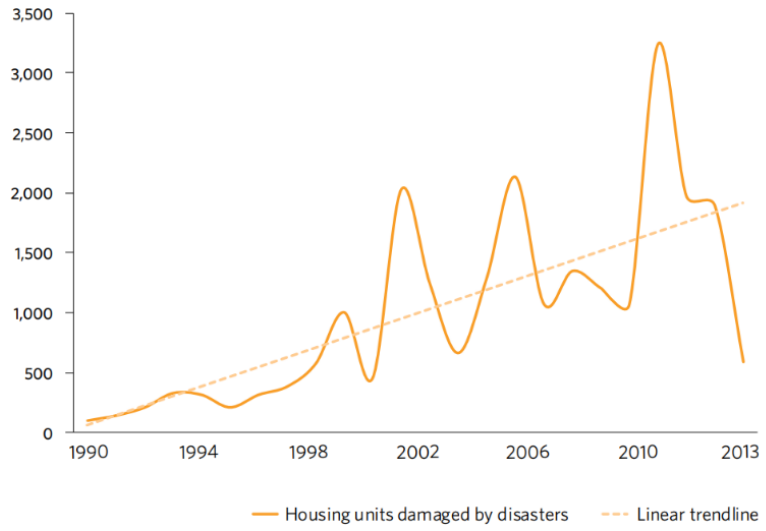

Figure 2.2 Total number of housing units damaged by disasters annually, 1990-2013 (data from 90 countries) (thousands)[2]

According to the data published by the Emergency Events Database (EM-DAT), the number of disasters, as shown in Figure 2.3, has risen from the 1990s.

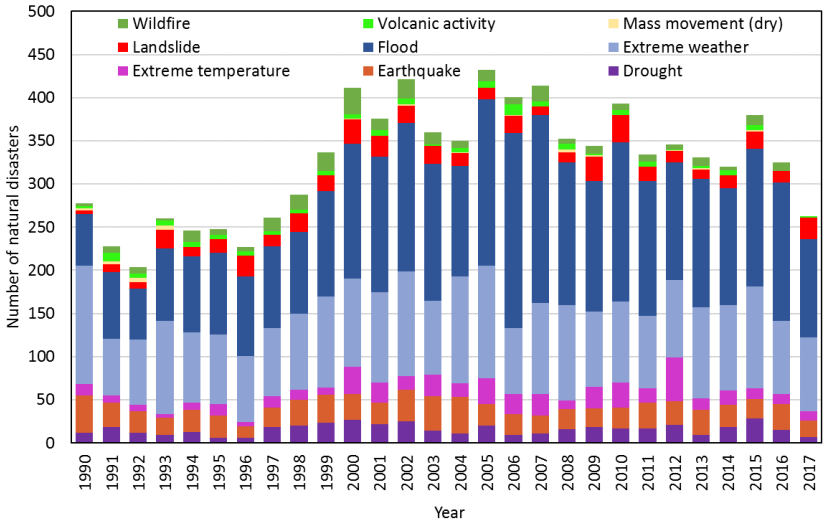

Figure 2.3 Number of reported disasters by type (edited by the author, sources obtained by EM-DAT[3])

Besides, as shown in Figure 2.4, the cost caused by natural disasters also increased. In 2011 it surpassed the US$ 350 billion mark.

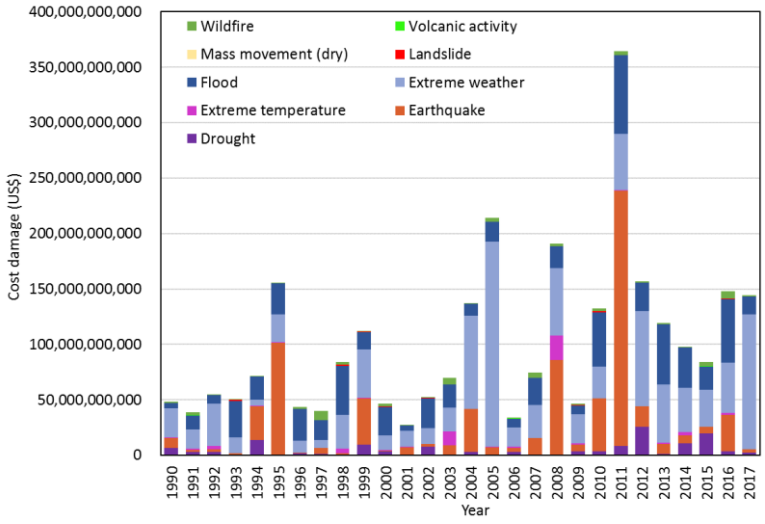

Figure 2.4 Total damage costs from global natural disasters (edited by the author, sources obtained by EM-DAT[3])

Although natural disasters have increased in recent decades, the global annual deaths caused by natural disasters are still virtually stable, considering that for years the numbers of deaths have risen suddenly, as shown in Figure 2.5.

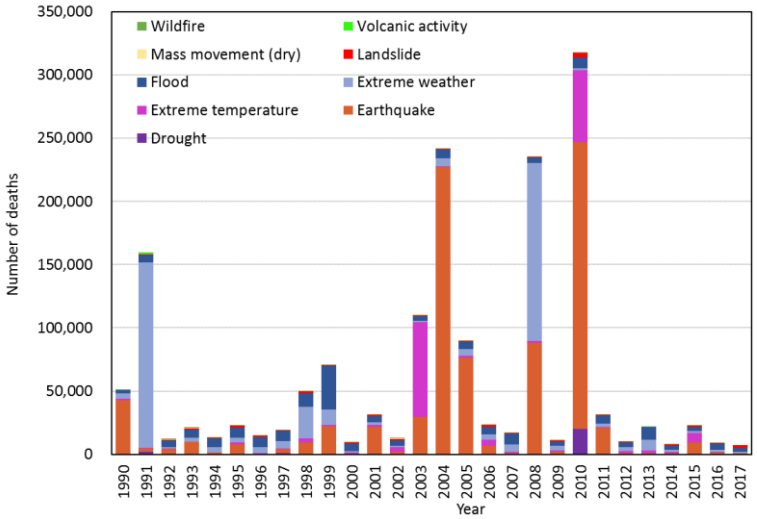

Figure 2.5 Absolute number of global deaths per year as a result of natural disasters (edited by the author, sources obtained by EM-DAT[3])

Many countries have developed measures to reduce disaster risk in vulnerable urban areas, including investments in disaster prevention structures[2]. However, natural disasters are still a global issue to be addressed. The high cost caused by natural disasters when they occur, which

is indirectly linked to human survival, and the high annual number of deaths, directly linked to human survival, are some examples. For both reasons, there is a need to reduce these numbers to make human settlements safe and sustainable.

2.2.1 Preventive measures for natural disasters

One of the most significant challenges of natural disaster prevention is that they may occur without notice at any time, anywhere. Although science and technology have advanced and brought many advancements to mitigate damages, they still require development because it is impossible to protect from all disasters. Nevertheless, methods that minimize the risk of damage against natural disasters, such as structural and nonstructural measures[4], are also called hard and soft measures.

In the case of hard measures, different types of mitigation can be classified into the following types:

- shotcrete;
- drainage;
- geogrids;
- anchors; and
- check dams.

In the case of the soft measures, there are three types of nonstructural measures against sediment disasters:

- development of warning and evacuation systems;
- restriction of land use in areas at risk for sediment disasters; and
- preparation and publication of hazard maps with public involvement.

Although both hard and soft measures are essential to mitigate damages of natural disasters, these measures are not perfect and always contain a weakness gap. For instance, in the case of hard measures, there are disadvantages such as the factor of the load on the environment that these structures cause and the high cost of the built structures. The high consumption of aggregates to make concrete, about 70% of the volume[5], is another concern since the mining of these aggregates destroys landscapes and releases a considerable amount of CO_2. For these reasons, using renewable and sustainable resources to construct prevention disaster structures may be a key to decreasing the load on the environment and collaborating to reduce structural costs.

2.3 Recent situation of the sugarcane

Sugarcane is of the oldest crops known to man; it has been cultivated since pre-historic times as a sugar source. Recently, around the world, 70% of sugar is manufactured from sugarcane[6]. Further, sugarcane has a great potential to be used for the production of bioethanol. Its global production is about 1.91 billion tons annually, concentrated in tropical regions, particularly in developing nations in Latin America and Asia[7]. According to the Food and Agricultural Organization (FAO) of the United Nations (UN), there are over 100 countries producing sugarcane today[8]. Table 2.1 illustrates the top 10 sugarcane producers in the world in 2013.

Table 2.1 World top 10 sugarcane production countries in 2013[9]

Country	Production		Area		Yield	
	Million Mg	Rank	×1000 ha	Rank	Mg ha^{-1}	Rank
Brazil	739.27	1	9835.2	1	75.17	29
India	341.20	2	5060.0	2	67.43	40
China	126.14	3	1827.3	3	69.03	39
Thailand	100.10	4	1321.6	4	75.74	26
Pakistan	63.75	5	1128.8	5	56.48	51
Mexico	61.18	6	782.8	6	78.16	25
Colombia	34.88	7	405.7	9	85.95	19
Indonesia	33.70	8	450.0	7	74.89	31
Philippines	32.00	9	435.4	8	73.49	37
USA	27.91	10	368.6	11	75.71	27
World total	2165.23		26522.7		81.64	

Figure 2.6 shows the map of sugarcane crops in Brazil. As evidenced in Figure 2.6, the sugarcane crops are distributed in all Brazil regions, except the northern region, where the Amazon Forest is located. Currently, Brazil leads the world production of sugarcane, with a planted area estimated at over nine million hectares. The sugar production in 2014/2015 harvest was 35.56 million tons, whereas ethanol production was around 29 billion liters[7]. In 1973, with the impacts of the global energy crisis and Brazil's inflation, the government was motivated to launch the National Alcohol Program, which started in November 1975[10].

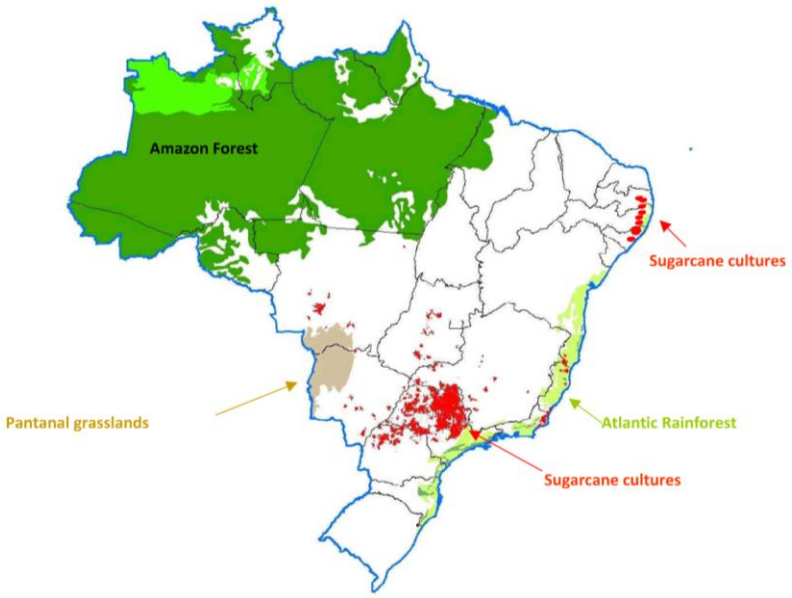

Figure 2.6 Map of sugarcane crops in Brazil[11]

In Japan, unlike Brazil, the sugarcane crops are concentrated in the southwestern islands. Sugar is produced at 25 sugar mills, 7 of those located in Kagoshima Prefecture and 18 in Okinawa Prefecture[12]. The current situation of sugarcane production in Japan is shown in Table 2.2, and the map of the sugarcane crop area is shown in Figure 2.7. As seen in Table 2.2, the annual total sugarcane production fluctuated widely year by year. The main reason for this variation is due to typhoon and drought conditions during the summer season.

Table 2.2 Current situation of sugarcane production in Japan[12]

Year	No. of small- holders planting sugarcane	Total harvest area (ha)	Average harvest area / small-holders (ha)	Total cane production (ton)	Average cane yield (ton / ha)	Total sugar production* (ton)
1994/95	37,161	24,761	0.67	1,601,222	64.7	190,507
1998/99	31,471	22,468	0.71	1,664,677	74.1	189,697
1999/00	30,775	22,813	0.74	1,569,612	68.8	192,291
2000/01	29,836	23,010	0.77	1,393,721	60.6	168,297
2001/02	29,761	22,769	0.77	1,497,430	65.8	185,138
2002/03	29,629	23,770	0.8	1,326,314	55.8	159,844
2003/04	29,012	23,844	0.8	1,387,510	58.2	168,203
2004/05	28,897	23,158	0.8	1,185,740	51.2	133,455

* Including both raw sugar and brown sugar. Data source: Sugar information No. 113 (2006). Total amount of brown sugar production is 6952 ton in 2004/05 season.

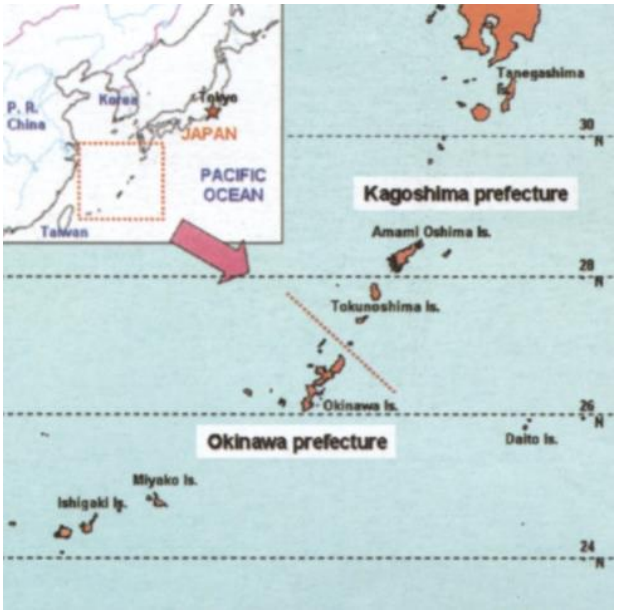

Figure 2.7 Map of sugarcane growing in the southwestern island of Japan[12]

2.3.1 Sugarcane by-products and disposal issues

In 1986, according to an FAO report, the interest in the by-products of the sugarcane industry had been developed from 1976. It had shown that the optimal use of by-products could provide non-negligible support to the sugarcane industry[13].

Three main by-products are generated by the sugarcane industry, as shown in Figure 2.8. They are the bagasse (25–30% cane), which is generated after the crushing of sugarcane; the mud (3–5% cane), which is generated after clarification and; the molasse (3.5–5% cane), which is generated after centrifugation[14]. These by-products of the sugar industry have significant economic value[15] and are vast potential reserves for human and animal consumption, and can provide energy as a renewable source. Sugarcane and its by-products are useful raw materials to over 25 industries[16]. Some examples are shown in Figure 2.8.

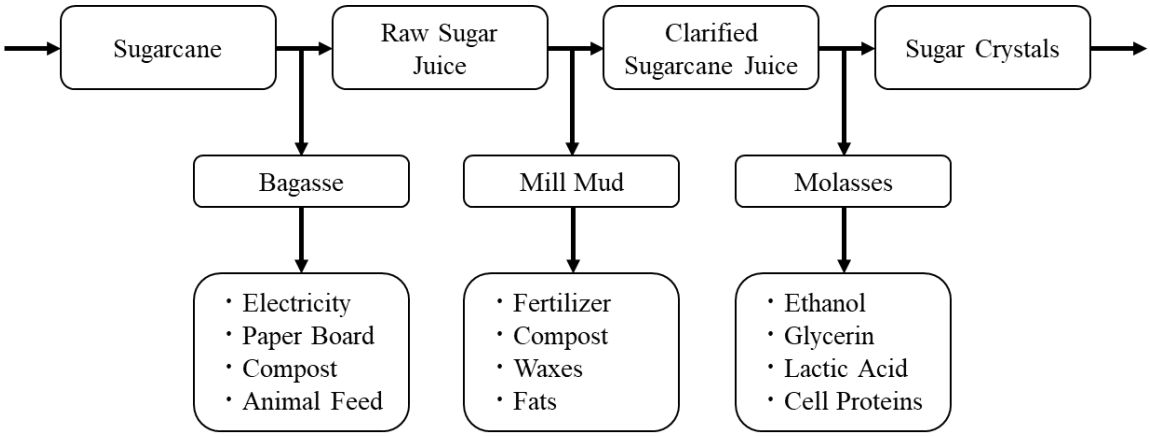

Figure 2.8 Sugar industry by-products at processing (edited by the author)[14]

The bagasse, which has 40 to 50% of water, 2 to 5% of dissolved sugar, and 40 to 45% of fibers, is used as a primary fuel source in sugar/ethanol mills[14, 17]. The bagasse burned as fuel in the boilers generates residual products composed of sand, ash[18, 19], and non-burned bagasse. The burned sugarcane residues are generated in large quantities and create a severe disposal problem to the ethanol-sugar industry, affecting the environment and public health[20].

In several countries, usually, the sugarcane residue has been mainly disposed of as soil fertilizer. However, given its environmental impact, this disposal method is far from being the most suitable one[21, 22].

2.3.2 Utilization of sugarcane residues on the construction industry

Recently, the application of agro-residues in concrete has gained interest due to the high amount available worldwide. Environmental issues as the wrong destination of these residues can also be argued. Among the several agro-residues, there is the bagasse which is a residue of sugarcane[23].

The use of bagasse ash/sand as a partial substitute for cement and/or bagasse ash/sand as a partial replacement for fine aggregates could reduce the environmental impacts caused by rock mining or sand extraction in rivers and reservoirs. Furthermore, it reduces the environmental impact caused by these residues' incorrect disposal in crops or inappropriate sites. Moreover, the use of bagasse ash may have positive downstream effects on cement's environmental impact through

the reduction of CO_2 emissions, a severe issue of the civil engineering industry[24, 25, 26, 27, 28, 29]. Other benefits, such as the decrease of the composite and local development costs, may be attractive factors to the use of these residues.

However, as mentioned in 2.3.1, once the bagasse is burnt at uncontrolled temperatures and time, there is also unburned bagasse mixed in with the sand and ash[30, 31, 32], as it can be seen in Figure 2.9. The bagasse ash is rich in silica, and it has a potential for pozzolanic reactivity and filler effect in concrete and mortar mixtures[25]. For this reason, in order to standardize and improve the quality of the ash collected from the boiler for possible use in concrete mixtures, a re-burning treatment process of sand, ash, and non-burned bagasse is applied[33, 34]. However, this re-burning treatment may be an unsustainable process due to additional CO_2 emissions. Moreover, the re-burning treatment requires specific equipment, making it inaccessible in some regions of the world.

Figure 2.9 Residual sand and ash with the presence of non-burned bagasse

On the other hand, the natural fiber reinforced cement composites have increased the interest of researchers and manufacturers seeking to improve construction materials. Due to their high mechanical performance and low cost, natural fiber reinforced cement composites have a high potential for replacing standard fiber materials[35, 36].

Using the sugarcane residues in their original form - that is, in the form that the residues are generated out of mills or boilers - a way to make both the civil engineering industry and the sugar/ethanol industry more sustainable seems possible.

2.4 Pozzolanic materials

Pozzolans are a broad class of materials that are either siliceous or both siliceous and aluminous. By themselves, they have little or do not have any cementitious properties. However, they react with calcium hydroxide at ordinary temperatures (e.g., room temperature) when combined with water forming other compounds, such as calcium silicate hydrate and calcium aluminate hydrate, which has cementitious properties[37, 38, 39]. This reaction is known as a pozzolanic reaction.

Pozzolans' chemical composition varies widely, depending on their sources and the techniques used to burn the source. However, in the case of coal fly ash, for example, silicon dioxide (SiO_2) (both amorphous and crystalline), aluminum oxide (Al_2O_3), and calcium oxide (CaO) are the major components, as shown in Table 2.3.

Table 2.3 Summary of worldwide coal fly ash chemical composition ranges[40]

Country	% Chemical composition											
	SiO_2	Al_2O_3	Fe_2O_3	CaO	K_2O	MgO	SO_3	TiO_2	Na_2O	P_2O_5	MnO	LOI
Australia	31.1-68.6	17-33	1-27.1	0.1-5.3	0.1-2.9	0-2	0-0.6	1.2-3.7	0-1.5	0-3.9	nd	na
Bagladesh	55	24.7	7.7	6.2	1.1	0.7	1.1	na	na	0.9	0.1	na
Bulgaria	30.1-57.4	12.5-25.4	5.1-21.2	1.5-28.9	0.8-2.8	1.1-2.9	0.4-12.7	0.6-1	0.4-1.9	0.1-0.4	0-0.2	0.8-32.8
Canada	35.5-62.1	12.5-23.2	3-44.7	1.2-13.3	0.5-3.2	0.4-3.1	0.2-7.8	0.4-1	0.1-7.3	0.1-1.5	na	0.3-9.7
China	35.6-57.2	18.8-55	2.3-19.3	1.1-7	0.8-0.9	0.7-4.8	1-2.9	0.2-0.7	0.6-1.3	1.1-1.5	nd	nd
Denmark	48-65	26-33	3.3-8.3	2.2-7.8	na	na	na	na	1.1-2.8	na	na	3.1-4.9
Europe	28.5-59.7	12.5-35.6	2.6-21.2	0.5-28.9	0.4-4	0.6-3.8	0.1-12.7	0.5-2.6	0.1-1.9	0.1-1.7	0-0.2	0.8-32.8
France	47-51	26-34	6.9-8.8	2.3-3.3	na	1.5-2.2	0.1-0.6	na	2.3-6.4	na	na	0.5-4.5
Germany	20-80	1-19	1-22	2-52	0-2	0.5-11	1-15	0.1-1	0-2	na	na	0-5
Greece	21-35	10-17.9	4.5-8.4	27.3-45	0.4-1	1.5-3.8	4-8.6	na	0.2-1	na	na	3-7
India	50.2-59.7	14-32.4	2.7-16.6	0.6-9	0.2-4.7	0.1-2.3	na	0.3-2.7	0.2-1.2	na	na	0.5-7.2
Israel	45.6-58.6	24.4-34.5	3-6.7	4.9-9.9	0.1	1.6-2.5	0.6-0.8	1.2-1.9	0-0.1	0.8-1.8	na	6
Italy	41.7-54	25.9-33.4	3-8.8	2-10	0-2.6	0-2.4	na	1-2.6	0-1	0-1.5	0-0.1	1.9-9
Japan	53.9-63	18.2-26.4	4.2-5.7	2-8.1	0.6-2.7	0.9-2.4	0.3-1.4	0.8-1.2	1.1-2.1	na	na	0.5-2.1
Korea	50-55.7	24.7-28.7	3.7-7.7	2.6-6.2	1.1	0.7-1.1	0.5-1.1	na	na	0.9	0.1	4.3-4.7
Mexico	59.6	22.8	5.6	3.1	1.3	0.9	0.4	0.9	0.5	0	na	na
Netherlands	45.1-59.7	24.8-28.9	3.3-9	0.5-6.8	0.6-2.9	0.6-3.7	0.2-1.3	0.9-1.8	0.1-1.2	0.1-1.5	0-0.1	2.7-8.1
Northern China	43.7	44	3.5	0.9	0.9	0.4	0.7	1.5	0.3	na	na	10
Poland	32.2-53.3	4-32.2	4.5-8.9	1.2-29.9	0.2-3.3	1.2-5.9	na	0.6-2.2	0.2-1.5	0.1-0.9	0-0.3	0.5-28
Russia	40.5-48.6	23.2-25.9	na	6.9-13.2	1.9-2.6	2.6-4	na	0.5-0.6	1.2-1.5	0.3-0.4	0.2-0.4	na
South Africa	46.3-67	21.3-27	2.4-4.7	6.4-9.8	0.5-1	1.9-2.7	na	1.2-1.6	0-1.3	0.3-0.9	0-0.5	na
Spain	41.5-58.6	17.6-45.4	2.6-16.2	0.3-11.8	0.2-4	0.3-3.2	0.1-2.2	0.5-1.8	0-1.1	0.1-1.7	0-0.1	1.1-9.7
Spain	41.5-58.6	17.6-35.6	2.6-16	0.8-11.8	0.4-4	0.9-2.5	0.1-2.2	0.5-1.6	0.2-0.8	0.1-1.7	0-0.1	1.1-5.2
Turkey	37.9-57	20.5-24.3	4.1-10.6	0.2-27.9	0.4-3.5	1-3.2	0.6-4.8	0.6-1.5	0.1-0.6	0.2-0.3	0	0.4-2.7
United State	34.9-58.5	19.1-28.6	3.2-25.5	0.7-22.4	0.9-2.9	0.5-4.8	0.1-2.1	1-1.6	0.2-1.8	0.1-1.3	na	0.2-20.5
Minimum	20.0	1.0	1.0	0.1	0.0	0.0	0.0	0.1	0.0	0.0	0.0	0.0
Maximum	80.0	55.0	44.7	52.0	4.7	11.0	15.0	3.7	7.3	3.9	0.5	32.8

Note: nd = Not detected, na = Not available.

Generally, pozzolanic materials have microscopic particles that can make the composite denser. The pozzolanic reaction can refine the pore structure, reducing the microcracks at the interfaces between the cement paste and aggregates. As a result, the compressive strength of concrete is increased, and the permeability is reduced. Consequently, the durability may increase. However, the concrete's early strength is reduced by pozzolanic materials when it replaces cement. This behavior is noted due to the pozzolanic reaction that occurs only after the initial hydraulic reactions that have produced the

calcium hydroxide required by the pozzolanic reaction.

Other essential physical properties of pozzolans include particle fineness, particle size, specific gravity, and water absorption - for instance, the pozzolanic materials' reactivity improves with particle size reduction[41, 42].

2.4.1 Bagasse ash

The produced quantity of bagasse ash has been rising rapidly during recent decades due to the high industrialization and the considerable improvement in living standards. Unfortunately, most of these waste quantities are not recycled but rather abandoned, causing severe problems such as the waste of natural resources and environmental pollution.

The sugar and ethanol industry seeks solutions to discard the sugarcane residues generated by sugar and ethanol production processes. The burnt bagasse residue is the last residue generated by the sugarcane chain. According to Sales et al., for each ton of bagasse burned, 25 kg of ash is generated. This ash is used as a fertilizer in plantations but does not have adequate mineral nutrients for this purpose[18].

The construction industry has shown significant gains in recycling industrial by-products and waste, including the bagasse ash materials. The recycling of this waste by converting it to aggregate components could save landfill space and reduce the demand for natural raw material extraction.

Cordeiro et al. investigated the role of mill type and grinding circuit configuration in grinding in laboratory and pilot plant-scale on the particle size, specific surface area, and pozzolanic activity of the produced ashes. Although the different mills and milling configurations produced different size distributions, they observed that the ground ash's pozzolanic activities directly correlated to its fineness, characterized by its 80% passing size or Blaine specific surface area[43].

Torres et al. characterized the sugarcane bagasse ash as supplementary material for Portland cement. As a result, the samples' chemical composition showed high percentages of silica, at 76.3 and 63.2%, indicating that sugarcane bagasse ash produced in the manufacture of commercial cement can be

recycled for use as pozzolanic material. Also, they suggest that the supplementary material can partially replace cement and therefore reduce CO_2 emissions[44].

Cordeiro et al. also investigated the pozzolanic and filler effects of residual sugarcane bagasse ash in mortars. They analyzed the influence of particle size of sugarcane bagasse ash on the packing density, pozzolanic activity of sugarcane bagasse ash, and compressive strength of mortars. According to Cordeiro et al., the sugarcane bagasse ash may be classified as a pozzolanic material, but its activity depends significantly on its particle size and fineness[45].

For this reason, in order to improve the quality of the ash collected from the boiler for possible use in concrete mixtures, a re-burning treatment process of bagasse ash and non-burned bagasse is applied[33, 34]. The burning conditions influence the bagasse ash's pozzolanic characteristics, which could contribute to the greater durability of the cementitious composite. The different burning processes at each sugar cane mill generate ashes with different characteristics and make their application more restricted. Ferreira et al., who analyzed the re-burning process to evaluate the homogenization and development of ashes' pozzolanic characteristics from different sources, revealed that the thermal treatment enables a better homogenization of different sugarcane ashes[46].

Nevertheless, the re-burning treatment may be an unsustainable process due to the additional CO_2 emissions, and its accessibility requires specific equipment. Rafael et al. prepared the bagasse ash without using any additional burning processes, with thermal control in the laboratory. They assessed the efficacy of the innovative micronization process of fly sugarcane bagasse ash using air-jet mills to obtain and prepare pozzolanic prerequisites. The performance of pozzolanic materials of milling fly sugarcane bagasse ash was also analyzed using the compressive strength method and the chemical reactivity analysis method. As stated by Rafael et al., the milling fly sugarcane bagasse ash samples presented satisfactory pozzolanic activity[47].

2.5 Fiber reinforced concrete

Cementitious composites are considered ceramic materials because they present this group of materials' typical properties, such as high rigidity, fragility, low tensile strength, and tendency to dry cracking.

The presence of fibers in the mortar and concrete promotes tensile strength, greater deformation capacity, and increased toughness. The fibers in cementitious materials can increase the impact resistance, flexural strength, and rupture modulus. Moreover, the addition of fibers in concrete has little or no effect on the compressive strength and the elasticity module[48]. Figure 2.10 shows the load-deformation curves for plain concrete and fiber reinforced concrete (FRC).

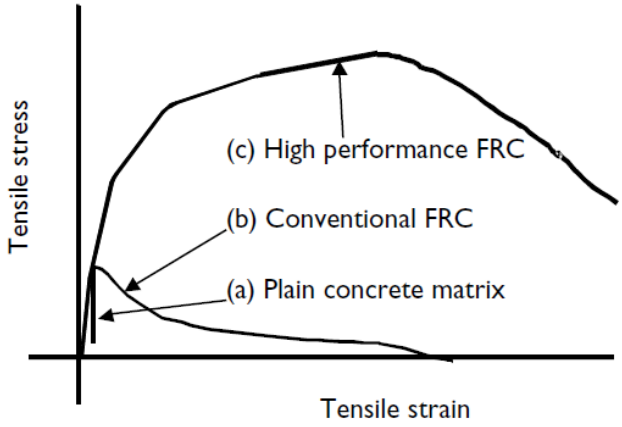

Figure 2.10 Relationship between stress and strain in three different types of concretes[48]

As shown in Figure 2.10, plain concrete rupture occurs suddenly when the deformation exceeds the ultimate tensile strength. On the other hand, FRC is capable of supporting considerable loads even with deformations greater than the deformation in the fracture of plain concrete. Therefore, the FRC after the beginning of the first crack does not break, unlike plain concrete.

In general, reinforced concrete performance depends on formulations and fiber characteristics, including type, geometry, distribution, orientation, and concentration[49, 50]. Many different types of fibers, such as metallic, polymeric, coated, uncoated, modified by irradiation, and natural fiber, have been used in cementitious composites.

2.5.1 Bagasse fibers

Conventionally, the concrete and mortar products, for example, are characterized by brittle behavior against tensile stress. The addition of the fibers into the cement matrix is expected to overcome this weakness by increasing the tensile strength and ductility, and consequently, improving durability since it can limit the propagation of cracks. Due to environmental awareness and an increasing

concern with the greenhouse effect, the construction industry has been stimulated to look for sustainable materials that can replace conventional synthetic polymeric fibers[51].

The use of bagasse fibers in cementitious composites is an alternative in construction materials. The bagasse is not entirely burned in the mills, with around 85% of bagasse production effectively burnt. Therefore, there is an excess of bagasse[52]. There is no significant difference between the common fiber reinforced concrete to the bagasse fiber cementitious composite, once both include cement, sand, water, fiber, and a few chemical additives. Also, the mixing procedure is still similar to that employed for the standard concrete. Compared with synthetic fibers, the production of natural fibers needs much less energy besides ecological, social, and economic benefits[53].

Bilba et al. prepared various bagasse fiber/cement composites, in which the fibers have a random distribution in the composites. The influence of different parameters on the setting of the composite material has been studied: (1) botanical components of the fiber, (2) thermal or chemical treatment of the fiber, (3) bagasse fiber content, and (4) added water percentage. This study showed a retarding effect of lignin on the composite setting; for a small amount of heat-treated bagasse (200 °C), the behavior of the composite is closely the same as the classical cement or cellulose/cement composite[54].

Matheus et al. performed a physical, chemical, morphological, and crystallographic analysis of the non-treated and treated (100°C during 30 min) sugarcane bagasse fibers. The effect of sugarcane bagasse fibers pre-treatment on Portland cement hydration was monitored by inhibition tests and differential scanning calorimetry in the first 24 hours. Furthermore, 28 days of age physical-mechanical properties of cement composite materials with sugarcane bagasse fibers were also evaluated. The inhibition index of treated sugarcane bagasse fibers was 5.9%, while for the non-treated sugarcane bagasse fibers, it was 67.3%. According to Matheus et al., the cement composites containing treated sugarcane bagasse fibers showed lower physical properties (water absorption and thickness swelling) than the cement composites reinforced with non-treated sugarcane bagasse fibers. Likewise, mechanical properties under flexure (modulus of rupture, MOR, and modulus of elasticity, MOE) of cement composites with treated sugarcane bagasse fibers showed higher values than the

cement composites with non-treated sugarcane bagasse fibers, thus proving the pre-treatment efficiency on sugarcane bagasse fibers for cement composites[55].

Henry et al. investigated the structure-property relation of fiber reinforced composites fabricated with Portland cement paste and sugarcane bagasse fibers. Pastes of 1.0 and 2.0 wt% of fibers were manufactured with a water to cement ratio (W/C) of 0.6. The mechanical properties were determined through three-point flexural tests, and the microstructural characterization was carried out through Scanning Electron Microscopy (SEM) tests. A Weibull distribution analysis for flexion damage was performed. Density, compressive strength, and ductility graphs were included. An analysis of the influence of capillaries pore size of the fiber over the flexural strength was made. The results showed that the fiber content improves the compressive strength, 9.7, 8.8, and 11.5 MPa for cement paste with 0, 1, and 2 wt% fibers contents, respectively. They conclude that these composites can be used as alternative green materials for houses in areas where sugarcane bagasse has low or no waste valorization[56].

2.6 Conclusion of chapter

Considering sugarcane residues as a partial substitute for cement or partial replacement of aggregates, they may reduce the environmental impact caused by rock mining or sand extraction in rivers and reservoirs. Furthermore, it reduces the environmental impact caused by these residues' incorrect disposal in crops or inappropriate sites. Besides, it can collaborate to reduce CO_2 emissions, which are a severe issue to the civil engineering industry. Therefore, besides its inaccessibility, re-burning treatments may be an unsustainable method: its CO_2 emissions may have a negative environmental impact.

With environmental awareness and an increasing concern with the greenhouse effect, the addition of the bagasse fibers in concrete may contribute to replacing conventional fibers. In several countries, sugarcane is the primary raw material used in the sugar/ethanol industry. The use of bagasse fiber in cement materials can be a way to increase the profit of local farmers, decrease the disposal and environmental issues, and, at the same time, collaborating with the construction industry in the development of green materials.

An easy classification method of sugarcane residues is proposed; the sugarcane residues were classified into different categories to use in the preparation of mortar and concrete composites.

Subsequently, several tests were performed on the sugarcane residues and cementitious composites with the addition of sugarcane residues to investigate the possible use of these residues on their original form in mortar and concrete for prevention disaster structures.

2.7 References

[1] United Nations, Transforming our world: the 2030 Agenda for Sustainable Development, A/RES/70/1, 2015.

[2] United Nations, The Sustainable Development Goals Report 2018, 2018.

[3] EM-DAT: The Emergency Events Database, Université catholique de Louvain (UCL) – CRED, Brussels, Belgium, [Online]. Available: www.emdat.be. [Accessed 30 12 2018].

[4] Takahisa MIZUYAMA, "Structural Countermeasures for Debris Flow," *International Journal of Erosion Control Engineering,* vol. 1, no. 2, pp. 38-43, 2008.

[5] K. Sakai, "Environmental design for concrete structures," *J. Adv. Concr. Technol.,* vol. 3, no. 1, pp. 17-28, 2003.

[6] Ghulam Mustafa, Faiz Ahmad Joyia, Sultana Anwar, Aqsa Parvaiz and Muhammad Sarwar Khan, "Biotechnological Interventions for the Improvement of Sugarcane Crop and Sugar Production," *Sugarcane - Technology and Research,* 2018.

[7] Edenis Cesar Oliveira, "Brazilian sugarcane sector: an economic and environmental approach," *Latin American J. of Management for Sustainable Development,* vol. 3, no. 1, pp. 35-46, 2016.

[8] FAO, "FAOSTAT online database, available at link http://faostat.fao.org/. Accessed on October 2019.," 2019.

[9] Zhao, Duli & Li, Yangrui, "Climate Change and Sugarcane Production: Potential Impact and Mitigation Strategies," *International Journal of Agronomy,* vol. 2015, pp. 1-10.

[10] Walter, Arnaldo & Galdos, Marcelo & Scarpare, Fabio & Leal, Manoel Regis & Seabra, Joaquim & Cunha, M.P. & Picoli, M.C.A. & Ortolan F. Oliveira, Camila, "Brazilian Sugarcane Ethanol: Developments so far and Challenges for the Future," *WIREs Energy and Environment,* pp. 70 - 92, 2014.

[11] Goldemberg, J, "The Brazilian biofuels industry," *Biotechnol Biofuels,* vol. 1, no. 6, 2008.

[12] Makoto Matsuoka, "Sugarcane cultivation and sugar industry in Japan," *Sugar Tech,* vol. 8, pp. 3-9, 2006.

[13] FAO, "Sugar as feed, " *FAO animal production and health papers,* 1988.

[14] Omprakash Sahu, "Assessment of sugarcane industry: Suitability for production,

consumption, and utilization," *Annals of Agrarian Science,* vol. 16, no. 6, pp. 389-395, 2018.

[15] Solomon, S., "Potential of developing sugarcane by-product based industries in India," *Sugar Tech,* vol. 13, pp. 408-416, 2011.

[16] Yadav, R.L. & Solomon, S., "Potential of developing sugarcane by-product based industries in India," *Sugar Tech,* vol. 8, pp. 104-111, 2006.

[17] Silvio Rainho Teixeira; Amanda Arenales; Agda Eunice de Souza; Renata da Silva Magalhães; Angel Fidel Vilche Peña; Davi Aquino; Rosane Freire, "Sugarcane bagasse: applications for energy production and ceramic materials," *The Journal of Solid Waste Technology and Management,* pp. 229-238, 2015.

[18] Almir Sales; Sofia Araújo Lima, "Use of Brazilian sugarcane bagasse ash in concrete as sand replacement," *Waste Management,* vol. 30, p. 1114–1122, 2010.

[19] Fernando C.R. Almeida; Almir Sales; Juliana P. Moretti; Paulo C.D. Mendes, "Sugarcane bagasse ash sand (SBAS): Brazilian agroindustrial by-product," *Construction and Building Materials,* vol. 82, pp. 31-38, 2015.

[20] Suzimara Rovani, Jonnatan J. Santos, Paola Corio and Denise A. Fungaro, "An Alternative and Simple Method for the Preparation of Bare Silica Nanoparticles Using Sugarcane Waste Ash, an Abundant and Despised Residue in the Brazilian Industry," *Journal of the Brazilian Chemical Society,* vol. 30, pp. 1524-1533, 2019.

[21] K.C.P. Faria, R.F. Gurgel, J.N.F. Holanda, "Recycling of sugarcane bagasse ash waste in the production of clay bricks," *Journal of Environmental Management,* vol. 101, pp. 7-12, 2012.

[22] Myrian Aparecida S. Schettino, José Nilson F. Holanda, "Characterization of Sugarcane Bagasse ash Waste for Its Use in Ceramic Floor Tile," *Procedia Materials Science,* vol. 8, pp. 190-196, 2015.

[23] Jnyanendra Kumar Prusty, Sanjaya Kumar Patro, S.S. Basarkar, "Concrete using agro-waste as fine aggregate for sustainable built environment – A review," *International Journal of Sustainable Built Environment,* vol. 5, no. 2, pp. 312-333, 2016.

[24] Miss Nimita A.Tijore; Vyom B. Pathak; Mr. Rushabh A. Shah, "Utilization of Sugarcane Bagasse Ash in Concrete," *International Journal for Scientific Research & Development,* vol. 1, no. 9, pp. 1938-1942, 2013.

[25] E. CÂMARA; R. C. A. PINTO; J. C. ROCHA, "Setting process on mortars containing sugarcane bagasse ash," *Ibracon Structures and Materials Journal,* vol. 9, no. 4, pp. 617-642, 2016.

[26] T. S. ABDULKADIR; D. O. OYEJOBI; A. A. LAWAL, "Evaluation of sugarcane bagasse ash as a replacement for cement in concrete works," *Acta Tehnica Corviniensis – Bulletin of Engineering,* pp. 71-76, 2014.

[27] Worrell E; Price L; Martin N; Hendriks C; Meida L O, "Carbon dioxide emission from the global cement industry," *Annu Rev Energy Environ,* vol. 26, pp. 303-329., 2001.

[28] Qing Xu; Tao Ji; San-Ji Gao; Zhengxian Yang; Nengsen Wu, "Characteristics and applications of sugar cane bagasse ash waste in cementitious materials," *Materials (Basel, Switzerland),* vol. 12, no. 1 39, 2018.

[29] Moisés Frías; Ernesto Villar; Holmer Savastano, "Brazilian sugar cane bagasse ashes from the cogeneration industry as active pozzolans for cement manufacture," *Cement & Concrete Composites,* vol. 33, pp. 490-496, 2011.

[30] J.F. Martirena Hernández; B. Middendorf, M. Gehrke; H. Budelmann, "Use of wastes of the sugar industry as pozzolana in lime-pozzolana binders: study of the reaction," *Cement and Concrete Research,* vol. 28, no. 11, pp. 1525-1536, 1998.

[31] Nuntachai Chusilp; Chai Jaturapitakkul; Kraiwood Kiattikomol, "Effects of LOI of ground bagasse ash on the compressive strength and sulfate resistance of mortars," *Construction and Building Materials,* vol. 23, p. 3523–3531, 2009.

[32] K. Umamaheswaran; Vidya S. Batra, "Physico-chemical characterisation of Indian biomass ashes," *Fuel,* vol. 87, p. 628–638, 2008.

[33] M.A. Tantawy; A.M. El-Roudi; A.A. Salem, "Immobilization of Cr(VI) in bagasse ash blended cement pastes," *Construction and Building Materials,* vol. 30, pp. 218-223, 2012.

[34] G.C. Cordeiro; R.D. Toledo Filho; E.M.R. Fairbairn, "Effect of calcination temperature on the pozzolanic activity of sugar cane bagasse ash," *Construction and Building Materials,* vol. 23, pp. 3301-3303, 2009.

[35] Kavitha S, T Felix Kala, "A review on natural fibres in the concrete," *International Journal of Advanced Engineering and Technology,* vol. 1, no. 1, pp. 1-4, 2017.

[36] Noor Zawati Zakaria, Mohd Zailan Sulieman, Roslan Talib, "Turning Natural Fiber Reinforced Cement Composite as Innovative Alternative Sustainable Construction Material A Review Paper," *International Journal of Advanced Engineering, Management and Science (IJAEMS),* vol. 1, no. 8, pp. 24-31, 2015.

[37] Deborah D.L. Chung, "6 - Cement-Matrix Composites," in *Carbon Composites (Second Edition)*, Butterworth-Heinemann, 2017, pp. 333-386.

[38] Ian Sims, Bev Brown, "16 - Concrete Aggregates," in *Lea's Chemistry of Cement and Concrete (Fourth Edition)*, Butterworth-Heinemann, 1998, pp. 907-1015.

[39] D.A. Spears, J.H. Sharp, D. Thompson, B.B. Argent, "PREDICTION OF THE PHASES PRESENT IN FLY ASH, THEIR COMPOSITION AND THE INFLUENCE OF THESE FACTORS ON ITS UTILITY AND DISPOSAL," *The Institute of Energy's Second International Conference on Combustion & Emissions Control,* pp. 71-87, 1995.

[40] Arpita Bhatt, Sharon Priyadarshini, Aiswarya Acharath Mohanakrishnan, Arash Abri, Melanie Sattler, Sorakrich Techapaphawit, "Physical, chemical, and geotechnical properties of coal fly ash: A global review," *Case Studies in Construction Materials,* vol. 11, 2019.

[41] Sanjay Kumar, Rakesh Kumar, "Mechanical activation of fly ash: Effect on reaction, structure and properties of resulting geopolymer," *Ceramics International,* vol. 37, no. 2, pp. 533-541, 2011.

[42] A Fernández-Jiménez, A Palomo, "Characterisation of fly ashes. Potential reactivity as alkaline cements," *Fuel,* vol. 82, no. 18, pp. 2259-2265, 2003.

[43] Guilherme Chagas Cordeiro, Romildo Dias Toledo Filho, Luís Marcelo Tavares, Eduardo de Moraes Rego Fairbairn, "Ultrafine grinding of sugar cane bagasse ash for application as pozzolanic admixture in concrete," *Cement and Concrete Research,* vol. 39, no. 2, pp. 110-115, 2009.

[44] Torres, J., Mejía, R., Escandón, C. E., González, L. O., "Characterization of sugar cane bagasse ash as supplementary material for Portland cement," *Ingeniería e Investigación,* vol. 34, no. 1, pp. 5-10, 2014.

[45] G.C. Cordeiro, R.D. Toledo Filho, L.M. Tavares, E.M.R. Fairbairn, "Pozzolanic activity and filler effect of sugar cane bagasse ash in Portland cement and lime mortars," *Cement and Concrete Composites,* vol. 30, no. 5, pp. 410-418, 2008.

[46] Ferreira, R. T. L., Nunes, F., Bezerra, A. C. d. S., Figueiredo, R. B., Cetlin, P. R., & da Aguilar, M., Teresa Paulino, "Influence of reburning on the pozolanicity of sugar-cane bagasse ashes with different characteristics," *Materials Science Forum,* vol. 869, pp. 141-146, 2016.

[47] Rafael G. D. Molin Filho, Jaciele M. Rosso, Eduardo A. Volnistem, Romel D. Vanderlei, Leda M. S. Colpini, Mateus M. Ferrer, Paulo R. Paraíso, Luiz M. de M. Jorge, "Sugarcane Bagasse Ash Micronized Using Air Jet Mills for Green Pozzolan in Brazil," *International Journal of Chemical Engineering ,* vol. 2019, 2019.

[48] Arnon Bentur and Sidney Mindess, Fibre Reinforced Cementitious Composites (Second Edition), Taylor & Francis, 2007.

[49] O Gencel, C Ozel, W Brostow & G Martínez-Barrera, "Mechanical properties of self-

compacting concrete reinforced with polypropylene fibres," *Materials Research Innovations,* vol. 15, no. 3, pp. 216-225, 2011.

[50] Ronald F. Zollo, "Fiber-reinforced concrete: an overview after 30 years of development," *Cement and Concrete Composites,* vol. 19, no. 2, pp. 107-122, 1997.

[51] Flavio de Andrade Silva, Nikhilesh Chawla, Romildo Dias de Toledo Filho, "Tensile behavior of high performance natural (sisal) fibers," *Composites Science and Technology,* vol. 68, no. 15-16, pp. 3438-3443, 2008.

[52] D. Verma, P.C. Gope, M.K. Maheshwari, R.K. Sharma, "Bagasse Fiber Composites-A Review," *Journal of Materials and Environmental Science,* vol. 3, no. 6, pp. 1079-1092, 2012.

[53] Tolêdo Filho, Romildo Dias, Joseph, Kuruvilla, Ghavami, Khosrow, & England, George Leslie, "THE USE OF SISAL FIBRE AS REINFORCEMENT IN CEMENT BASED COMPOSITES," *Revista Brasileira de Engenharia Agrícola e Ambiental,* vol. 3, no. 2, pp. 245-256, 1999.

[54] K Bilba, M-A Arsene, A Ouensanga, "Sugar cane bagasse fibre reinforced cement composites. Part I. Influence of the botanical components of bagasse on the setting of bagasse/cement composite," *Cement and Concrete Composites,* vol. 25, no. 1, pp. 91-96, 2003.

[55] Matheus R. Cabral, Erika Y. Nakanishi, Valdemir dos Santos, Joahnn H. Palacios, Stéphane Godbout, Holmer Savastano Junior, Juliano Fiorelli, "Evaluation of pre-treatment efficiency on sugarcane bagasse fibers for the production of cement composites," *Archives of Civil and Mechanical Engineering,* vol. 18, no. 4, pp. 1092-1102, 2018.

[56] Henry A Colorado, John F Zapata, "Composites of Portland cement paste and sugarcane bagasse fibers: structure-property relation and Weibull statistics," *Journal of Materials and Environmental Sciences,* vol. 10, no. 11, pp. 1162-1171, 2019.

3 CLASSIFICATION OF THE SUGARCANE RESIDUES AND THEIR CHARACTERISTICS

3.1 Introduction

For several countries with limited resources base and small land areas, it is imperative to conduct environmentally friendly production activities from the viewpoints of waste reduction, resource-saving, and prevention of global warming. There is no exception to the civil construction industry since this field is one of the most pollutants in the world[1, 2]. Efforts to develop a mortar/concrete with less cement than conventional ones are being taken as a measure against global warming. Also, the agro-residues in concrete are a sustainable way to reduce natural resources consumption. Other benefits, such as the decrease of the composite and local development cost, can be attractive factors to the use of these residues.

Natural fibers are produced by plants, such as vegetables, leaves, and wood. Researchers have used plant fibers as an alternative source of materials like steel. Artificial fibers have been used in composites, such as cement paste mortar and concrete, to increase their strength properties. These plant fibers could be originated from coir, sisal, jute, Hibiscus cannabinus, Eucalyptus grandis pulp, malva, ramie bast, pineapple leaf, kenaf bast, sansevieria leaf, abaca leaf, vakka, date, bamboo, palm, banana, hemp, flax, cotton and sugarcane[3].

The bagasse, a residue derived from sugarcane, is one of the most natural fibers produced in the world. The sugarcane residues can be classified into two broad groups as follows:

1. non-burned residues, for example, the bagasse, which still in the raw phase; and
2. burned residues, for instance, the bagasse ash, the residues originated from the burn of the bagasse in the boilers of the mill.

Although there are several types of research about those residues, there is no established standardization about their classification. However, there are different manners to use them ecologically in concrete. This chapter aims to propose a straightforward method of categorizing sugarcane residues and investigating their chemical, physical, and mechanical characteristics.

3.2 Research design and methodology

3.2.1 Flow chart of the experimental approach

This chapter aims to describe the classification of the sugarcane residues, methods used, and the

experimental procedure. Both the non-burned and the burned sugarcane residues used in this research were acquired from a sugar mill in Okinawa Prefecture, Japan.

Figure 3.1 shows the flow chart of the experimental approach. The first step was washing the bagasse. After the bagasse was washed, the classification of the residues was started. The classification was carried out in two groups: the burned and non-burned bagasse residues.

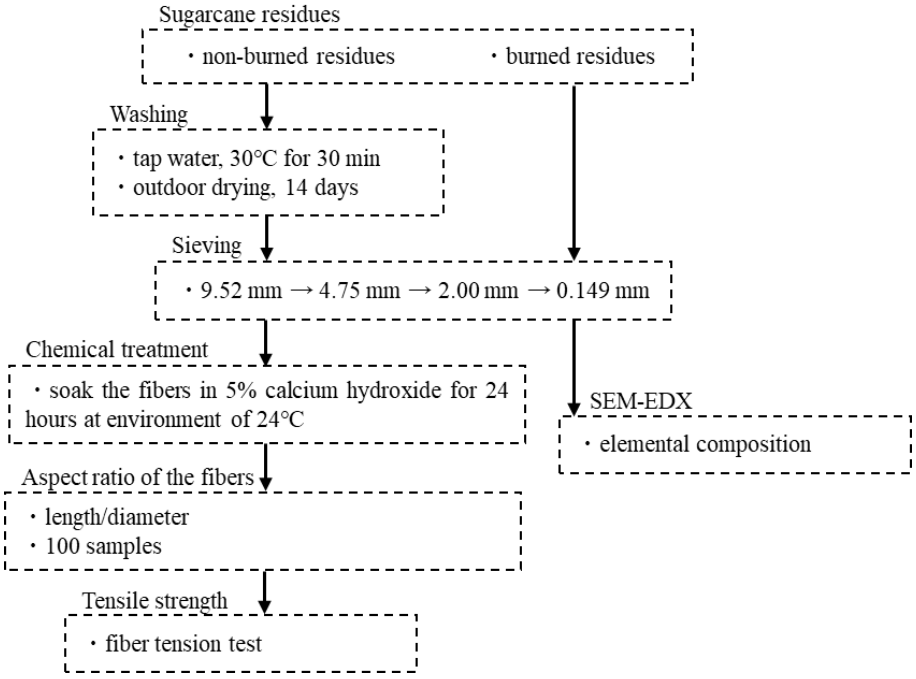

Figure 3.1 Flow chart of the experimental approach

After classification of the residues, samples were prepared to be applied to physical and mechanical tests to evaluate the properties and characterize the residues; all focused on preparing fibers and ashes for use in a cementitious medium. Furthermore, some care has been taken, such as applying ecological methods, which do not require a high degree of energy to be performed. These methods and procedures and the testing devices used are explained in detail. The chemical composition of the sugarcane bagasse ash was also investigated.

3.2.2 Process of washing of the bagasse fiber

In a simple washing process, the bagasse (non-burned residues) was dipped in water at 30°C for 30 minutes and then dried in the open air, as shown in Figure 3.2. This procedure aimed to reduce the residual sugar content of the bagasse and eliminate the impurities.

Figure 3.2 Washing (left) and drying (right) process of the bagasse fiber

After the washing, the fibers were placed to dry in an open-air area.

3.2.3 Process of sieving of the bagasse fiber

Afterward, the process of sieving the bagasse fiber had begun. The apertures of the sieve mesh sizes were 9.52, 4.76, and 2.00 mm. The sieved bagasse fiber is shown in Figure 3.3.

Figure 3.3 Original state and the sieved bagasse fiber

Concerning the mortar or concrete workability, the materials classified above 4.76 mm should be reprocessed, such as cutting the bagasse, to be used in mortar or concrete. Otherwise, it should be reused for a different purpose.

The bagasse fibers (BF) used in this study were passed through a 4.76 mm sieve and remained in a 2 mm sieve.

3.2.4 Alkali treatment of the bagasse fiber

Before the preparation of specimens, the fibers were treated with an alkali solution (see Figure 3.4) to improve the strength of fibers against the alkaline attack[4, 5]. The fibers were soaked in a solution of 5% $Ca(OH)_2$ for 24 hours[6, 7].

Figure 3.4 Bagasse fibers after the alkali treatment

3.2.5 Analysis of the reducing sugar content of the bagasse fiber

The reducing sugar content of the raw bagasse (RB), washed bagasse (WB), and bagasse fiber (BF, washed and alkali-treated) was analyzed. 4 g of each sample was cut, and 40 ml of H_2O was added. Subsequently, it was allowed to rest for about 2 hours. Later, this mixture was centrifuged at 8000 rpm at 20°C for 30 min. Then, 10 ml supernatant was lyophilized and dissolved in 1 ml of acetonitrile/water (CH_3CN/H_2O=75/25). This solution was used as a sample to analyze the reducing sugar. Afterward, 0.2 ml of sample, 0.4 ml of reagent A ($NaCO_3$ (40g/L), glycine (16g/L), $CuSO_4 \cdot 5H_2O$ (0.45g/L)) and 0.4 ml of reagent B (neocuproine hydrochloride (0.15g/100ml)) were mixed. The mixture was heated at 100°C for 12 minutes and rapidly cooled. 1 ml of H_2O was added, and the absorbance at 450 nm was measured. The sample's reducing sugar content was determined as a glucose equivalent from the calibration curve prepared with glucose.

3.2.6 Density test of the bagasse fiber

The density determination of bagasse fiber was made according to JIS A 1109, with some modifications. The sample's weight was changed from 500 grams to 100 grams, and the liquid used was ethanol to better compact the fibers into the flask since the ethanol has a smaller density than water.

3.2.7 Aspect ratio of the bagasse fiber

In order to determine the fibers' aspect ratio, a digital camera (16 Megapixels) was used to take a photo of the fiber (see Figure 3.5) and, by using a software (Adobe Photoshop), the diameter and length were measured before the mechanical tests. The average diameter is obtained after the measurement of at least 2 measurements throughout the fiber length. The measurements were made by pixels and then converted to millimeters.

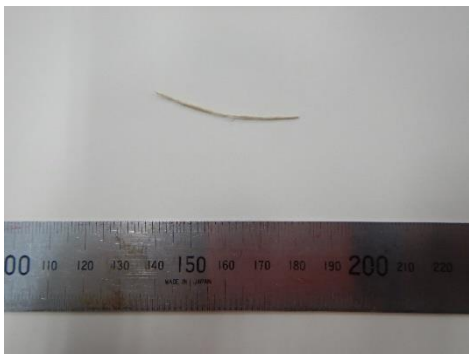

Figure 3.5 Aspect of the bagasse fiber

After the measurements of the length and the diameter, the aspect ratio was obtained by the following equation:

$$\textbf{Aspect Ratio} = \frac{\textbf{Length (mm)}}{\textbf{Diameter (mm)}}$$

3.2.8 Tensile strength of the bagasse fiber

The tensile properties of the single fiber of the bagasse were determined according to JIS R 7606 and JIS K 7161. Single fibers are manually separated from the bundles. The fibers' diameter is determined individually by the average of 2 points throughout the length of the fiber, as mentioned in 3.2.7. As Figure 3.6 illustrates, before testing, the fiber was glued to the paper frame with epoxy. The distance between the 2 glued borders was 5 mm. Then, the frame is clamped on the Autograph AG-X universal testing machine (see Figure 3.7). After the clamping of the ends of the paper frame in the test machine, the paper frame sides were carefully cut in the middle with small scissors before starting the tensile test. The tests were displacement-controlled with a loading rate of 0.5 mm/min at 20 ± 2°C and 60% relative humidity. The test was conducted 30 times, and the average values are reported.

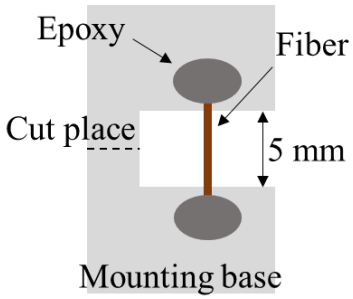

Figure 3.6 Preparation of specimen for the tensile test

Figure 3.7 Set up of the tensile test

The tensile strength is calculated by dividing measured load values by the original cross-sectional area of the fiber sample, as the following equation shows:

$$\textbf{Tensile strength} = \frac{\textbf{Load } (N)}{\textbf{Section area } (mm^2)}$$

3.2.9 Process of sieving of the bagasse sand and ash

The bagasse sand and ash (burned residues) were not washed to avoid small particles of ash coming into contact with water. The sieve mesh size's apertures used to categorize the bagasse sand and ash were 9.52, 4.76, and 2.00 mm. The sieved burned residues are shown in Figure 3.8.

Figure 3.8 The original state and the sieved burned bagasse

The burned residues passed through a 2 mm sieve were classified as bagasse sand (BS). This bagasse sand was then sieved in a 0.149 mm sieve. The residues which passed through a 0.149 mm sieve were classified as bagasse ash (BA), as shown in Figure 3.9.

Figure 3.9 Bagasse ash

It should be noted that, in the case of BS, there are burned fibers, bagasse sand, and bagasse ash (in a small amount) mixed in the sample.

3.2.10 Density test of the bagasse sand and ash

In order to determine the density of the bagasse sand and the bagasse ash, measurements were made according to JIS A 1109. However, some modifications were made, such as the weight of the samples was changed from 500 grams to 250 grams, and the liquid used was ethanol to better compact the samples into the flask, as mentioned in 3.2.6.

3.2.11 Chemical composition of the bagasse sand and ash

The scanning electron microscopy (SEM) and energy dispersive spectroscopy (EDS) were carried out to analyze the microstructure and determine the elemental composition of bagasse ash.

3.2.12 Loss ignition of the bagasse sand and ash

The loss on ignition and the moisture were measured according to JIS A 6201.

3.3 Results and discussions

In this section, the analysis results of the performance of sugarcane residues from experimental observations and measurements are shown. First, the results of the chemical components and weight ratio are shown and discussed. Afterward, the physical, mechanical properties result of bagasse fibers are argued and debated.

3.3.1 Cumulative passing rate of bagasse fiber

The cumulative passing rate of burned bagasse fibers made by sieving the bagasse fiber is shown in Figure 3.10.

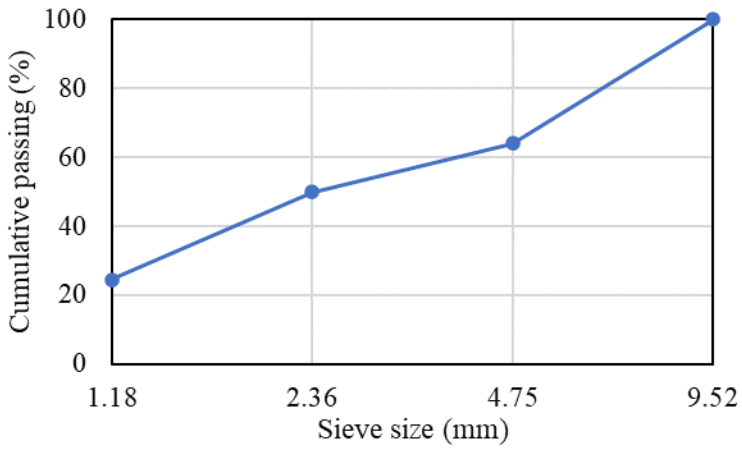

Figure 3.10 Cumulative passing rate of bagasse fiber

According to Figure 3.10, the bagasse fiber, which was smaller than 4.76 mm and larger than 2.36 mm, was around 14% of the total. This result means that approximately 14% of the non-burned residues acquired from the mill can be added to mortar or concrete without any particular process, such as cutting. In the bagasse fiber smaller than 2.36 mm, the fibers sizes are more uniform. However, there is bagasse powder mixed. For this reason, the use of bagasse fiber smaller than 2.36 mm should be considered since it may contain a high amount of soluble sugar, which can influence the mortar or concrete setting.

3.3.2 Reducing sugar analysis

The result of reducing sugar analysis is shown in Figure 3.11.

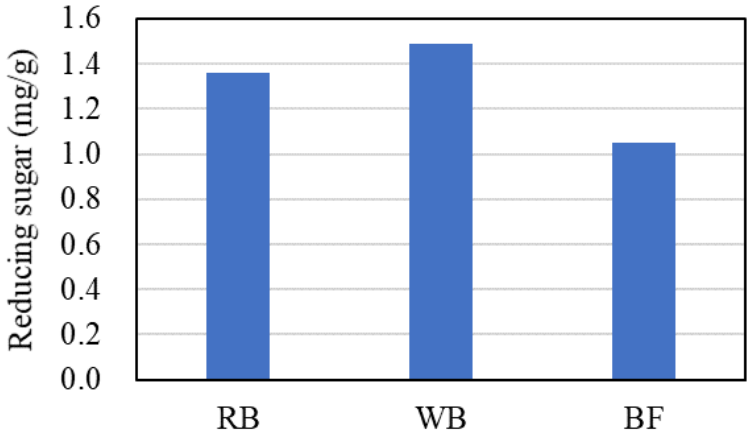

Figure 3.11 Reducing sugar content

From Figure 3.11, it is possible to see that the RB contains a certain amount of reducing sugar since the glucose is derived from sugarcane. However, in WB, where the bagasse was dipped in water at 30°C for 30 minutes, the reducing sugar content increased compared to RB. Since sugarcane contains

various enzymes[8, 9], the bagasse may contain similar enzymes. Those may remain inactivated in the case of RB. However, in the case of WB, it seems that they were activated and accelerated the sucrose hydrolysis reaction, releasing reducing sugars. Usually, hydrolysis is a slow reaction[10, 11], where sucrose can sit for an extended period with minor changes. However, with water heating in WB, the reaction could have been accelerated by breaking the glycosidic bond and converting sucrose into glucose and fructose. Consequently, this increased the reducing sugar content. Also, due to the short time that the bagasse was dipped in the water, it may not be enough to reduce the sugar released into water. Furthermore, the hydrolysis reaction may still be reacting during the bagasse's drying time remaining. In the case of the alkali-treated bagasse fiber, the reducing sugar content decreased in comparison with WB. This may be due to the longer time that the washed bagasse was dipped in the solution.

3.3.3 Characteristics of the bagasse fiber

The characteristics of the alkali-treated bagasse fibers are shown in Table 3.1. As shown in Table 3.1, the density of the alkali-treated fibers was 0.71 g/cm^3. The average length and the diameter were 17.9 and 0.56 mm, respectively, resulting in an aspect ratio of 32. The tensile strength of the fibers was 132 N/mm^2.

Table 3.1 Characteristics of the bagasse fibers

	BF
Surface-dry density (g/cm^3)	0.71
Length (mm)	17.9 (average)
Diameter (mm)	0.56 (average)
Aspect ratio	32
Tensile strength (N/mm^2)	132

3.3.4 Cumulative passing rate of burned bagasse residues

The cumulative passing rate of burned bagasse residues made by sieving the burned bagasse is shown in Figure 3.12.

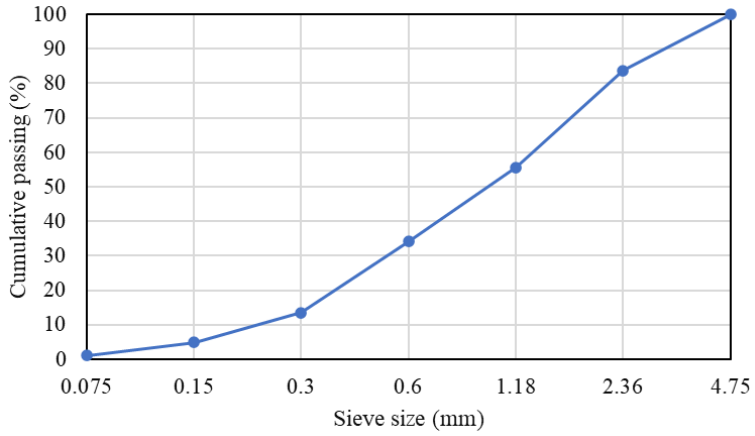

Figure 3.12 Cumulative passing rate of burned bagasse residues

From Figure 3.12, it is possible to see that around 79% of the total of the burned bagasse were smaller than 2.36 mm and bigger than 0.15 mm. More than half of the weight of the burned bagasse residues acquired could be classified as bagasse sand (BS). Also, Figure 3.12 indicates that around 5% of the total was smaller than 0.15 mm. However, this percentage could vary with different factors such as the environment and the mill's temperature, among others.

3.3.5 Chemical composition of the bagasse sand and ash

Figure 3.13 shows the microstructure of the bagasse ash from an SEM image. Microstructural examination of bagasse ash shows angular and irregular particles. The EDS analysis was done by selecting the whole area from Figure 3.13.

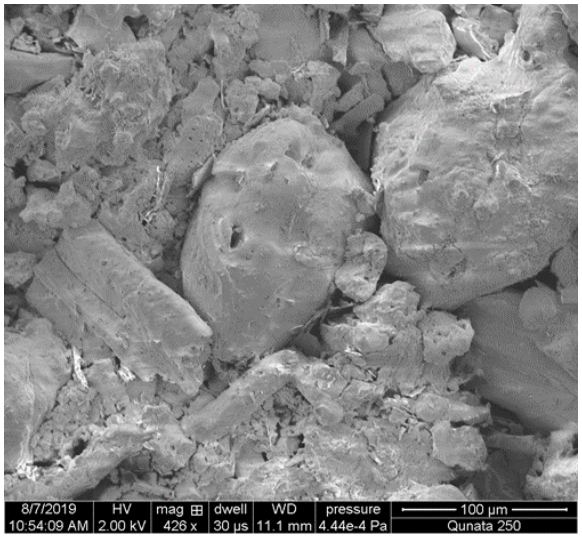

Figure 3.13 SEM image of the bagasse ash

As Table 3.2 shows, in the selected EDS analysis area, the predominately chemical composition was

silicon dioxide, aluminum oxide, potassium oxide, calcium oxide, phosphorus pentoxide, magnesium oxide, and iron(III) oxide.

Table 3.2 Chemical composition of sugarcane bagasse ash

Element component	Concentration
SiO_2	68.54
Al_2O_3	8.46
K_2O	6.54
CaO	6.53
P_2O_5	4.20
MgO	3.67
Fe_2O_3	2.04

According to the chemical analysis results from Table 3.2, the selected sample shows that the sum of significant oxides, SiO_2, Al_2O_3, and Fe_2O_3, is approximately 79%. This value is larger than 70%, which is required as the chemical composition of natural pozzolans according to ASTM C 618.

3.3.6 Loss of ignition

The loss on ignition and the moisture of the BA were 5.0% and 1.0%, respectively. Table 3.3 shows a comparison between the required standards (JIS A 6201) of fly ash and BA used in this study.

Table 3.3 Comparison between the required standards of fly ash and BA

	Fly ash Type 1	Fly ash Type 2	Fly ash Type 3	Fly ash Type 4	BA
SiO_2 (%)	≧45				68.5
Moisture (%)	≦1.0				1.0
Loss on ignition (%)	≦3.0	≦5.0	≦8.0	≦5.0	5.0
Density (g/cm^3)	≧1.95				2.1
Specific surface area (cm^2/g)	≧5000	≧2500		≧1500	—

Although the BA results achieved the standard of fly ash type 2, BA's shape was not the same as fly ash, which has a fine spherical particle. For this reason, more studies about the physical properties of BA should be done to determine the workability of the mortar and the influence of the BA in the case of replacement of cement for BA. Besides, supplementary investigations should be done to confirm the pozzolanic activity of the bagasse ash.

3.4 Conclusion of chapter

The results obtained in this study can be summarized as follows:

1. Approximately 14% of the non-burned residues acquired from the mill can be added to mortar or concrete without any particular process, such as cutting.
2. 1.36 mg/g of reducing sugar was detected in raw bagasse. This value increased when the raw bagasse was dipped in water at 30°C for 30 minutes to 1.49 mg/g. However, when the washed bagasse is alkali-treated, the reducing sugar content decreased to 1.05 mg/g.
3. The tensile strength of the fibers was 132 N/mm^2.
4. 79% of the total weight of the burned bagasse was smaller than 2.36 mm. From this total, around 5% of the total weight was smaller than 0.15 mm.
5. The chemical analysis showed that the sum of major oxides, SiO_2, Al_2O_3, and Fe_2O_3, was approximately 79%, 9% more than the required chemical composition of natural pozzolans according to ASTM C 618.
6. Although the bagasse ash (burned bagasse smaller than 0.15 mm) has an angular and irregular particle, the results indicate that BA conforms to the requirements prescribed standard (JIS A 6201) of fly ash type 2.

3.5 References

[1] Bas J. van Ruijven, Detlef P. van Vuuren, Willem Boskaljon, Maarten L. Neelis, Deger Saygin, Martin K. Patel, "Long-term model-based projections of energy use and CO_2 emissions from the global steel and cement industries," *Resources, Conservation and Recycling,* vol. 112, pp. 15-36, 2012.

[2] Lizhen Huang, Guri Krigsvoll, Fred Johansen, Yongping Liu, Xiaoling Zhang, "Carbon emission of global construction sector," *Renewable and Sustainable Energy Reviews,* vol. 81, no. 2, pp. 1906-1916, 2018.

[3] Kavitha S, T Felix Kala, "A review on natural fibres in the concrete," *International Journal of Advanced Engineering and Technology,* vol. 1, no. 1, pp. 1-4, 2017.

[4] Marie-Ange Arsène; A. Okwo; Ketty Bilba; A. B. O. Soboyejo; W. O. Soboyejo, "Chemically and thermally treated vegetable fibers for reinforcement of cement-based composites," *Materials and Manufacturing Processes,* vol. 22, no. 2, pp. 214-227, 2007.

[5] Cristel Onésippe; Nady Passe-Coutrin; Fernando Toro; Silvio Delvasto; Ketty Bilba; Marie-Ange Arsène, "Sugar cane bagasse fibres reinforced cement composites: Thermal considerations," *Composites: Part A,* vol. 41, p. 549–556, 2010.

[6] M.N.M. Ibrahim; G.R. Pearce, "Effects of chemical pretreatments on the composition and In vitro digestibility of crop by-products," *Agricultural Wastes,* vol. 5, no. 3, pp. 135-156, 1983.

[7] Jairo Alexander Osorio Saraz; Fredy Varón Aristizabal; Jhonny Alexander Herrera Mejí, "Mechanical behavior of the concrete reinforced with sugar cane bagasse fibers (in Spanish)," *Dyna (Medellin, Colombia),* vol. 74, pp. 69-79, 2007.

[8] Alexander, A.G., "The Action Pattern of Sugarcane-Leaf Amylase," *The Journal of Agriculture of the University of Puerto Rico,* vol. 51, no. 2, pp. 154-166, 1967.

[9] Alexander, A. G., "Sucrose-enzyme relationships in immature sugarcane as affected by varying levels of nitrate and potassium supplied in sand culture," *The Journal of Agriculture of the University of Puerto Rico,* vol. 48, no. 3, pp. 165-231, 1964.

[10] M. Satish Kumar, Practical Physical Chemistry, Sankalp Publication, 2019.

[11] Martin F. Chaplin, Christopher Bucke, Enzyme Technology, Cambridge University Press, 1990.

4 A STUDY ON MECHANICAL PROPERTIES OF MORTAR WITH SUGARCANE BAGASSE FIBER AND BAGASSE ASH

4.1 Introduction

Concrete structures are essential for the infrastructure of many countries in the world[1]. However, under inappropriate conditions and environment[2], these structures deteriorate rapidly, surpassing the usage planned period[3]. This happens because several factors can damage the structure, not only after its construction but also before and during its construction, causing significant economic losses each year[4]. Therefore, durability is a necessary performance requirement for a structure that must be considered during the design step. As a fragile material, low tensile strength can easily cause cracks in mortar and concrete[5]. This is an issue not only considering mechanical properties but also the durability of the structure. For this reason, the addition of short fibers is often adopted as one of the effective methods to increase the durability of mortar and concrete since it can control crack propagation[6].

Zhang et al. studied the effect of different fly ash and silica fume content on the compressive strength, flexural strength, and toughness of high-performance FRCC (Fiber Reinforced Cementitious Composite), based on the development and application of high-performance FRCC. According to Zhang et al., the addition of fly ash and silica fume significantly affects the mechanical properties of high-performance FRCC. The specific optimization content with 50% ash and 15% silica fume can make the flexural strength of high-performance FRCC up to 19.5 MPa, the compressive strength to 75.2 MPa, and the ratio of bending strength to compressive strength to about 0.26. Compared with ordinary fiber reinforced cementitious composite, its flexural strength and compressive strength are increased by 35 and 40%, respectively. The ratio of bending strength to compressive strength is increased by about 6%. It can be seen that the optimization mixture can significantly enhance the compressive strength, flexural strength, and toughness of high-performance FRCC and may provide a reference for practical use[7].

Vanathi et al. examined the potential use of sugarcane bagasse ash as a partial cement replacement material. They characterized the bagasse ash physically and partially replaced cement with ratios of 0, 10, 20, and 30% in the addition of steel fiber by weight of cement in concrete. The compressive strength, tensile strength, and flexural strength of concrete mixed with bagasse ash as cement substitute were measured. The test results indicated that up to 10% replacement of cement by bagasse ash in concrete with steel fiber could be considered an optimum replacement material[8].

In this chapter, the mechanical properties of the sugarcane residues in mortar were studied. The fibers and ashes mortar specimens were prepared, and strength tests (compressive, split tensile, flexural, and adhesion strength) were performed. Besides, the porosity rate, water retention rate, and drying strain shrinkage were measured. All tests were performed in a short, medium, and extended period of 7, 28, and 91 days of curing, respectively, to analyze the behavior of sugarcane fiber and ash in mortar in different periods.

4.2 Research design and methodology

4.2.1 Flow chart of the experimental approach

This section describes the experimental approach and test procedures. The raw materials used in this work are bagasse fiber, bagasse sand, bagasse ash, cement, sand, and fly ash. The research design is summarized in Figure 4.1.

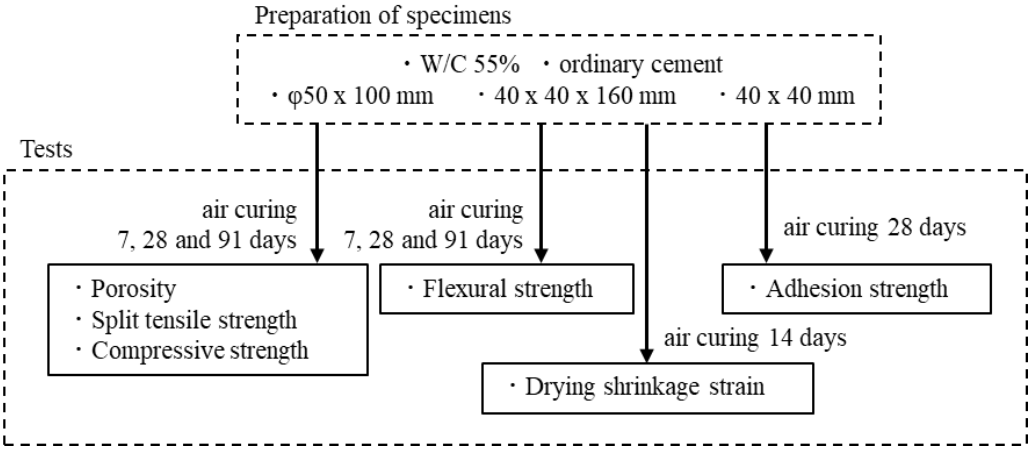

Figure 4.1 Overall flow of this research

As shown in the flow chart of research in Figure 4.1, after the specimens' preparation, the strength tests were performed to determine the mechanical properties of the specimens when added with the sugarcane residues.

4.2.2 Materials

All specimens were prepared using ordinary Portland cement (C) and fine aggregates (S). Commercially available PVA fiber (VF) of 18 mm length for mortar and fly ash (FA) was used for comparisons. The physical properties of materials and the fibers' characteristics are given in Table 4.1 and Table 4.2, respectively.

Table 4.1 Physical properties of cement and aggregates

Properties	Materials				
	C	S	BS	BA	FA (grade Ⅱ)
Density (g/cm^3)	3.16	2.60	1.29	2.10	2.24
R_2O (%)	0.56	—	—	—	—
Specific surface area (cm^2/g)	3280	—	—	—	3420
Loss on ignition %	—	—	—	—	2.2

Table 4.2 Characteristics of the fibers

	BF	VF
Surface-dry density (g/cm^3)	0.71	1.10
Length (mm)	17.9 (average)	18.0
Diameter (mm)	0.56 (average)	0.2
Aspect ratio	32	90
Tensile strength (N/mm^2)	132	975

4.2.3 Mortar mixture

The mix proportions of mortar are shown in Table 4.3. The mortar mixture N was prepared in the laboratory, with water to binder ratio (W/C) of 55% and S/C=4.2. Mortar mixture N represents the control specimens and contains no bagasse materials. In BF specimens, three mixtures were prepared with fiber volume ratios of 0.5, 1.0, and 2.0%. A mortar specimen using PVA fibers (VF) was made with a fiber volume ratio of 2.0% to compare the bagasse fibers' performance. Also, a mortar specimen using BF and VF was prepared. In this case, the bagasse fiber volume ratio was 0.5%, and the PVA fiber volume ratio was 0.5%, for a total fiber volume ratio of 1.0%. Besides, specimens were made using bagasse sand (BS), bagasse ash (BA), and fly ash (FA). In these cases, the volume ratio of the BS, BA, and FA was 5.0% and was used in the place of sand. In the case of BA and FA, the bagasse ash and fly ash acted as a binder. Thus, the W/B becomes 50% and 46%, respectively. In all cases, the fibers were used instead of sand.

Table 4.3 Mix proportions of the mortar specimens

Composites	Fiber addition amount (Vol. %)	W/B (%)	Unit (kg/m^3)							
			C	W	S	BS	BA	FA	BF	VF
N	—	55	400	220	1698	—	—	—	—	—
BF0.5	0.5				1687	—	—	—	3.15	—
BF1.0	1.0				1675	—	—	—	6.65	—
BF2.0	2.0				1649	—	—	—	13.65	—
VF2.0	2.0				1649	—	—	—	—	21.30
BF0.5 +	0.5				1674	—	—	—	3.50	—
VF0.5	0.5					—	—	—	—	5.45
BS5.0	—		400	220	1613	42	—	—	—	—
BA5.0 + BF2.0	2.0	50			1566	—	41	—	13.65	—
FA5.0 + BF2.0	2.0	46			1566	—	—	74	13.65	—

4.2.4 Mortar specimens and the tests applied

The mixing of mortar was performed following JIS R 5201. However, some steps were altered to improve the workability. All the mortar mixtures were mixed using a laboratory pan-type mixer. First, the cement and the fine aggregate were placed into the mixer. The mixer was immediately started at low speed (rotation speed: 30 ± 5 rpm) for 30 seconds. Afterward, the specified amount of water containing the fibers was added and mixed for 30 more seconds. After that, the mixer speed was changed to high speed (rotation speed: 60 ± 5 rpm), and the mixing continued for 30 seconds. After that, the mixer was stopped for 90 seconds. While the mixer was idle, during the first 30 seconds, the mortar that had adhered to the paddle was scraped off with a spatula and put at the mixer's center. After the break, the mortar was mixed for 60 seconds more at high speed. The total mixing time, including the break time, was 4 minutes. When the mixing was completed, the mortar was removed from the mixer and stirred ten times with an appropriate spoon.

The outline of mortar specimens is shown in Figure 4.2. For each mortar mixture, specimens of φ50 × 100 mm were cast to determine the compressive strength (JIS A 1108), modulus of elasticity (JIS A 1149), split tensile strength (JIS A 1113), porosity rate, and water retention rate of mortar. The porosity rate test was based on the mass of the specimen. First, the specimens were completely dried in a drying furnace at 80°C for 24 hours. Afterward, the specimens were

stored in a room at 20°C and relative humidity of 60% until the temperature of specimens decreased, equaling the ambient temperature. Then the mass of the specimens was weighed. Subsequently, the specimens were immersed in water at 20°C for 48 hours, and then the surface-dry mass of specimens was weighed. The following equation determined the porosity rate:

$$\boldsymbol{\varepsilon = \frac{W_s - W_d}{\rho \times V} \times 100}$$

Where:

ε: porosity rate (%);

W_d: mass of specimen absolute dried (g);

W_s: mass of specimen surface dried (g);

ρ: density of water (g/cm^3); and

V: volume of the specimen (cm^3).

After the porosity rate test, the moistened specimens were placed in a room at 20°C and relative humidity of 60%, and the mass change of specimens was recorded every 24 hours for 7 days. This mass change was determined as water retention rate. Furthermore, 40 × 40 × 160 mm specimens were prepared to determine the flexural strength (JIS A 1106) and drying shrinkage strain (JIS A 1129–2). For all specimens, the mortar was compacted in the formwork in three layers with a tamping rod. Subsequently, the formwork was placed on the vibration table for the physical test of cement and vibration was given for 120 seconds.

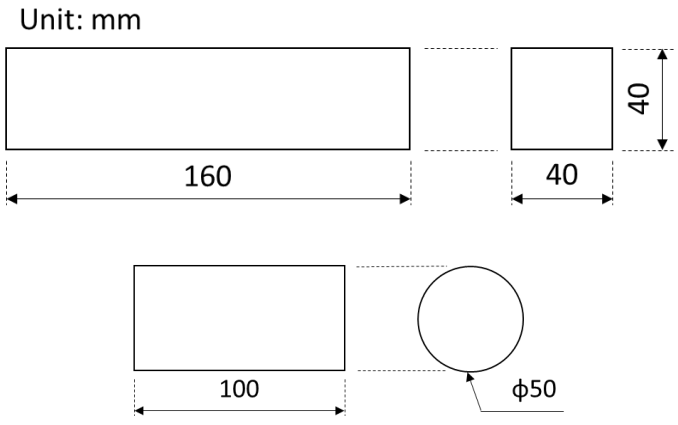

Figure 4.2 Outline of mortar specimens

Also, to find several possibilities for using mortar added with bagasse residues, the use of this mortar as a section restoration material was considered. Specimens of 30×40×40 mm were

prepared to determine the adhesion strength (JSCE-K 561-2013) of mortar. After 28 days of curing, a new mortar was placed on the surface of the 30×40×40 mm specimens and then compacted in the formwork with a tamping rod. Afterward, the specimen was placed on the vibration table for the physical test of cement and vibration was given for 120 seconds. The outline of the specimen for the adhesion strength test is shown in Figure 4.3. The adhesion strength test's specimen was fixed with epoxy resin on the center of a concrete specimen of 100×100×400 mm, W/C 60%, as shown in Figure 4.4.

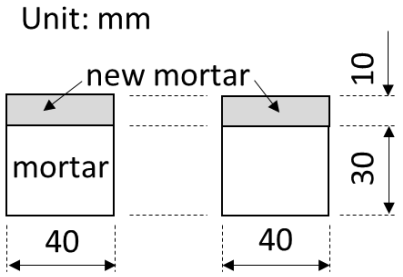

Figure 4.3 Outline of specimen for adhesion strength test

Figure 4.4 Overview of the adhesion strength test

After the casting, all specimens were cured in the laboratory at 20°C and 60% RH for 24 hours. After that, the specimens were de-molded and cured in air under room temperature of 20°C and 60% RH. Except for the elastic modulus and adhesion strength tests, which were applied after 28 days, all tests were applied at 7, 28, and 91 days of curing. Three specimens were used for

each test.

4.3 Results and discussions

In this section, the results of mechanical tests performed on bagasse residues cementitious composite materials are presented and discussed.

4.3.1 Porosity rate and water retention rate

The porosity of mortars at 7, 28, and 91 days is shown in Figure 4.5. The porosity of the specimens containing fibers is higher than N after 7, 28, and 91 days of curing. The increase in porosity with the addition of bagasse fiber can be explained once bagasse fiber is porous and, consequently, absorbs a high amount of water. Furthermore, it may be due to fine bubbles of air clumping together while the mortar mixes and eventually turning into empty space.

The porosity at 7 days of VF2.0 is slightly larger than that of BF2.0. This may be attributed to the fact that the PVA fiber diameter is approximately three times smaller than that of bagasse fiber (see Table 4.2). As a result, the number of PVA fibers was higher than the bagasse fiber specimens, increasing fine bubbles of air while the mortar was mixing. In the cases of BS5.0, BA5.0 + BF2.0, and FA5.0 + BF2.0, the porosity was higher than that of the other cases. The rise in porosity may be caused by the lower hydration of the ashes, especially at the earliest age where the pozzolanic reaction is small.

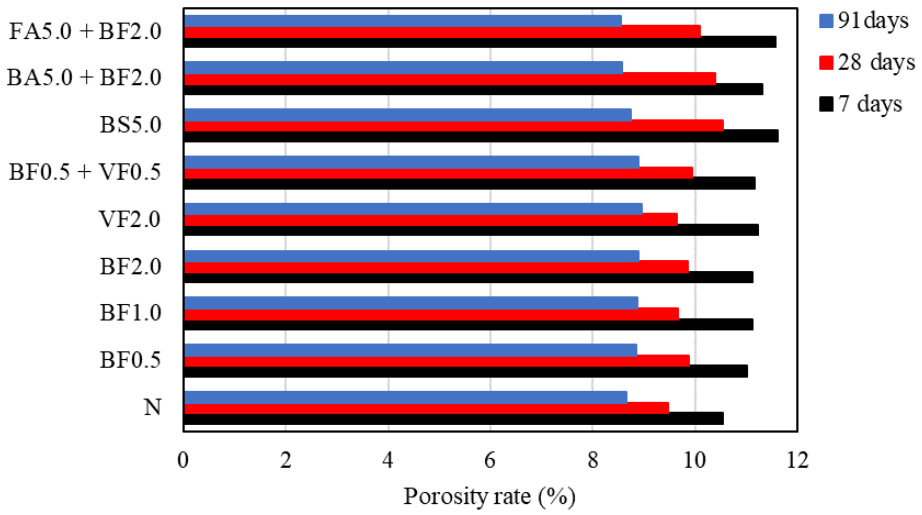

Figure 4.5 Porosity rate of each mixture

However, the porosity rate of each mortar reduced with time due to the increase in the hydration of cementitious materials. After 91 days of curing, particularly in the cases of BS5.0,

BA5.0 + BF2.0, and FA5.0 + BF2.0, the porosity rate decreased relatively, reaching the values of 8.7, 8.6, and 8.5%, respectively. This decrease is probably due to the increased pozzolanic reaction of the ashes since the pozzolanic reaction of ash tends to progress after a more extended period[9].

The water retention rate of each mortar mixture after 7, 28, and 91 days are shown in Figure 4.6, Figure 4.7, and Figure 4.8, respectively.

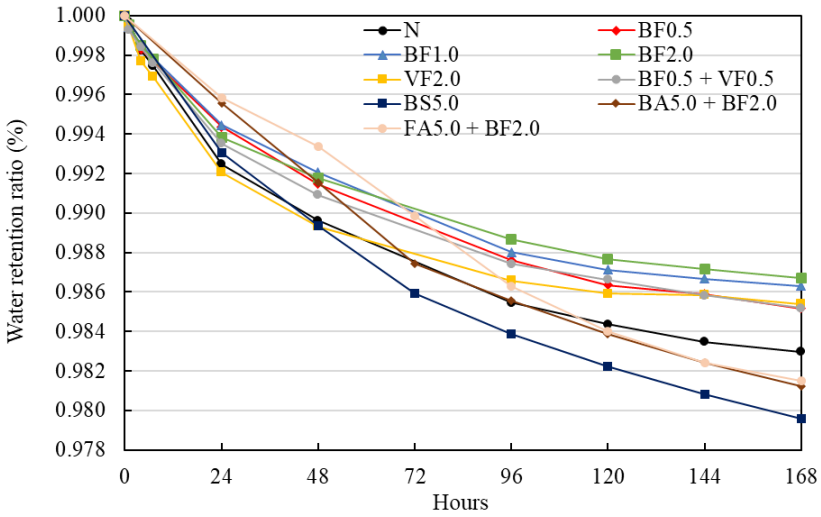

Figure 4.6 Water retention rate of each mixture at 7 days

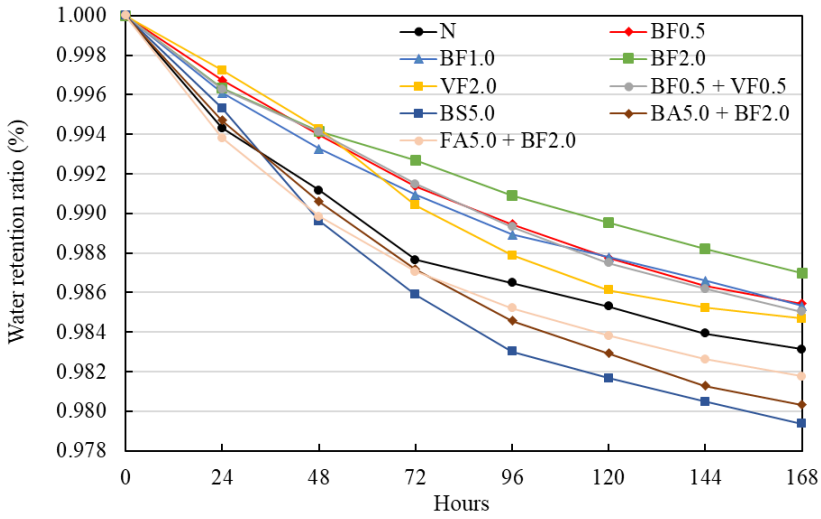

Figure 4.7 Water retention rate of each mixture at 28 days

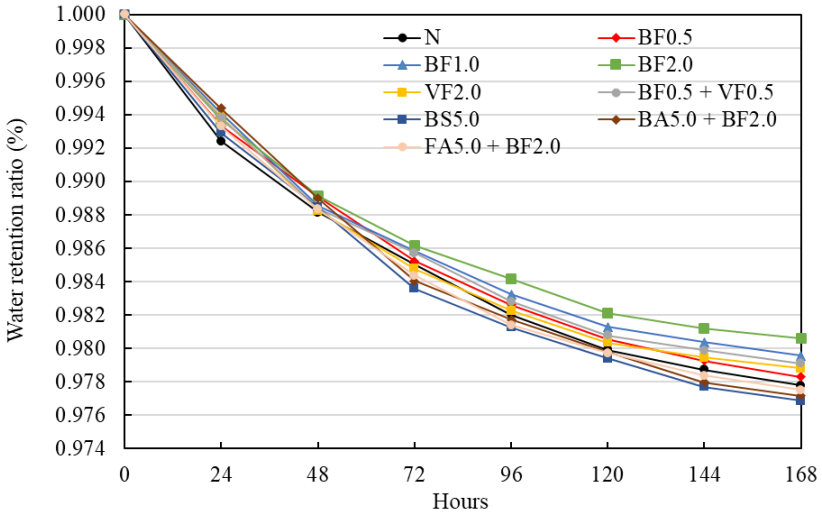

Figure 4.8 Water retention rate of each mixture at 91 days

As shown in Figure 4.6, Figure 4.7**,** and Figure 4.8, the water retention ratio is higher in the case of BF2.0 as compared to other cases. The high retention of water in BF2.0 is due to the high percentage of fibers used and bagasse fiber characteristics, which has a high absorption and retention capacity of water.

In the cases of BS5.0, BA5.0 + BF2.0, and FA5.0 + BF2.0, the water retention ratio is smaller than that of other cases. The smaller retention of water may be due to the water consumption during the pozzolanic reaction.

4.3.2 Compressive strength test

Figure 4.9 shows the results of the compressive strength of mortar. The mortar's strengths containing BF, VF, BS, BA, and FA were relatively low compared to N specimens after 7 days of curing. However, after 91 days, the difference in compressive strength between N and the other cases is reduced. In general, the greater the porosity, the smaller is the compressive strength.

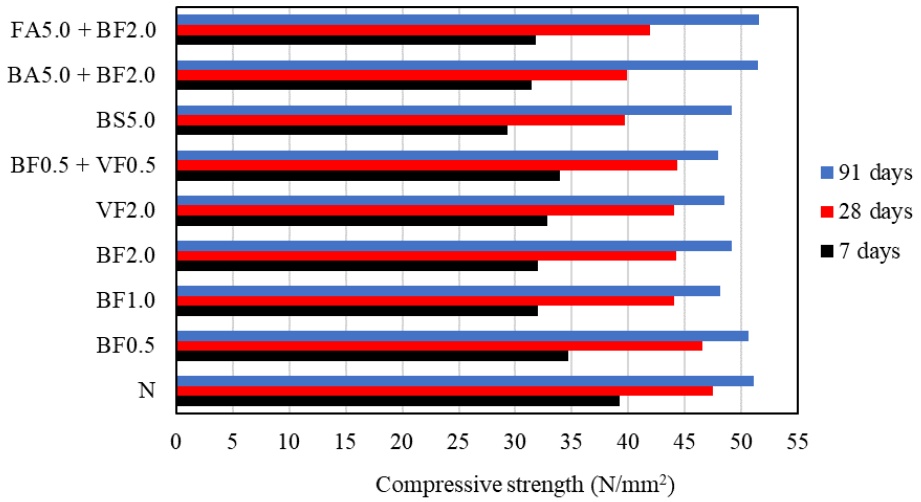

Figure 4.9 Compressive strength of mortars at 7, 28, and 91 days

In the cases of FA5.0 + BF2.0 and BA5.0 + BF2.0, the compressive strength after 91 days exceeds that of N. The pozzolanic reaction progress may increase the compressive strength since the porosity of FA5.0 + BF2.0 and BA5.0 + BF2.0 decreased after 91 days.

4.3.3 Elastic modulus

Figure 4.10 shows the results of the modulus of elasticity for each mixture. The modulus of elasticity is defined as the ratio between stress and reversible strain (elastic strain). The higher the elastic modulus, the harder the material is. Conversely, if the elastic modulus is low, the material will be ductile.

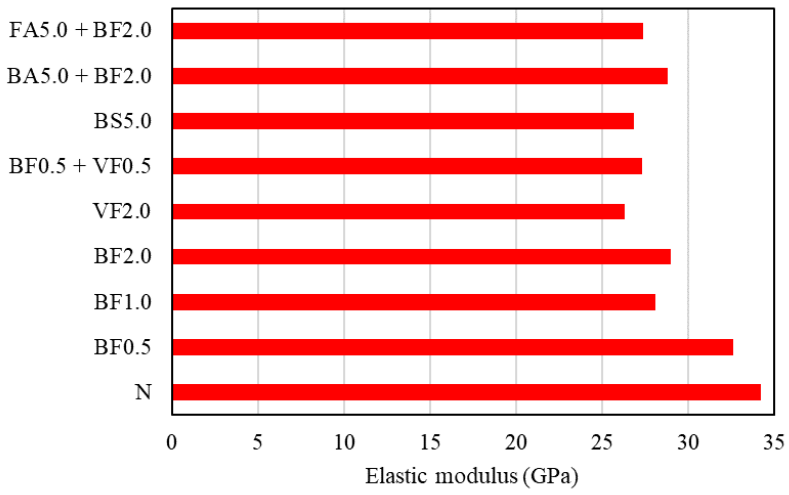

Figure 4.10 Elastic modulus of mortar after 28 days of curing

As shown in Figure 4.10, the modulus of elasticity of the mortar decreases with the addition of fiber. In general, in ordinary concrete with a compressive strength of 24-50 N/mm^2, the elastic modulus is in the range of 25-33 GPa[10]. Despite the transient decrease in the compressive strength, the addition of fiber is advantageous because of the gains in ductility compared to N.

4.3.4 Flexural strength test

The flexural strength test results after 7, 28, and 91 days are shown in Figure 4.11.

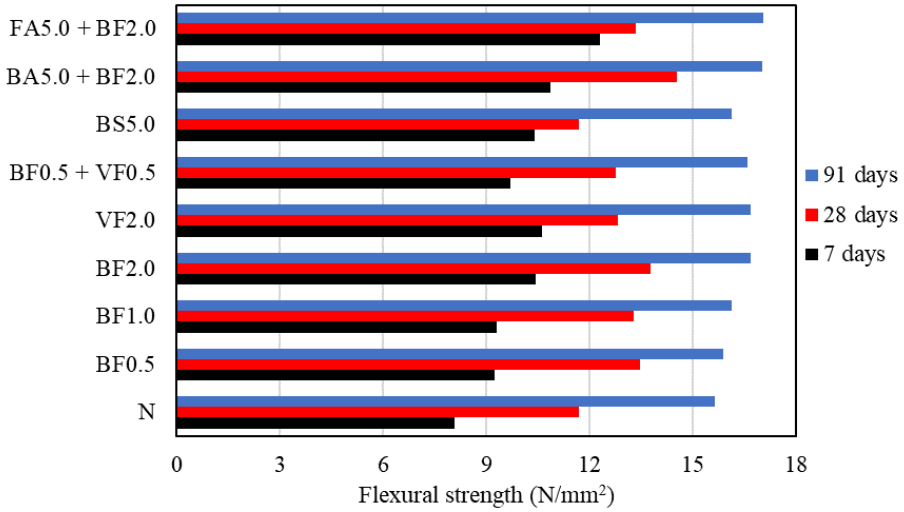

Figure 4.11 Flexural strength of mortar at 7, 28, and 91 days

According to Figure 4.11, the flexural strength of all-fiber mortar specimens exceeds the value of N. These high flexural strengths are caused by the fibers acting as a stress transfer bridge, which contributes to minimizing crack propagation, controlling their openings, and possibly delaying the breakage of the mortar. In other words, the fiber addition increases the flexural resistance, making the mortar more flexible against different stress conditions.

4.3.5 Split tensile strength test

Figure 4.12 summarizes the average splitting tensile strength results of the mortar after 7, 28, and 91 days of curing.

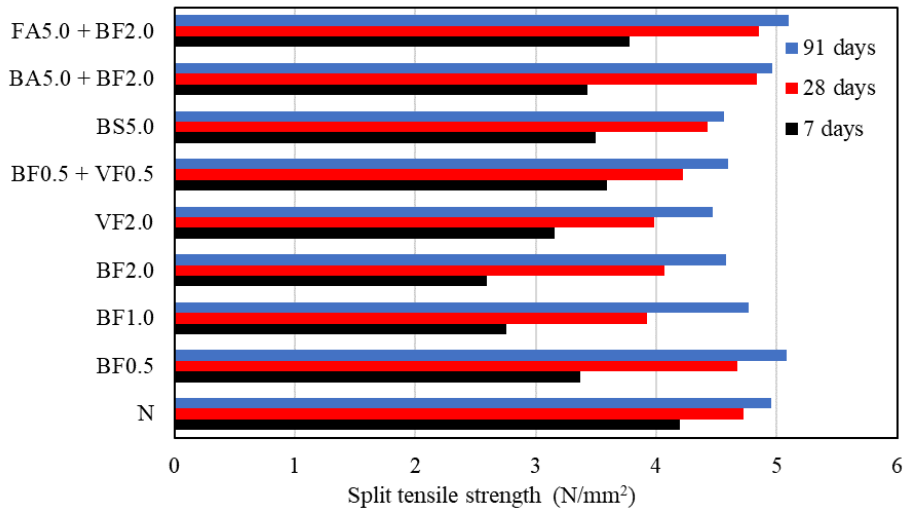

Figure 4.12 Split tensile strength of mortar at 7, 28, and 91 days

While the flexural strength tended to increase as the bagasse fiber content increased, the split tensile strength tended to decrease, as shown in Figure 4.12. In the flexural test case, the tensile stress in the bottom side is uniformly distributed in the constant flexural moment span. So, although the flexural cracking is localized at a particular cross-section, the effect of fiber bridging re-distributes the tensile stress to another cross-section. On the other hand, the tensile failure section is limited to the one in the splitting tensile test. However, as shown in Figure 4.12**,** after 91 days of curing, the difference in split tensile strength between N and the other cases is reduced due to decreased porosity. In the cases of FA5.0 + BF2.0 and BA5.0 + BF2.0, the split tensile strength exceeds that of N due to the pozzolanic reaction progress.

4.3.6 Shrinkage strain measurements

Figure 4.13 shows the shrinkage strain derived from the length change measurement due to the drying shrinkage.

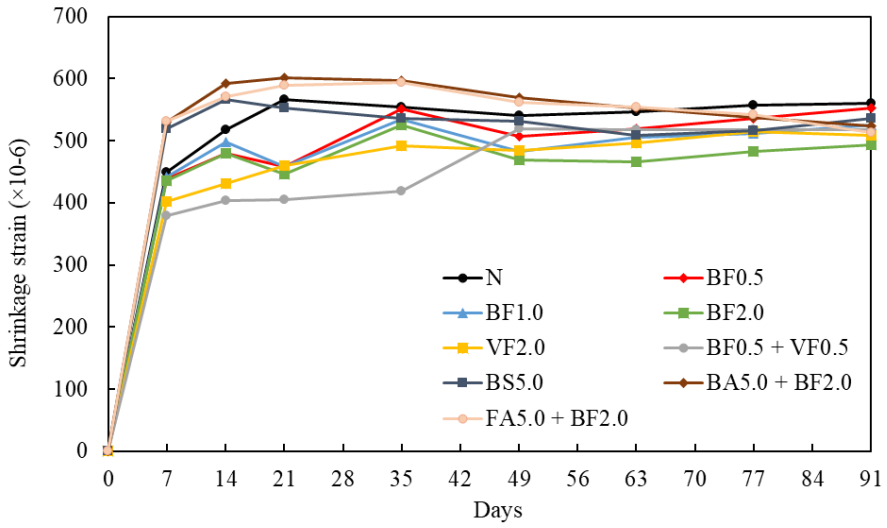

Figure 4.13 Shrinkage strain of mortar

According to Figure 4.13, regardless of the fiber type and the amount of the fiber mixed into the mortar, mortars containing fiber show a slight shrinkage strain when compared to N. In VF2.0, the drying shrinkage is smaller than that of the other cases. As explained before, the PVA fiber diameter is approximately three times smaller compared with that of bagasse fiber. Consequently, the number of fibers in VF2.0 was higher in comparison to other cases, which may have suppressed the progression of drying shrinkage. However, with the addition of bagasse fiber, the drying shrinkage strain can be reduced to approximately the same level as VF2.0. After 49 days, the drying shrinkage strain of BF2.0 becomes smaller than that of VF2.0. This may be attributed to the high amount of water retention in BF2.0, which may have suppressed the progression of drying shrinkage.

On the other hand, when the bagasse sand (BS5.0), bagasse ash (BA5.0 + BF2.0), and fly ash (FA5.0 + BF2.0) are added to the mortar, the drying shrinkage strain becomes higher than N at the early period. This is probably because bagasse ash and fly ash, which substituted the fine aggregate, increased the amount of binder compared to other mixtures, resulting in a high drying shrinkage strain due to the self-shrinkage. Additionally, it might be hard to suppress the shrinkage due to the reduction of the aggregate amount, which may provide resistance against the shrinkage.

4.3.7 Adhesion strength test

Figure 4.14 shows the mortar adhesion strength at 28 days of age. Notably, the specimens broke at the adhesive surface due to the cohesive failure of the adhesive.

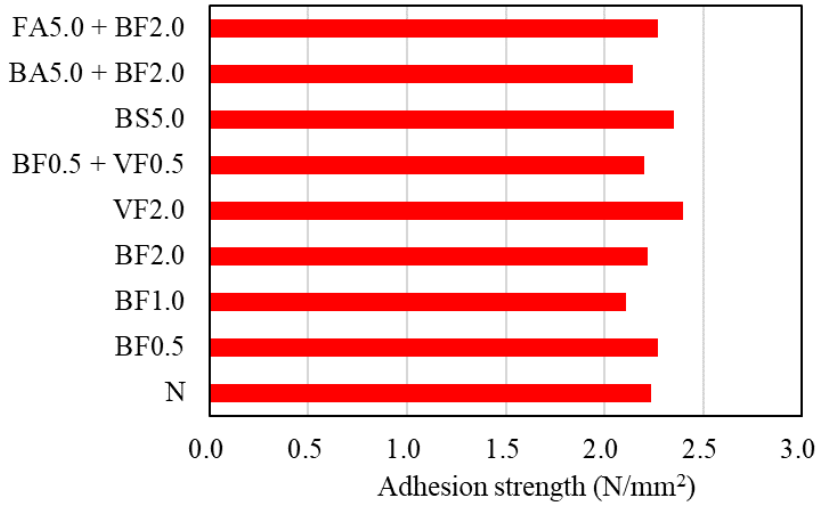

Figure 4.14 Adhesion strength of mortar after 28 days of curing

Although it is difficult to see a trend, according to Figure 4.14, the adhesion strength at the age of 28 days of all mortar mixtures is higher than the value of 2.0 N/mm^2, exceeding the adhesion strength standard of 1.5 N/mm^2[11].

4.4 Conclusion of chapter

This study revealed that the residues of sugarcane, even without special procedures, are viable to use as material in civil construction. The results obtained in this study can be summarized as follows:

1. The water retention ratio was higher when 2% of bagasse fiber was added compared to other cases due to the high percentage of fibers used, which can retain a high amount of water.
2. Despite a slight decrease in compressive strength, with the addition of fiber, the specimens' ductility increased compared to the control specimen. However, when 5% of fly ash with 2% of bagasse fiber and when 5% of bagasse ash with 2% of bagasse fiber were added, the compressive strength exceeded the control specimen's compressive strength after 91 days.
3. The flexural strength of all-fiber mortar specimens exceeded the control specimen's value after 7, 28, and 91 days of curing.
4. With the addition of bagasse fiber, the drying shrinkage strain could be reduced to approximately the same level as that of the mixtures added with 2% of PVA fibers. After 49 days, when 2% of bagasse fiber was added, the drying shrinkage strain becomes smaller than that of the mixtures added with 2% of PVA fibers.
5. The adhesion strength at 28 days of all mortar mixtures is higher than 2.0 N/mm^2. These values exceed the adhesion strength standard of 1.5 N/mm^2.

4.5 References

[1] Erik Schlangen, "Foreword," in *Eco-Efficient Repair and Rehabilitation of Concrete Infrastructures*, Woodhead Publishing, 2018, p. xvii.

[2] A.J. Boyd, J. Skalny, "Environmental deterioration of concrete," *Environmental Deterioration of Materials,* pp. 143-184, 2007.

[3] Daman K. Panesar, "3 - Supplementary cementing materials," in *Developments in the Formulation and Reinforcement of Concrete (Second Edition)*, Woodhead Publishing, 2019, pp. 55-85.

[4] Angst, UM, "Challenges and opportunities in corrosion of steel in concrete," *Materials and Structures,* vol. 51, no. 4, 2018.

[5] A. Turatsinze, J.-L. Granju, S. Bonnet, "Positive synergy between steel-fibers and rubber aggregates: Effect on the resistance of cement-based mortars to shrinkage cracking," *Cement and Concrete Research,* vol. 36, no. 9, pp. 1692-1697, 2006.

[6] Fernando Pelisser, Almir Barros da S. Santos Neto, Henriette Lebre La Rovere, Roberto Caldas de Andrade Pinto, "Effect of the addition of synthetic fibers to concrete thin slabs on plastic shrinkage cracking," *Construction and Building Materials,* vol. 24, no. 11, pp. 2171-2176, 2010.

[7] Zhang Pan, Xiaohui Zeng and Zhongwei Hu, "Effect of Fly Ash and Silica Fume on Mechanical Properties of High-Performance FRCC," *Materials Science and Engineering,* vol. 562, 2019.

[8] Vanathi, M. and T.S. Thandavamoorthy, "Potential Utilization of BAGASSE Ash Steel Fiber Reinforced Concrete-An Experimental Study," *Australian Journal of Basic and Applied Sciences,* vol. 8, no. 6, pp. 239-244, 2014.

[9] P. Sargent, "21 - The development of alkali-activated mixtures for soil stabilisation," in *Handbook of Alkali-Activated Cements, Mortars and Concretes*, Woodhead Publishing, 2015, pp. 555-604.

[10] Japan Society of Civil Engineers, Standard Specifications for Concrete Structures - 2017, Design, Japan Society of Civil Engineers, 2017.

[11] NEXCO (Nippon Expressway Company), Structure Construction Management Guidelines, 2019.

5 A STUDY ON THE REDUCTION IN HYDRATION HEAT AND THERMAL STRAIN OF CONCRETE WITH ADDITION OF SUGARCANE BAGASSE FIBER

5.1 Introduction

As mentioned in 2.2.1, hard measures to prevent or mitigate natural disasters have disadvantages like the impact of the load on the environment that hard structures cause and the structures' high cost. Also, the increased consumption of aggregates to make concrete, which is about 70% of the volume[1], is another concern since the mining of these aggregates causes the destruction of the environment's landscape and releases a considerable amount of CO_2.

Some structures to prevent or mitigate natural disasters are massive concrete structures like dams, pavements, and piers. In those structures, the reaction between water and cement produces heat and increases the concrete's temperature[2]. It occurs primarily at its internal part, where high temperatures are reached. This process is referred to as cement hydration, and it requires some unique methods to control the temperature. High temperatures may cause thermal stress, and reducing the heat generated during cement hydration prevents the development of cracks in the concrete at the early stage of use.

Several researchers have tried to reduce hydration heat by replacing a certain amount of cement with pozzolanic materials, such as silica fume, fly ash, and oil palm fuel ash. Their results show that when a certain amount of these materials is used in place of cement, it is possible to decrease the concrete's temperature.

Nili et al. investigated the effects of supplementary cementitious materials on the temperature rising profile, heat evolution, and early-age strength development of medium- and high-strength concrete. A total of 13 different mixtures were prepared, with two different water-cement ratios (0.3 and 0.46). Natural pozzolan, fly ash, and silica fume was included in the specimens. The results showed that natural pozzolan, mainly fly ash, decreased the amplitude of peak temperature, delay the peak occurrence, and decreased the sharpness of the temperature rising profiles. In contrast, the temperature profile of silica fume specimens was similar to those without silica fume. It was found that the best mixture, the highest early-age strength and the lowest heat liberation corresponded to the specimen containing fly ash at 15% (by cement weight). This result justifies fly ash's advantage effect, which can develop sufficient tensile strength to resist thermal cracking potential in massive high-strength concrete[3].

Awal et al. investigated the performance behavior of palm oil fuel ash (POFA) in reducing the heat of hydration of concrete. Two concrete mixes, namely OPC concrete (concrete with 100% ordinary Portland (OPC) cement as control) and POFA concrete (concrete with 30% POFA and 70% OPC were prepared), and the temperature rise due to hydration heat in both the mixes was recorded. It has been found that palm oil fuel ash reduced the total temperature rise and delayed the time at which the peak temperature occurred. The results obtained clearly demonstrate that the partial replacement of cement by palm oil fuel ash is advantageous, particularly for mass concrete, where thermal cracking due to excessive heat rise is of great concern[4].

Several countermeasures can improve crack resistance and decrease the effect of the strain shrinkage of concrete. The utilization of fibers is one of these countermeasures.

Sarabi et al. used the waste turnery steel fibers in massive concrete to control the generated cement hydration heat and consequently the potential of cracking due to the thermal stress expansion. The amount of used cement was reduced without changing the compressive strength. By substituting a part of the cement with waste steel fibers, the costs and the generated hydration heat were reduced, and the tensile strength was increased. The results showed that by using 0.5% turnery waste steel fibers and consequently decreasing to 32% the cement content, the hydration heat reduced to 23.4% without changing the compressive strength. Moreover, the maximum heat gradient reduced from 18.5% in the plain concrete sample to 12% in the fiber reinforced concrete sample[5].

Mezencevova et al. examined the efficiency of thermomechanical pulp (TMP) fibers, both untreated and after chemical treatment, to produce holocellulose and α-cellulose for internal curing. Also, they investigated the effect of TMP fibers on early hydration behavior. The results show that TMP and α-cellulose fibers had a negligible impact on cement hydration. Holocellulose, conversely, significantly reduced the rate of hydration, noticeably delaying setting time. The fibers' addition in dosages to provide an additional amount of entrained water of 0.05 g per gram of cement resulted in a decrease of early autogenous shrinkage of cement paste. Holocellulose reduced autogenous shrinkage of cement paste by 93%, being the most effective for internal curing. However, its adverse effect on cement hydration may require acceleratory admixtures when used in concrete. Thermomechanical pulp and α-cellulose showed a similar efficiency in mitigating autogenous shrinkage: these fibers reduced cement paste shrinkage by approximately 51 and 45%, respectively[6].

Ataie investigated the impact of the addition of rice straw fibers (RSF) on the compressive and flexural strengths of concrete, drying shrinkage, and the heat of cement hydration. RSF was saturated

before being added to concrete. The addition of RSF in concrete reduced concrete strength, increased concrete drying shrinkage, and increased the induction period of cement hydration. It was suggested that water squeezed out of RSF during mixing and sample consolidation increased effective water-to-cement ratios (w/c) and reduced concrete strength, and increased the concrete drying shrinkage. The rise in retardation time was attributed to the leaching of organic and inorganic compounds out of RSF into the pore solution. It was shown that samples containing washed RSF did not have noticeable improvement in compressive strength over samples containing unwashed (as received) RSF. However, samples containing washed RSF had lower drying shrinkage and a shorter induction period than those containing unwashed RSF[7].

However, the combination of both pozzolanic materials and bagasse fibers to decrease the heat of hydration and control the cracking generation due to the thermal stress expansion in massive concrete structures with fibers remains unclear. In the present research, sugarcane residues were used in massive concrete to investigate the behavior of cement hydration heat and, consequently, to evaluate the potential resistance these residues materials have against the generation of cracks.

5.2 Research design and methodology

5.2.1 Flow chart of the experimental approach

This section explains the experimental design and the methodologies to obtain the mechanical properties of concrete added with sugarcane residues materials. Also, specimens of 300 × 300 × 300 mm were used to investigate the temperature and strain due to the thermal expansion. Figure 5.1 shows the overall flow of this research.

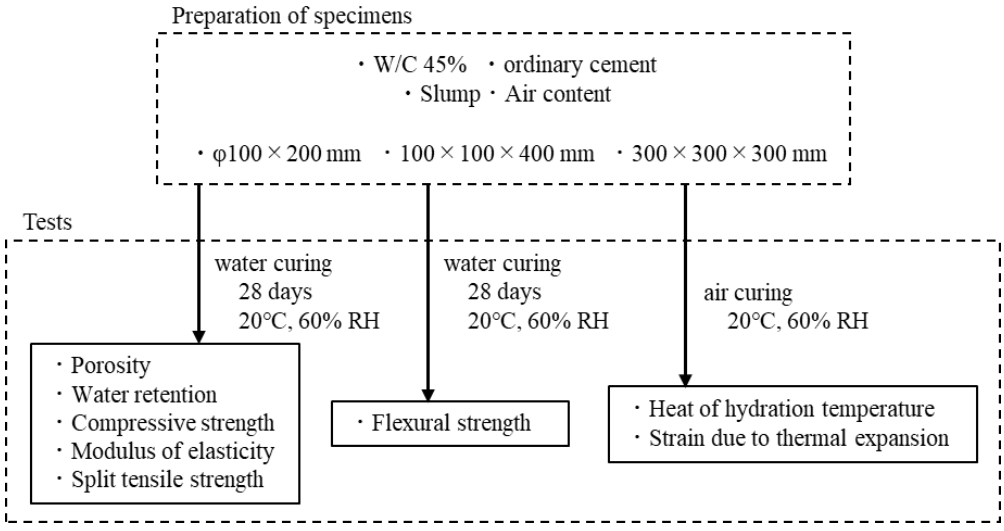

Figure 5.1 Overall flow of this research

5.2.2 Materials

The specimens were made using ordinary Portland cement (C). The fine aggregates (S) and the coarse aggregates (G) were acquired from manufacturer Nishijima, Hyogo, Japan. In order to perform the comparisons, commercially available fly ash (FA) grade II was used. The physical properties of those materials are given in Table 5.1.

Table 5.1 Physical properties of cement and aggregates

Properties	Materials				
	C	S	G	BA	FA
Density (g/cm^3)	3.16	2.57	2.57	2.1	2.24
Total alkali content (%)	0.56	—	—	—	—
Specific surface area (cm^2/g)	3280	—	—	—	3420
Loss of ignition	—	—	—	—	2.2

For the concrete mixture, two kinds of admixtures were used in this study to satisfy the fresh concrete requirements. The properties of the water-reducing agent (WRA) and air-entraining agent (AEA) are shown in Table 5.2; the bagasse fibers' characteristics are shown in Table 5.3.

Table 5.2 Properties of admixtures

Admixtures	Main components	Color	Density (20°C, g/cm^3)	Total alkali content (%)	Cl^- content (%)
WRA (No.70)	Complexes of lignin sulfonic acid compound and polyol	Dark brown	1.23-1.27	1	0.03
AEA (303A)	Alkyl ether type anionic surfactant	Light yellow	1.02-1.06	1.1	0.01

Table 5.3 Characteristics of the fibers

	BF
Density (g/cm^3)	0.71
Length (mm)	17.9 (average)
Diameter (mm)	0.56 (average)
Aspect Ratio	32
Tensile strength (N/mm^2)	132

5.2.3 Concrete mixture

The mix proportions of the concrete are shown in Table 5.4. Mixture C was prepared in the laboratory, with a water to binder ratio (W/C) of 45%. Mixture C represents the control specimens and contains no sugarcane residue materials. In the case of BF specimens, two mixtures were prepared with bagasse fiber volume ratios of 2.0% (BF2) and 5.0% (BF5) in comparison to the total mixture volume. Besides, specimens were made using bagasse ash (BA) and fly ash (FA). In these cases, the volume ratio of the bagasse ash and fly ash was 5.0% compared to the total volume of sand. In BA and FA cases, the specimens were prepared with the same volume of fibers as BF2, and the bagasse ash and fly ash acted as a binder. Thus, the W/B becomes 43 and 41%, respectively. In all cases, the fibers were replaced by sand. The maximum size of the coarse aggregate (G_{max}) was 15 mm.

Table 5.4 Mix proportions of the concrete specimens

Composites	Fiber	W/B	Unit (kg/m^3)								
	(Vol. %)	(%)	C	W	S	G	BA	FA	BF	WRA	AEA
C	—	45	389	175	876	950	—	—	—	1.17	0.0125
BF2	2				824		—	—	14		
BF5	5				746		—	—	36		
BA	2	43			780		22	—	14		
FA	2	41					—	39			

5.2.4 Preparation of Concrete Specimens and the Tests Applied

The outline of specimens is shown in Figure 5.2. For each concrete mixture, specimens of φ100 mm × 200 mm were cast in order to determine the compressive strength (JIS A 1108), elasticity modulus (JIS A 1149), split tensile strength (JIS A 1113), porosity rate, and water retention rate of concrete. Furthermore, specimens of 100 × 100 × 400 mm were prepared to determine the flexural strength (JIS A 1106). Three samples were used for each test.

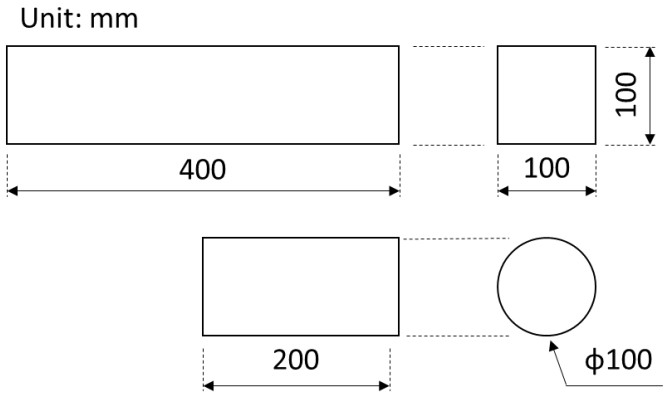

Figure 5.2 Outline of concrete specimen

The porosity rate test was based on the mass of the specimen. First, the specimens were completely dried in a drying furnace at 105 °C for 24 hours. Afterward, the specimens were stored in a room at 20 °C and relative humidity of 60% until the sample's temperature decreased and became equal to the ambient temperature. The mass of the specimen was weighed. Subsequently, the specimens were immersed in water at 20 °C for 48 hours, and the surface-dried mass of the specimen was weighed. The following equation determined the porosity rate:

$$\boldsymbol{\varepsilon = \frac{W_s - W_d}{\rho \times V} \times 100}$$

Where:

ε: porosity rate (%);

W_d: mass of absolutely dried specimen (g);

W_s: mass of surface-dried specimen (g);

ρ: density of water (g/cm^3); and

V: volume of specimen (cm^3).

After the porosity rate test, the moistened specimens were placed in a room at 20°C and relative humidity of 60%, and the mass change of specimen was recorded every 24 hours for 7 days. This mass change was determined as water retention rate.

Besides, to simulate a massive concrete structure, two specimens of 300 × 300 × 300 mm of each concrete mixture were prepared. The concrete's temperature and strain were measured by two thermocouples (T-G-0.65) and two mold strain gauges (PMFL-60) embedded in concrete, respectively. The thermocouples and the gauges were settled at the surface (cover thickness of 20 ± 2 mm) and the center (cover thickness of 145 ± 2 mm), as shown in Figure 5.3.

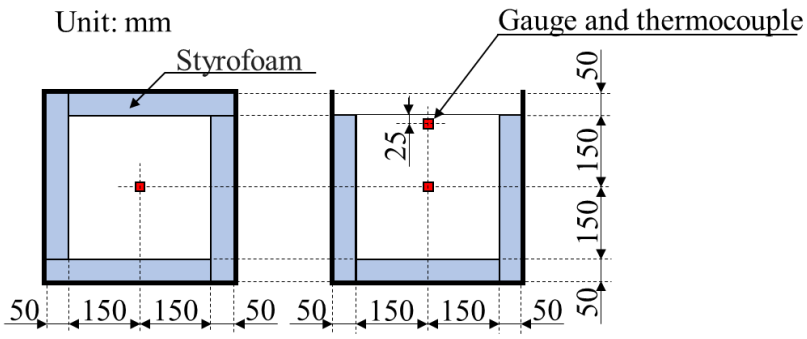

Figure 5.3 Outline of massive concrete specimen

All the concrete mixtures were mixed using a laboratory pan-type mixer. First, the coarse aggregate, cement/ashes, and fine aggregate were put in the mixer and mixed for 30 seconds. Next, the water/fibers were placed in the mixer and mixed for an additional 120 seconds. Before casting, the slump flow and the air content were conducted on the concrete mixture to determine its workability.

After the casting, all specimens were cured in the laboratory at 20°C for 24 hours. The samples were then de-molded and cured underwater at 20°C for 28 days. However, the massive concrete specimens were not de-molded and were instead cured in the air at a room temperature of 20°C and 60% RH for 28 days. During the curing period, the temperature and the strain due to the thermal expansion of concrete were measured using thermocouples and gauges, as shown in Figure 5.3.

5.3 Results and discussions

5.3.1 Fresh properties

The slump test and air content test results are shown in Figure 5.4 and Figure 5.5, respectively.

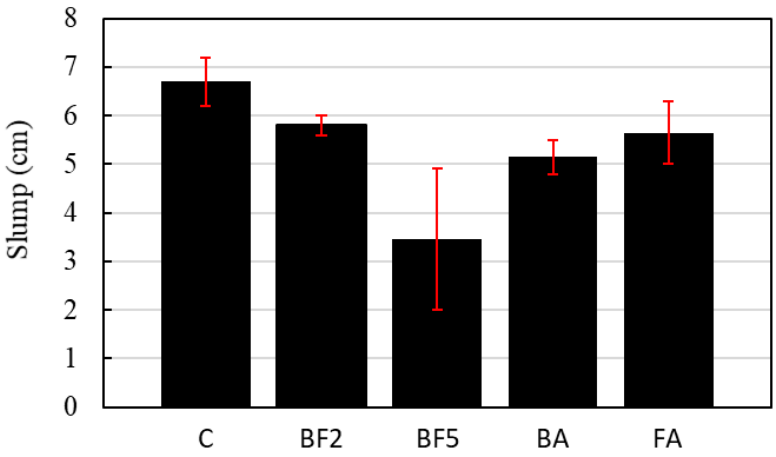

Figure 5.4 Slump test results

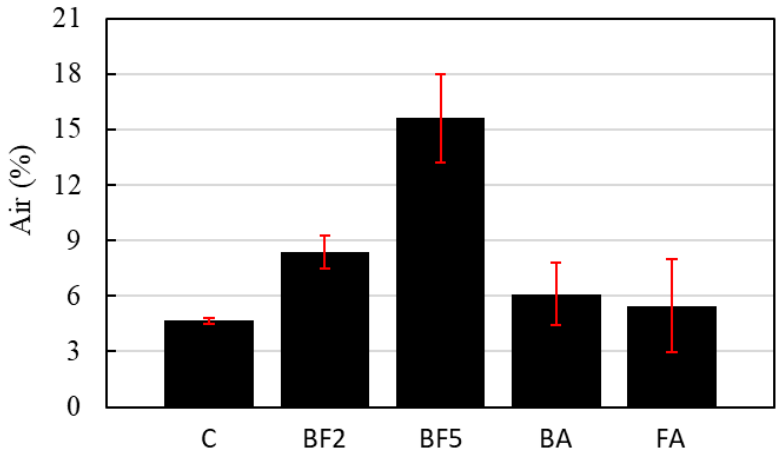

Figure 5.5 Air content test results

As shown in Figure 5.4, the slump of concrete decreased with the addition of the bagasse fiber. The control concrete slump is 6.7 cm, while in the cases of BF2, BA, and FA, the fraction volume of the fiber was 2%, the slump was reduced to 5.8, 5.2, and 5.7 cm, respectively. In the case of BF5, where 5% of the volume was bagasse fiber, the slump decreased to 3.5 cm. This decrease is because of the formation of a bridge network of fibers that restrained the fresh concrete's deformation during the test. As a result, the more bagasse fiber is added to the concrete mix, the greater the fiber network is, which decreases the concrete workability. Another factor contributing to this decrease is that a certain amount of water may have been absorbed by the bagasse fiber during the mixture due to the hydrophily of bagasse fiber[8, 9]. In the cases of BA and FA, with the addition of ashes and the increase in the binder amount, the viscosity of concrete increased, resulting in a brief decrease in the slump compared to BF2.

Figure 5.5 shows that the air content in the concrete without fibers is about 4.7%. However, the air percentage increases as the amount of mixed fibers increases. For the cases of BF2, BF5, BA, and FA, the air content values obtained were 8.4, 15.6, 6.1, and 5.5%, respectively. The rise in the air content with the addition of bagasse fiber can be explained due to fine bubbles of air clumping together while the concrete mixes; consequently, the amount of empty space may increase.

Figure 5.5 further reveals that the air content of BA and FA cases, which contain 5% of pozzolanic materials, is lower than that of BF2. These results are a consequence of the filler effect: due to the replacement of sand with ashes, the ashes occupy the micro and macro empty spaces created during the mixing.

5.3.2 Heat of hydration

The plot of temperature versus time for the different mixtures and the ambient temperature can be seen in Figure 5.6.

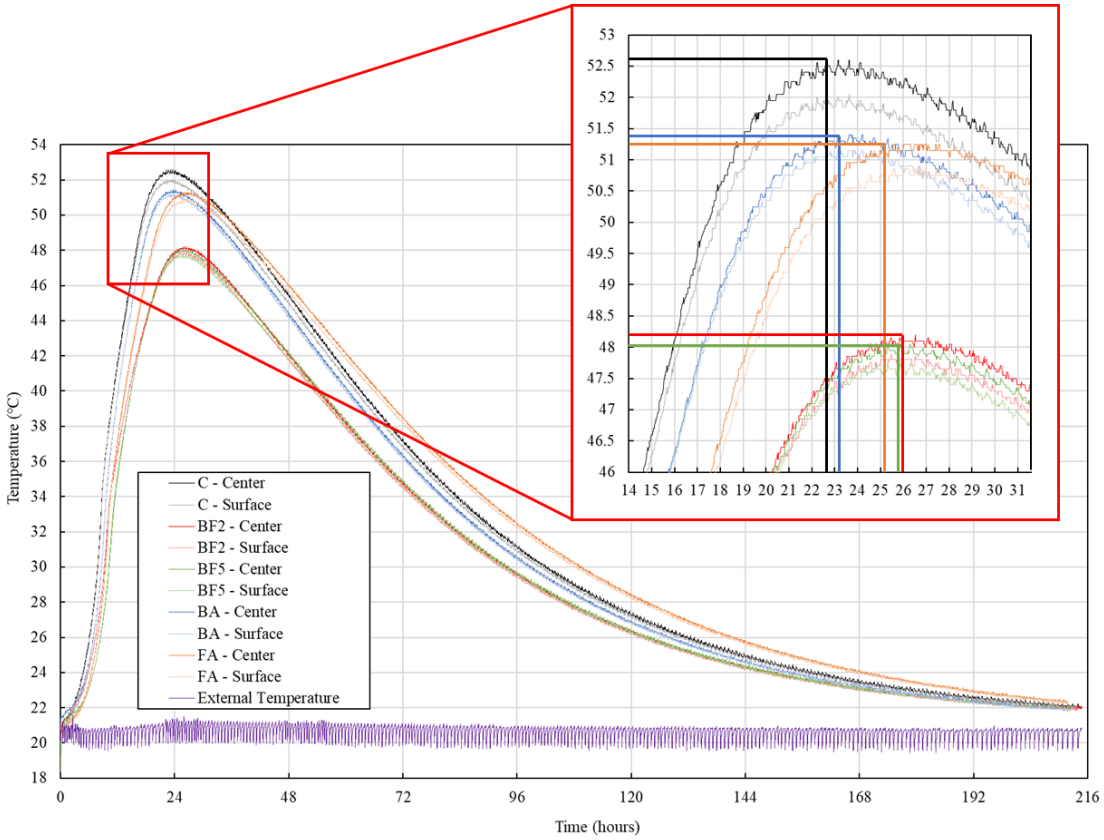

Figure 5.6 Heat of hydration of cement

As Figure 5.6 illustrates, the peak of hydration heat in the center of the specimens in the control mixture was nearly 52.5°C; the highest temperature reached in this study. In the cases of BF2, BF5, BA, and FA, this value decreases to around 48.3, 48.0, 51.4, and 51.3°C, respectively. It can be concluded from Figure 5.6 that the hydration heat of all mixture added with bagasse fiber was reduced. These findings are consistent with previous studies, which indicate that the composites (cement paste) made with components of bagasse exhibit setting temperatures that are lower than the reference[10]. According to Bilba et al. [10] and Fisher et al. [11], two phenomena can explain this temperature decrease: the exothermic reaction between water and cement and the endothermic reactions between water and components of bagasse fiber.

In BF2 and BF5, the difference in the peak temperature of the heat of hydration was around 0.3°C. As the amount of fibers increases in BF5, a high number of empty spaces between the fiber and the matrix are created, reducing the thermal conductivity. Therefore, the hydration heat absorption by

the surrounded fiber components becomes difficult, resulting in the same temperature as BF2.

Where the bagasse ash and the fly ash were added into the mixture to replace the sand, the temperature was approximately 1°C lower than C; however, the temperature was about 3°C higher than for those mixtures where bagasse fibers were added. This increase in temperature in the cases of BA and FA, compared to BF2 and BF5, is due to the difference in the water to binder ratio. As shown in Table 5.4, the W/B of BA and FA is 43% and 41%, respectively, or 2 or 4% smaller than the other cases.

Furthermore, from Figure 5.6, it can be observed that, in the mixtures with the bagasse fiber, the peak temperature is reached later than C, around 22:30 hours after the placement. For BF2, BF5, BA, and FA, the temperature peak was achieved, respectively, 26:00, 27:00, 24:10, and 25:10 hours after the concrete placement. The probable explanation is that the presence of some water-soluble sugars may have retarded the setting of concrete[10]. In order to verify the presence of sugar, 4 g of bagasse fiber (BF) was cut, and 40 ml of H_2O was added. Subsequently, it was allowed to rest for about 2 hours. Later, this mixture was centrifuged at 8000 rpm at 20°C for 30 min. Then, 10 ml supernatant was lyophilized and dissolved in 1 ml of acetonitrile/water (CH_3CN/H_2O=75/25). This solution was used as a sample to analyze the reducing sugar. Afterward, 0.2 ml of sample, 0.4 ml of reagent A ($NaCO_3$ (40g/L), Glycine (16g/L), $CuSO_4 \cdot 5H_2O$ (0.45g/L)) and 0.4 ml of reagent B (neocuproine hydrochloride (0.15g/100ml)) were mixed. The mixture was heated at 100°C for 12 minutes and rapidly cooled. 1 ml of H_2O was added, and the absorbance at 450 nm was measured. From the calibration curve prepared with glucose, the reducing sugar content of the sample was determined as a glucose equivalent. The result indicates that the reducing sugar content was 1.05 mg/g, confirming the presence of water-soluble sugars that affected the hardening and hydration of cement. These soluble sugars may form a protective layer around the hydrating cement[12], preventing water from percolating to hydrate further the cement grain[13, 14]. As a consequence, the heat of hydration was reduced, and the setting of concrete was retarded.

Moreover, Figure 5.6 reveals a difference between the internal and surficial temperature. The peaks of the surface (cover 2 cm) temperature for C, BF2, BF5, BA, and FA were approximately 52.0, 47.9, 47.8, 51.2, and 50.8°C, respectively. In the case of C without the sugarcane bagasse fiber, the surface and center temperature difference achieves a value of about 0.5°C. In the other mixtures with the bagasse fiber, this value varies between 0.2 and 0.3°C. Usually, the difference between the internal and surficial temperature is notably higher because the concrete surface is influenced by the ambient temperature[15, 16, 17]. However, the difference between internal and surficial temperature obtained in this research was not higher due to the styrofoam as thermal insulation, completely isolating the

concrete from the outside temperature influence.

5.3.3 Relationship between the heat of hydration and strain

The relationship between the heat of hydration and each mixture's strain is shown in Figure 5.7, Figure 5.8, Figure 5.9, Figure 5.10, and Figure 5.11. The strain of each mixture is then compared in Figure 5.12.

Figure 5.7, Figure 5.8, Figure 5.9, Figure 5.10, and Figure 5.11 show that, after the concrete placement, the strain gauges are pressed initially, resulting in decreasing the strain. Subsequently, the concrete expands due to the increase in temperature due to hydration heat.

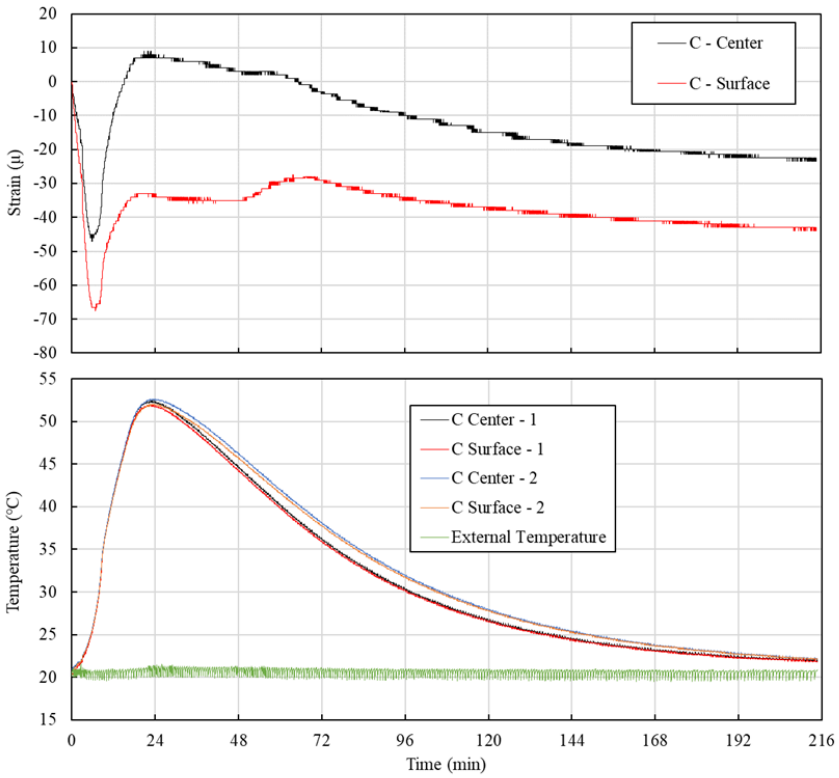

Figure 5.7 Relationship between the heat of hydration and strain of C

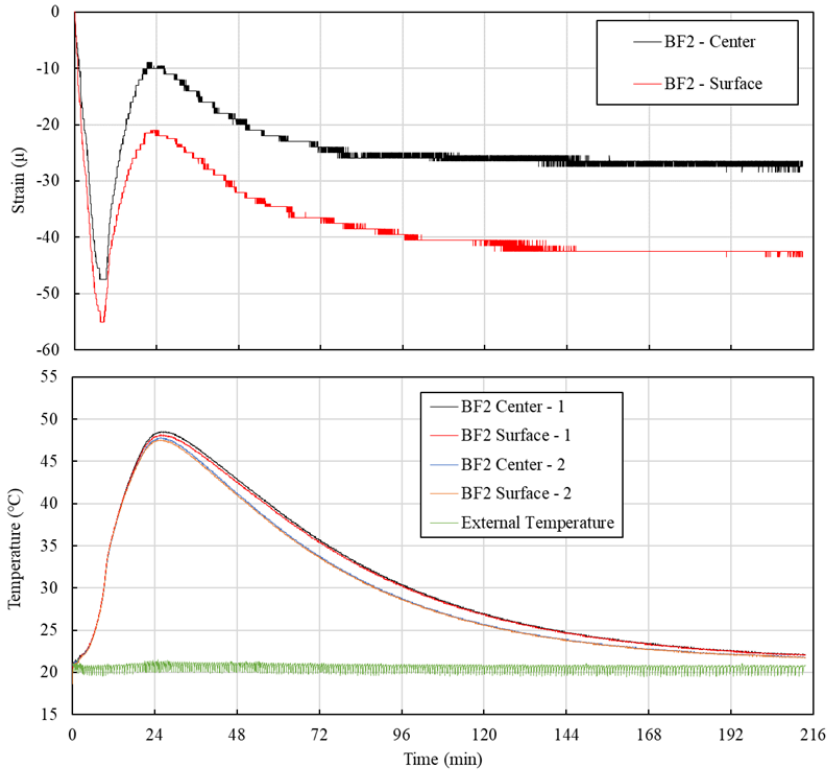

Figure 5.8 Relationship between the heat of hydration and strain of BF2

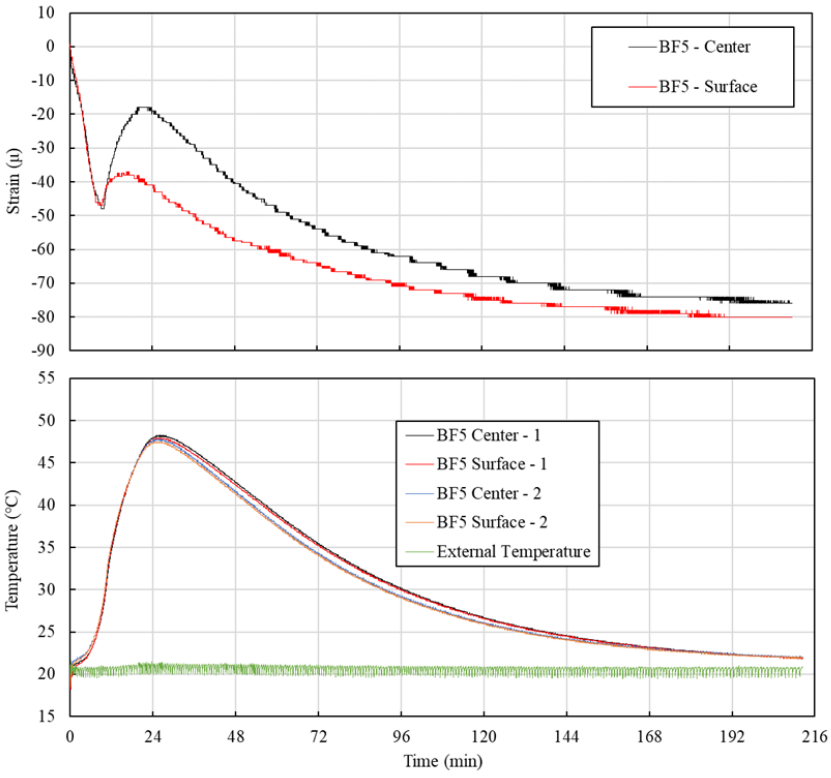

Figure 5.9 Relationship between the heat of hydration and strain of BF5

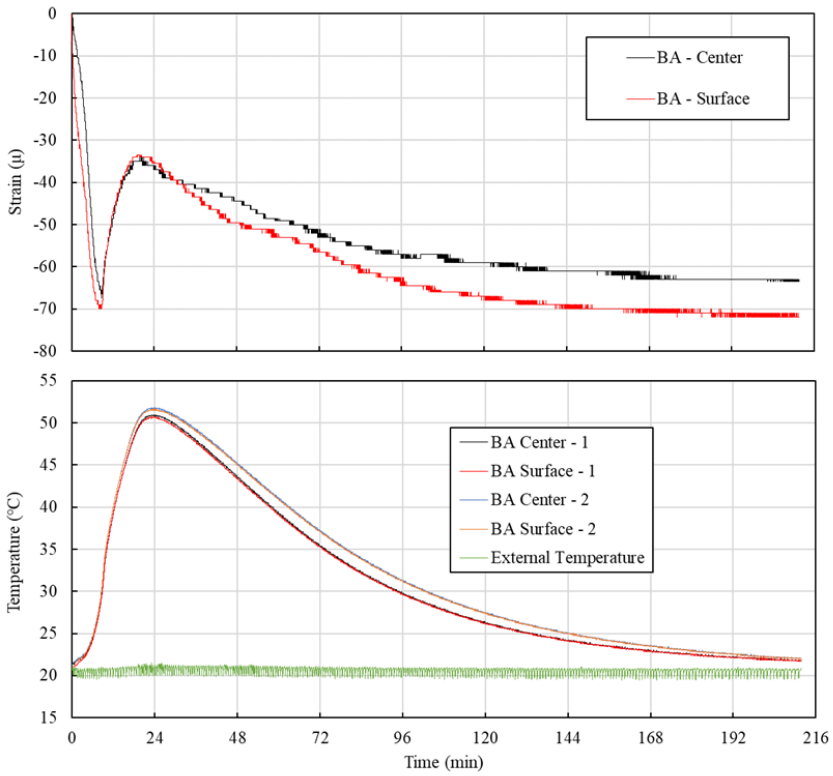

Figure 5.10 Relationship between the heat of hydration and strain of BA

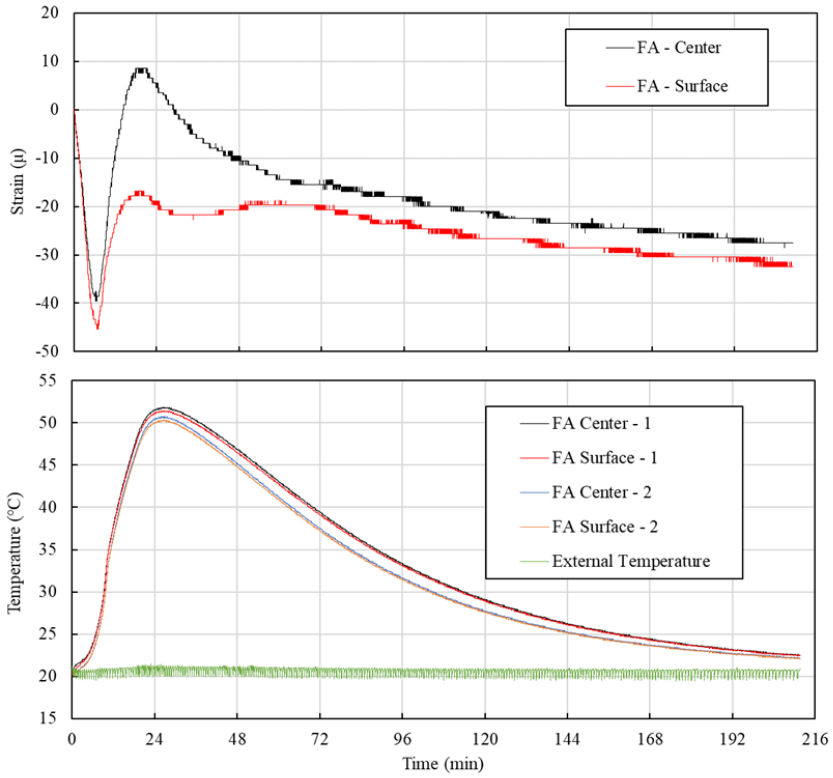

Figure 5.11 Relationship between the heat of hydration and strain of FA

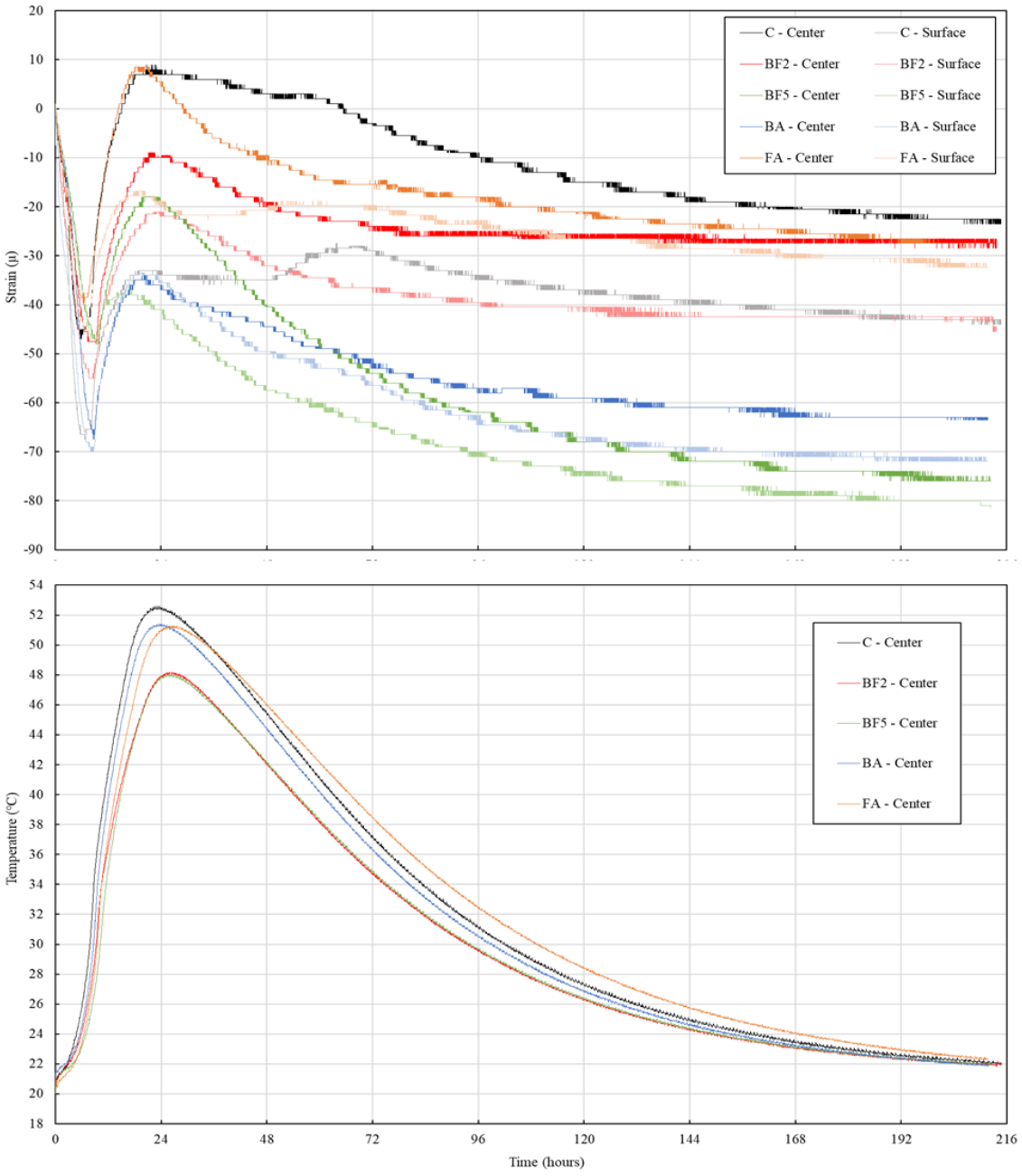

Figure 5.12 Comparison of the strain of each mixture

The strain due to the thermal expansion of each mixture is shown in Figure 5.13. Note that the initial strain value was set right after the thermal expansion began. As Figure 5.13 shows, in C, the strain rose to a value of approximately 55 μ, while in the cases of BF2, BF5, BA, and FA, the strain achieved 39, 30, 44, and 48 μ, respectively. When bagasse fiber is added to the mixture, there is a tendency to decrease the concrete's strain. As well as the increase in the concrete temperature, which can influence the strain, the fibers may have reduced the expansion due to the transference of stress among the network of bagasse fiber bridges to other cross-sections.

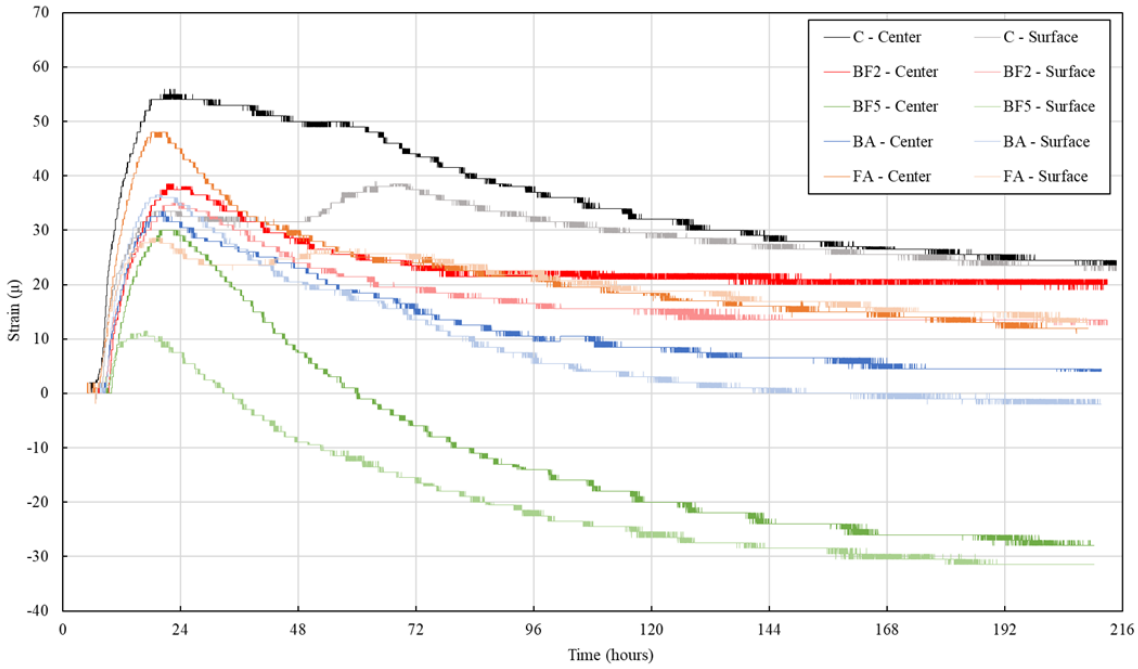

Figure 5.13 Thermal expansion

Furthermore, Figure 5.13 shows that the specimen surface strain is lower than the strain in the center. This is because the strain gauge used in this study measured only the horizontal direction (see Figure 5.3). Also, just one gauge in the center and one on the surface (cover 25 mm) were used. Therefore, the measurement of the strain in other directions was not able to be measured. Although the surface and center temperatures are almost the same, the vertical strain may have been more affected than the horizontal strain on the concrete's surface. However, supplementary studies should be done to measure the strain in different directions to clarify this point.

5.3.4 Porosity rate and the water retention rate

Figure 5.14 shows the porosity rate test results.

As shown in Figure 5.14, the porosity rate increased as the replacement rate of bagasse fiber increased. This is because a higher amount of entrapped air in the mixture with bagasse fibers is created during the mixing than in that without bagasse fibers.

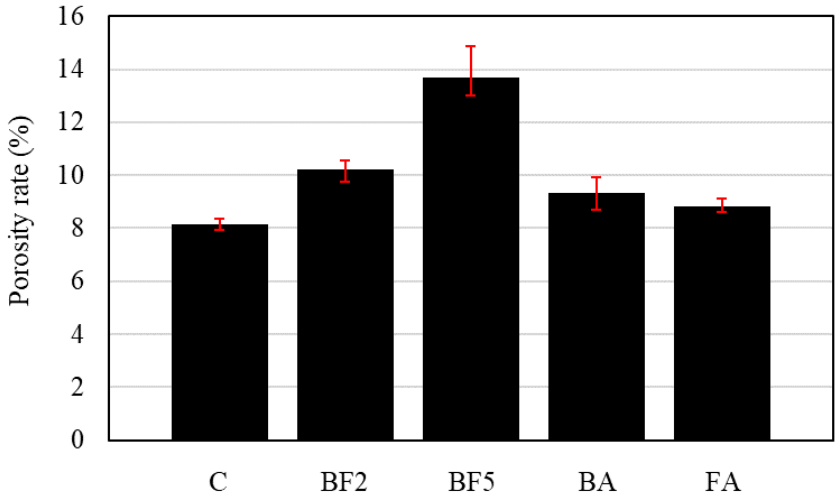

Figure 5.14 Porosity rate of each concrete mixture

However, in BA and FA, where the ash was added, the concrete's porosity rate decreases compared to BF2, which contains the same fiber volume. Although the solid content per cubic meter of BA and FA is higher than the solid content of BF2, this decrease may be related to the ash's filler effect. When adding ashes to concrete mixtures, the ashes act to filling the voids and reduce the number of pores and probable microcracks of the concrete during pozzolanic reactions.

The water retention rate of each concrete mixture is shown in Figure 5.15.

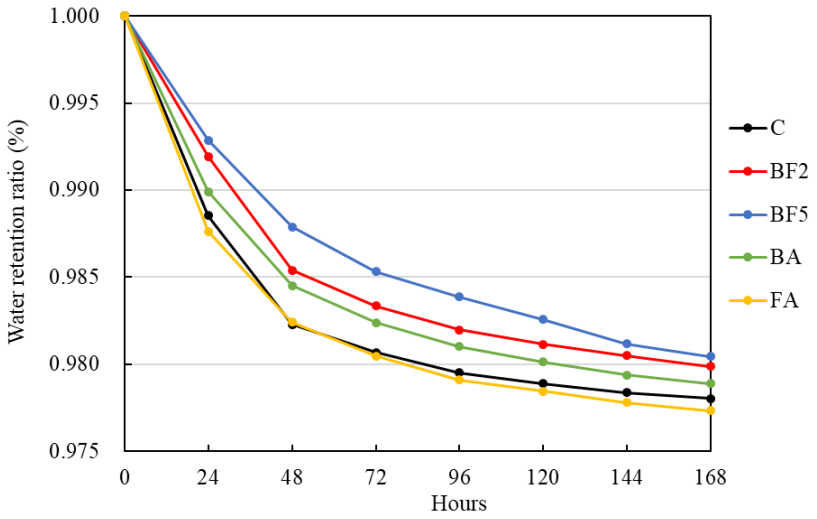

Figure 5.15 Water retention rate of each mixture

As shown in Figure 5.15, the water retention ratio of mixtures in which fibers were added increased compared to the control mixture. It is also possible to see that the higher the amount

of fiber added, the higher the water retention in the specimen is. The high retention of water in BF5 is due to the high percentage of fibers used and bagasse fiber characteristics, which have a high capacity to absorb and retain water.

However, after 120 hours, the water retention of BF5 decreases nearly to BF2 values. The natural fibers are very hydrophilic[8, 9]. For this reason, the wetness of the whole specimen tends to be balanced. The water may be transferred from the center of the specimen to the surface since the specimen's surface is more affected by natural drying.

When 5% of ashes were added, the water retention ratio is smaller than BF2, even though they contain 2% of fibers added in the mixture. In particular, in the case of FA, the water retention was smaller than the control mixture. This reduction may be related to the ashes' pozzolanic reaction, in which the reaction consumes the water.

5.3.5 Compressive strength

Figure 5.16 illustrates the compressive strength of each concrete mixture. From Figure 5.16, it is possible to see that, with the addition of 2% of bagasse fiber, the compressive strength briefly decreases, probably due to the increase in the porosity of the concrete. In the case of BF5, which resulted in a higher porosity, the compressive strength decreases by about 16% compared to C. Since the entrapped air tends to increase during the mixing and decrease the compressive strength, the use of proper vibration techniques can help remove entrapped air.

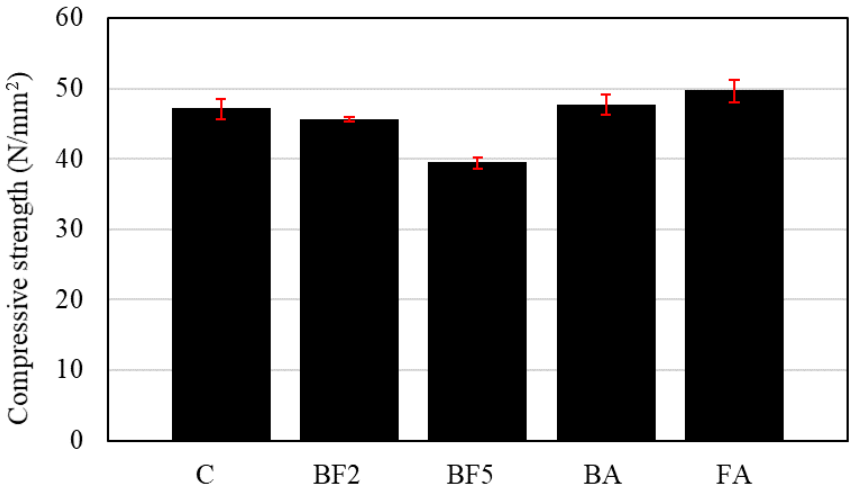

Figure 5.16 Compressive strength of each concrete mixture

On the other hand, Figure 5.16 demonstrates that the compressive strength increased in BA and

FA, where the ashes were added into the mixtures. Usually, the low reactivity and slow reaction rate of fly ash at ambient temperatures lead to the low strength of the concrete at an early age[18, 19, 20]. However, the increase in BA and FA's compressive strength is because when the ashes are added into the mixture, the amount of powder used increases the binder amount, as shown in Table 5.4. Another probable reason may be due to the alkali activation, which effectively accelerates the pozzolanic reaction of ash[20]. Since the fibers were treated with a solution of 5% $Ca(OH)_2$ for 24 h, the fibers' internal alkali solution may have been activated on the surface of the ash particles at an early age, accelerating the pozzolanic reaction during the water immersion curing period.

5.3.6 Modulus of elasticity

Figure 5.17 shows the elasticity modulus of the concrete. As illustrated in Figure 5.17, the moduli of elasticity for C, BF2, BF5, BA, and FA were 35.0, 31.8, 28.3, 32.1, and 33.9 GPa, respectively. From these results, it is possible to conclude that the modulus of elasticity of the concrete decreases with the addition of fiber, which gains ductility in comparison to C.

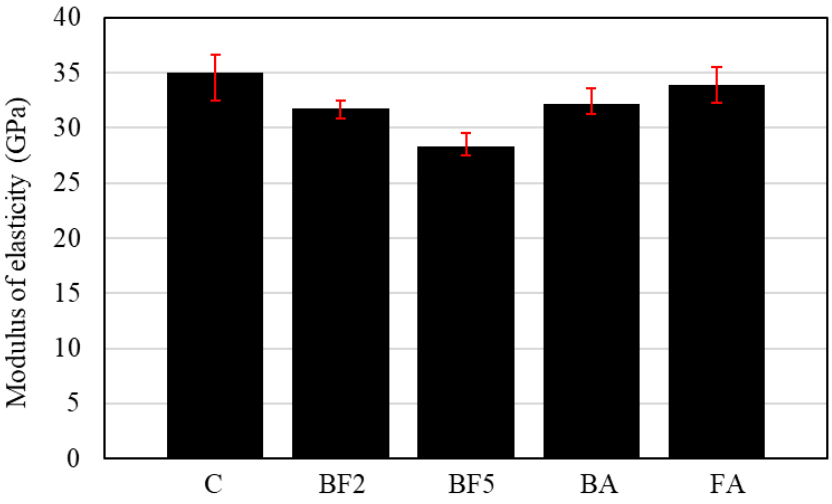

Figure 5.17 Modulus of elasticity of each mixture

According to the JSCE (Japan Society of Civil Engineers)[21], in ordinary concrete with a compressive strength of 40-50 N/mm^2, the elastic modulus is in the range of 31-33 GPa. Although the modulus of elasticity in C and FA is slightly higher than this range, in the case of BF5, the elastic modulus decreases drastically to around 28 GPa. This is due to the high amount of fiber added to the mixture, which increased the porosity and reduced the modulus of elasticity.

5.3.7 Flexural strength

Figure 5.18 shows the flexural strength of each concrete mixture. As shown in Figure 5.18, the

flexural strength was 4.63, 4.77, 4.83, 5.30, and 5.35 N/mm^2 for C, BF2, BF5, BA, and FA, respectively. From these results, it can be concluded that the higher the amount of fiber added, the higher the acquired flexural strength is. However, in BF5, the flexural strength was not proportional, resulting in a flexural strength near to that of BF2. This tendency indicates that when a high amount of fibers are added into concrete, they may not effectively transfer the stress to the other cross-sections. This may be because with the addition of a high amount of fibers, the concrete density tends to decrease and, consequently, the porosity tends to increase. Therefore, the high number of interfacial voids between the fiber and the matrix may increase, affecting stress transmission.

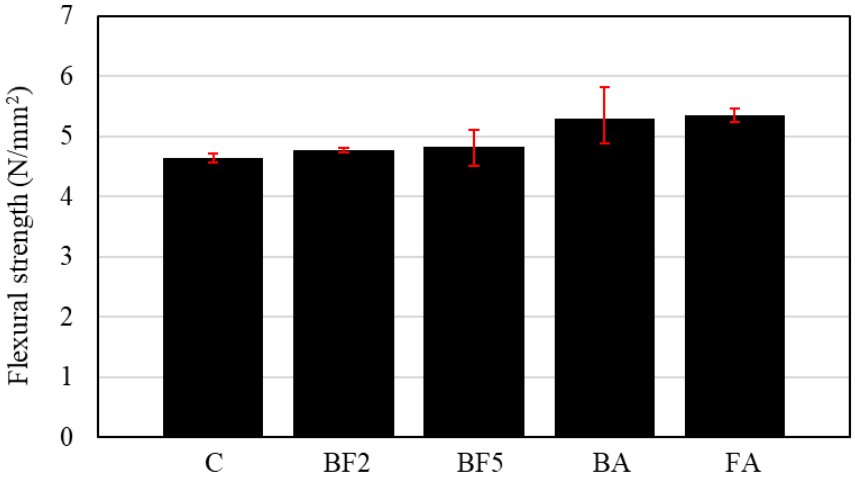

Figure 5.18 Flexural strength of each concrete mixture

Besides, Figure 5.18 shows that, compared to BF2, the flexural strength increased when the ashes are added into the mixture. This increase is related to the pozzolanic reaction. The pozzolanic reaction leads to the formation of additional C-S-H gel[22], which may have filled up the interfacial voids between the fiber and the matrix. Consequently, the flexural strength increases as the fiber/matrix interface contact increases, allowing for the homogeneous distribution of stress to other cross-sectional parts of the specimens.

5.3.8 Split tensile strength

Figure 5.19 shows the results of the split tensile strength test.

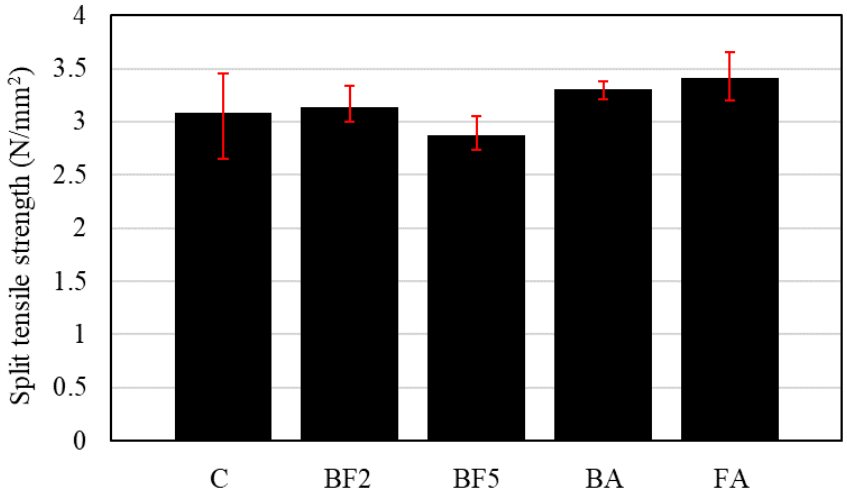

Figure 5.19 Split tensile strength of each concrete mixture

Figure 5.19 shows that the 28-day split tensile strength increased when 2.0% of fiber content was added to the mixture. This increase was more significant when 5% of ashes were added to the mixture. In BA and FA, the split tensile strength was 3.30 and 3.41 N/mm^2, respectively.

However, when 5% of fiber was added, the split tensile strength decreased to around 2.87 N/mm^2, approximately 7% lower than the control mixture. Since the tensile failure section is limited to the one in the tensile splitting test, the effect of fiber bridging to redistribute the stress to another cross-section is limited, a phenomenon in which is even more pronounced due to the high number of voids in the fiber/matrix interface.

5.4 Conclusions

The use of sugarcane residues to replace sand may be a way to make low-cost and environmentally friendly materials. Their use in concrete could also reduce the heat of hydration and the strain due to the thermal expansion, which may be a countermeasure against the generation of cracks in massive concrete. The results obtained in this study can be summarized as follows:

1. The slump decreased with the addition of the fiber amount compared to the control mixture. However, the amount of air increased as the amount of mixed fibers increased.
2. With the addition of bagasse fiber, the heat of hydration of all mixtures was reduced. When 5% of the bagasse fiber was added, the peak temperature neared 48°C, approximately 4.5°C lower than the control mixture.
3. When the bagasse fiber was added, the peak temperature was reached later than the control mixture. When 2% of the bagasse fiber was added, the temperature peak was achieved 26 hours

after the concrete placement, while the control mixture temperature peak was reached 4 hours earlier.

4. In the case of the control mixture, the strain rose to a value of approximately 55 μ, while, in the case of the mixture in which 5% of bagasse fiber was added, the strain value was 30 μ, a difference of about 25 μ.
5. In the case where the bagasse fiber was added, the compressive strength decreased. However, the compressive strength increased when the ashes were added to the mixtures, thereby exceeding the control mixture.
6. The flexural strength of all concrete specimens with added fiber exceeded the value of the control specimen.
7. The split tensile strength increased when 2.0% of the fiber content was added to the mixture. On the other hand, with 5.0% of the fiber, the split tensile strength decreased.

5.5 References

[1] K. Sakai, "Environmental design for concrete structures," *J. Adv. Concr. Technol.,* vol. 3, no. 1, pp. 17-28, 2003.

[2] Nguyen, Trong-Chuc & Luu, Bach, "Reducing temperature difference in mass concrete by surface insulation," *Magazine of Civil Engineering,* vol. 88, no. 4, pp. 70-79, 2019.

[3] Nili, Mahmoud & Salehi, Amir., "Assessing the effectiveness of pozzolans in massive high-strength concrete," *Construction and Building Materials,* vol. 24, no. 11, pp. 2108-2116, 2010.

[4] Awal, A.S.M. Abdul & Hussin, M., "Effect of Palm Oil Fuel Ash in Controlling Heat of Hydration of Concrete," *Procedia Engineering,* vol. 14, p. 2650–2657, 2011.

[5] Sahar Sarabi, Hossein Bakhshi, Hamed Sarkardeh, and Hamed Safaye Nikoo, "Thermal stress control using waste steel fibers in massive concretes," *The European Physical Journal Plus,* vol. 132, 2017.

[6] Andrea Mezencevova; Victor Garas; Hiroki Nanko; and Kimberly E. Kurtis, "Influence of Thermomechanical Pulp Fiber Compositions on Internal Curing of Cementitious Materials," *JOURNAL OF MATERIALS IN CIVIL ENGINEERING,* vol. 24, no. 8, 2012.

[7] Ataie, Feraidon, "Influence of Rice Straw Fibers on Concrete Strength and Drying Shrinkage," *Sustainability,* vol. 10, no. 7, 2018.

[8] He Tian, Y.X. Zhang, "The influence of bagasse fibre and fly ash on the long-term properties of green cementitious composites," *Construction and Building Materials,* vol. 111, pp. 237-250, 2016.

[9] Obinna Onuaguluchi, Nemkumar Banthia, "Plant-based natural fibre reinforced cement composites: A review," *Cement and Concrete Composites,* vol. 68, pp. 96-108, 2016.

[10] K Bilba, M-A Arsene, A Ouensanga, "Sugar cane bagasse fibre reinforced cement composites. Part I. Influence of the botanical components of bagasse on the setting of bagasse/cement composite," *Cement and Concrete Composites,* vol. 25, no. 1, pp. 91-96, 2003.

[11] F.D Fisher, N.R Wienhau, J Olbrecht, vol. 15, no. 11, pp. 12-19, 1974.

[12] Byung-Wan Jo, Sumit Chakraborty, Kwang Won Yoon, "A hypothetical model based on effectiveness of combined alkali and polymer latex modified jute fibre in controlling the setting and hydration behaviour of cement," *Construction and Building Materials,* vol. 68, pp. 1-9, 2014.

[13] Sumit Chakraborty, Sarada P. Kundu, Aparna Roy, Basudam Adhikari, and S. B. Majumder, "Effect of Jute as Fiber Reinforcement Controlling the Hydration Characteristics of Cement Matrix," *Industrial & Engineering Chemistry Research,* vol. 52, no. 3, pp. 1252-1260, 2013.

[14] Maximilienne Bishop and Andrew R. Barron, "Cement Hydration Inhibition with Sucrose, Tartaric Acid, and Lignosulfonate: Analytical and Spectroscopic Study," *Industrial & Engineering Chemistry Research,* vol. 45, no. 21, pp. 7042-7049, 2006.

[15] Abhilash Patil, "Heat of Hydration in the Placement of Mass Concrete," *International Journal of Engineering and Advanced Technology (IJEAT),* vol. 4, no. 3, pp. 1-4, 2015.

[16] NT. Chuc, Le Quy Don, P.V. Thoan, BA. Kiet, "The Effects of Insulation Thickness on Temperature Field and Evaluating Cracking in the Mass Concrete," *Electronic Journal of Structural Engineering,* vol. 18, no. 2, 2018.

[17] Mohammad Tahersima, Tyler Ley, Paul Tikalsky, "Hydration Heat in a Mass Concrete and a Thin Slab with Limestone Blended Cement," *International Journal of Materials Science and Engineering,* vol. 5, pp. 79-86, 2017.

[18] Phuong Trinh Bui, Yuko Ogawa, Kenji Kawai, "Long-term pozzolanic reaction of fly ash in hardened cement-based paste internally activated by natural injection of saturated Ca(OH)2 solution," *Materials and Structures,* vol. 55, no. 144, 2018.

[19] P. Kumar Mehta, "High-performance, high-volume fly ash concrete for sustainable development," *Proceedings of international workshop on sustainable development and concrete technology,* pp. 3-14, 2004.

[20] C.Y. Lee, H.K. Lee, K.M. Lee, "Strength and microstructural characteristics of chemically activated fly ash–cement systems," *Cement and Concrete Research,* vol. 33, no. 3, pp.

425-431, 2003.

[21] Japan Society of Civil Engineers, "Standard Specifications for Concrete Structures - 2017, Design," 2017.

[22] Baoju Liu, Youjun Xie, Jian Li, "Influence of steam curing on the compressive strength of concrete containing supplementary cementing materials," *Cement and Concrete Research,* vol. 35, no. 5, pp. 994-998, 2005.

6 A STUDY ON MECHANICAL PROPERTIES OF SHOTCRETE WITH ADDITION OF SUGARCANE RESIDUES

6.1 Introduction

As presented in Chapter 2, there are different classifications of prevention measures or mitigation against natural disasters. Shotcrete on the steep slopes has been widely used because it can prevent surface weathering and erosion, and in some cases, small-scale control rock falls[1] since it can block the penetration of outside air and rainwater. However, once shotcrete is directly affected by the external environment, the water of the shotcrete may immediately evaporate after its placement due to the influence of the sunlight or when the atmosphere is dry. Naturally, if the volume of the shotcrete decreases fastly, the development of cracks may begin.

The use of sugarcane residues on shotcrete may be an alternative to decrease aggregates' extraction from nature, avoiding environmental exploitation. Other benefits, such as decreasing the composite and local development cost, can be an attractive factor in using these residues[2]. Moreover, the high retention of water of the bagasse fiber and the effect of fiber bridging[3], which re-distributes the stress to another cross-section, may suppress the cracking development and the progression of the cracking propagation[4]. Therefore, from the viewpoint of promoting the effective use of sugarcane residues materials, bagasse fiber as a reinforcing material and bagasse ash for shotcrete were studied.

6.2 Research design and methodology

6.3 Flow chart of the experimental approach

This section describes the experimental approach of shotcrete added with sugarcane bagasse fibers and bagasse ash. This research design is summarized in Figure 6.1.

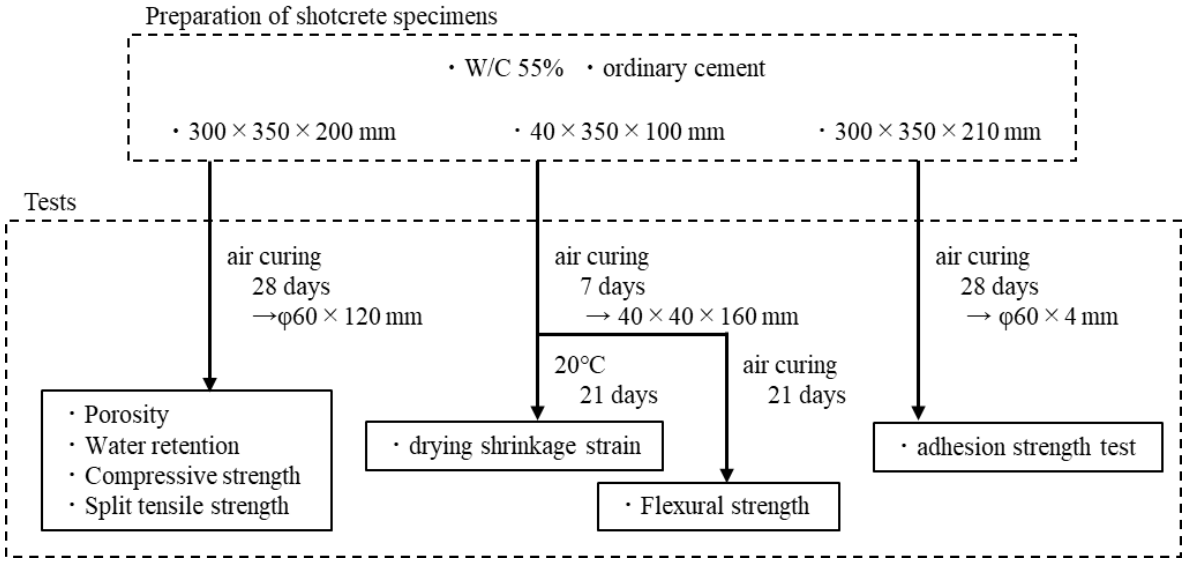

Figure 6.1 Overall flow of this research

As shown in the flow chart of research in Figure 6.1, after the preparation of shotcrete specimens, the specimens were exposed outdoors for the stipulated curing period. After the curing, the samples used for strength tests were drilled and cut. Right after, the mechanical properties of the specimens added with the sugarcane residues were investigated.

6.4 Preparation of the specimens

6.4.1 Materials

All specimens were made using ordinary Portland cement (C) and fine aggregates (S). For comparisons, a commercially available PVA fiber (VF) of 18 mm length for mortar, fly ash (FA), bagasse sand (BS), and bagasse ash (BA) were used. The physical properties of materials and the fibers' characteristics are given in Table 6.1 and Table 6.2.

Table 6.1 Physical properties of cement and aggregates

Properties	Materials				
	C	S	BS	BA	FA
Density (g/cm^3)	3.16	2.63	1.29	2.1	2.33
Total alkali content (%)	0.46	—	—	—	—
Specific surface area (cm^2/g)	3320	—	—	—	6980
Loss of ignition	2.2	—	—	—	1.4

Table 6.2 Characteristics of the fibers

Properties	Bagasse Fiber (BF)	PVA Fiber (VF)
Density (g/cm^3)	0.71	1.09
Length (mm)	17.9 (average)	18.0
Diameter (mm)	0.56 (average)	0.2
Aspect Ratio	32	90
Tensile strength (N/mm^2)	132	975

6.4.2 Shotcrete mixture

The mixed proportions of shotcrete are shown in Table 6.3. The shotcrete mixture C was prepared outdoors, with a water to binder ratio (W/C) of 55%. Shotcrete mixture C represents the control specimens and contains no bagasse materials. In the BF specimen case, it was prepared with a fiber volume ratio of 2.0%. A shotcrete specimen using PVA fibers (VF) was prepared with a fiber volume ratio of 2.0% to compare the bagasse fibers' performance. Also, samples were made using bagasse sand (BS), bagasse ash (BA), and fly ash (FA). In these cases, the volume ratio of the BS, BA, and FA was 5.0% and was used in the place of sand. In the case of BA and FA, the bagasse ash and fly ash acted as a binder. Thus, the W/B becomes 50% and 46%, respectively. In all cases, except C and BS, the fibers were used instead of sand.

Table 6.3 Mix proportions of the mortar specimens

Composites	Fiber type	Fiber (Vol. %)	W/B (%)	Unit (kg/m^3)						
				C	W	S	BS	BA	FA	Fiber
C	—	—	55	400	220	1698	—	—	—	—
BF	Bagasse	2.0	55	400	220	1649	—	—	—	14
VF	Vinylon	2.0	55	400	220	1649	—	—	—	21
BS	—	—	55	400	220	1613	42	—	—	—
BA	Bagasse	2.0	50	400	220	1566	—	41	—	14
FA		2.0	46	400	220	1566	—	0	74	14

6.4.3 Shotcrete specimens and the tests applied

The specimens used in this study were made according to JSCE-F 561. Figure 6.2 shows the preparation of specimens, and Figure 6.3 illustrates the outline of formworks used to drill and cut the specimens. As shown in Figure 6.3, three types of shotcrete specimens with 300 × 350 × 200 mm (a), 40 × 350 × 100 mm (b), and 300 × 350 × 210 mm (c) were made.

Figure 6.2 Preparation of specimens

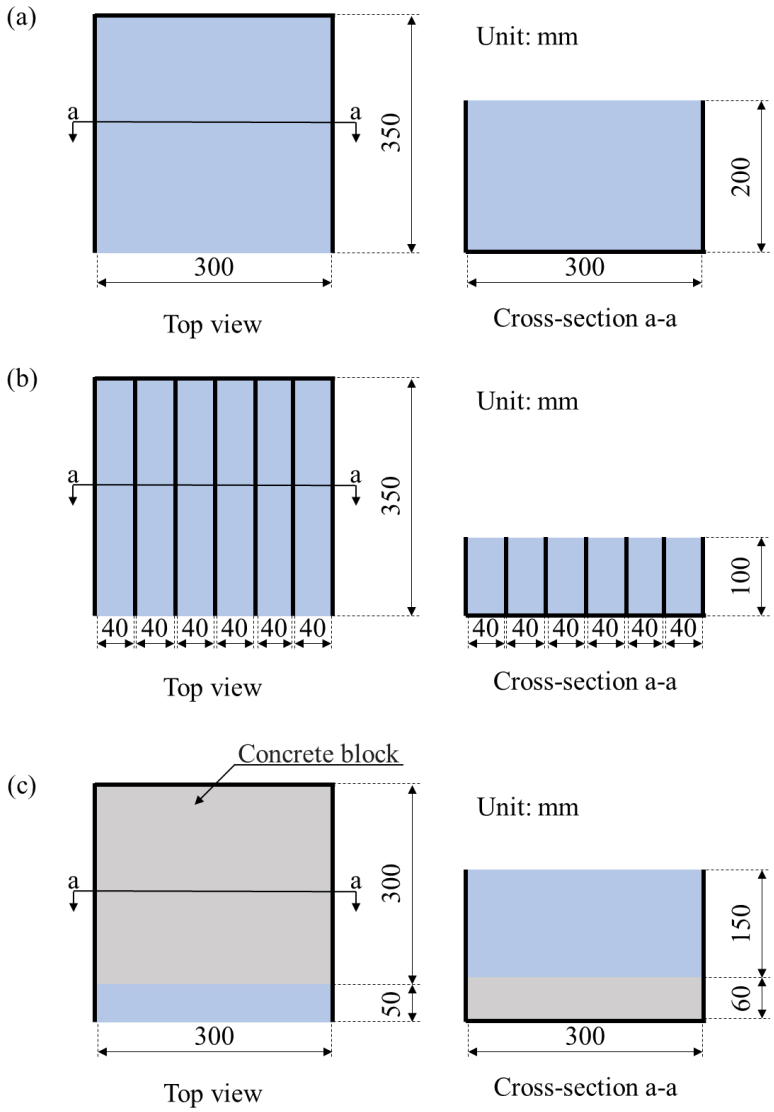

Figure 6.3 Outline of formworks for the shotcrete

In the case of the 300 × 350 × 200 mm specimens, cores were drilled and cut forming cylinder

specimens of φ60 × 120 mm. These specimens were made to determine the compressive strength (JIS A 1108) and split tensile strength (JIS A 1113) and measure the porosity and water retention. In the case of 40 × 350 × 100 mm specimens, samples of 40 × 40 × 160 mm were prepared by cutting to determinate the flexural strength (JIS A 1106) and drying shrinkage strain (JIS A 1129–2). The outline of shotcrete specimens is shown in Figure 6.4.

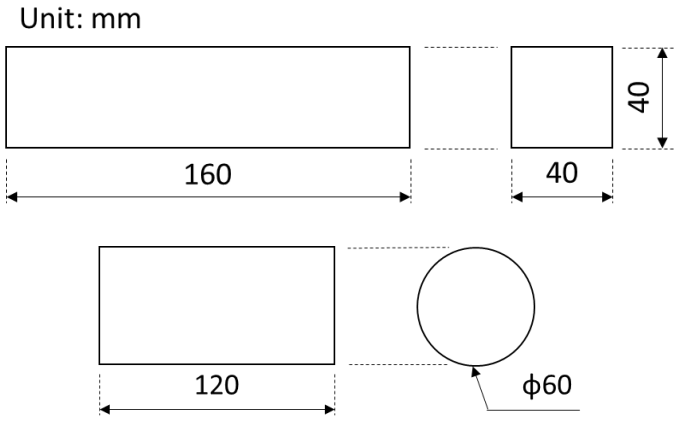

Figure 6.4 Outline of shotcrete specimens

The porosity rate test was based on the mass of the specimen. First, the samples were completely dried in a drying furnace at 105°C for 24 hours. Afterward, the specimens were stored in a room at 20°C until their temperature decreased, equaling the ambient temperature. Then, the mass of the specimens was weighed. Subsequently, they were immersed in water at 20°C for 48 hours, and then the surface-dry mass was weighed. The following equation determined the porosity rate:

$$\boldsymbol{\varepsilon = \frac{W_s - W_d}{\rho \times V} \times 100}$$

Where,

ε: porosity rate (%);

W_d: mass of specimen absolute dried (g);

W_s: mass of specimen surface dried (g);

ρ: density of water (g/cm^3); and

V: volume of the specimen (cm^3).

After the porosity rate test, the moistened specimens were placed in a room at 20°C, and the mass change of specimens was recorded every 24 hours for 7 days. This mass change was determined as water retention rate.

Finally, in the case of 300 × 350 × 210 mm specimens, the shotcrete was sprayed on a precast unreinforced concrete block (see Figure 6.3 (c)) with a flexural strength higher than 4 N/mm^2 (JIS A 5371 : 2016). Then, cores were drilled and cut in samples of φ60 × 40 mm, as demonstrated in Figure 6.5. These specimens were used to determine the adhesion strength (JSCE-K 561-2013) of shotcrete.

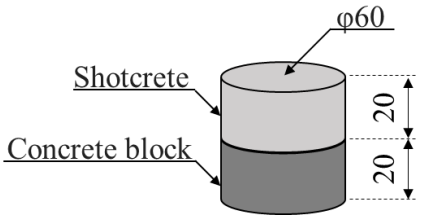

Figure 6.5 Outline of specimen for the adhesion strength test

The shotcrete was cured outdoor, exposed to the weather for 28 days from July 18 to August 15, 2020. During this period, the average humidity, temperature, and precipitation were 81.1%, 29.6°C, and 4.9 mm, respectively. The weather's detailed conditions during the curing period of the specimens can be seen in Figure 6.6.

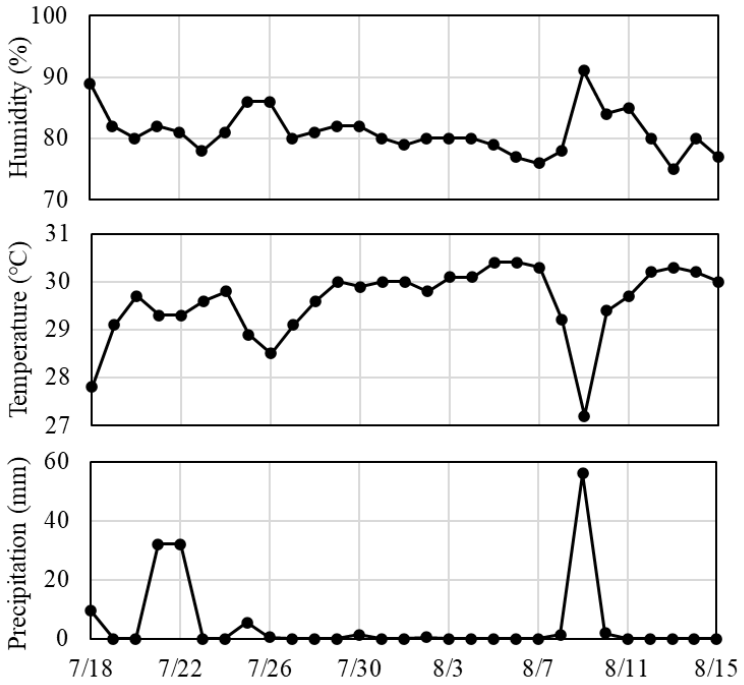

Figure 6.6 Weather conditions during the curing of specimens

The cores were drilled per JIS A 1107, right after the curing period. In the cases of 40 × 350 × 100

mm specimens, however, the specimens were demolded from the formwork after 7 days of curing, cut in 40 × 40 × 160 mm, and then left again to dry. From these specimens, three of them were used to measure the drying shrinkage. In this case, they were kept in a controlled room of 20 °C for 56 days.

6.5 Results and discussions

This section discussed the strength performance of shotcrete with sugarcane residues from experimental observations and measurements.

6.5.1 Porosity rate and water retention rate

Figure 6.7 shows the results of the porosity of shotcrete after 28 days of curing. As shown in Figure 6.7, the porosity rate for C, BF, VF, BS, BA, and FA is 14.7, 15.8, 17.2, 14.9, 15.4, and 15.2%, respectively. As explained in Chapter 4, the increase in porosity rate of the specimens with the addition of bagasse fiber can be because the bagasse fiber is porous, consequently absorbing a high amount of water.

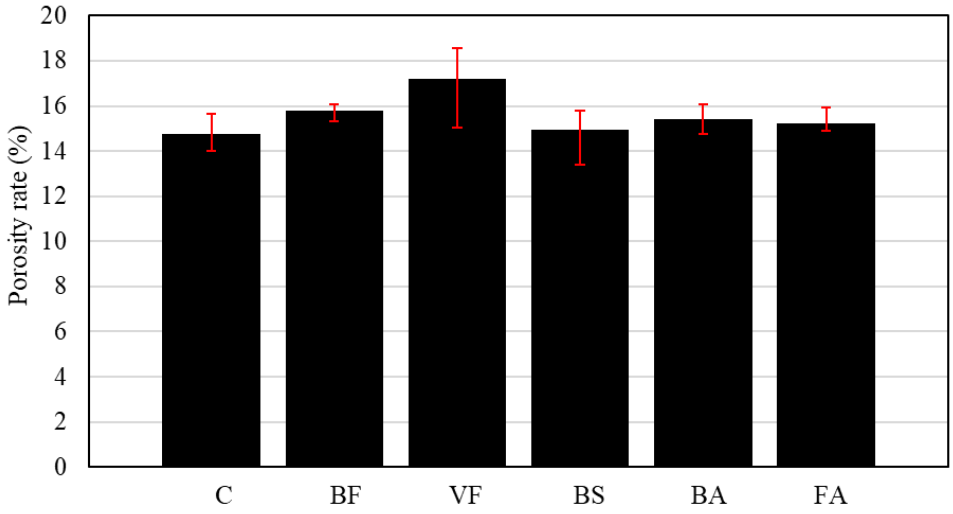

Figure 6.7 Porosity rate of each mixture

However, in VF's case, the shotcrete samples' porosity rate is higher in comparison to shotcrete with added sugarcane residues. This tendency was also observed in Chapter 4 and may be attributed to the fact that the PVA fiber diameter is approximately three times smaller than bagasse fiber. This difference may increase the number of fine bubbles of air while the mortar was mixing.

In the case of BS, the porosity rate is similar to that of the control mixture. For BA and FA, the porosity rate is lower than BF. This may be due to the pozzolanic reaction of the ashes, which tends

to progress through time. However, since the specimens were cured in the air, the pozzolanic reaction tends to be slower once the water supply is limited.

Figure 6.8 illustrates the water retention rate of each mixture.

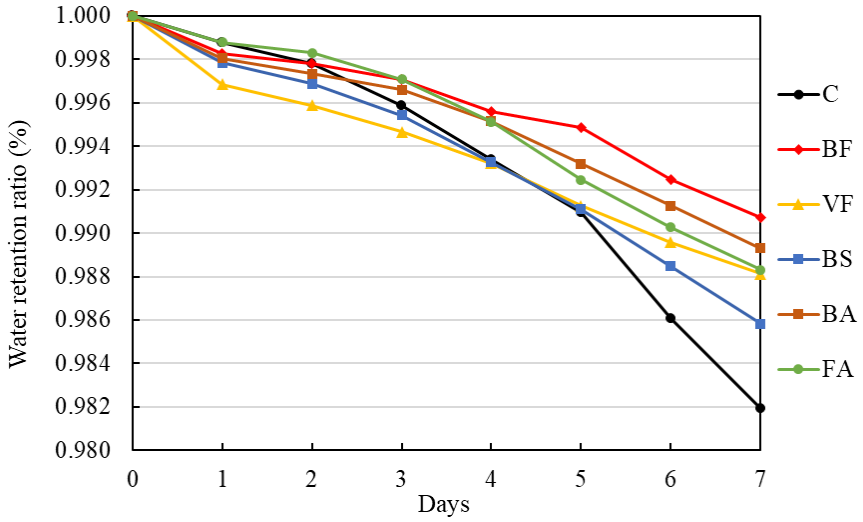

Figure 6.8 Water retention rate of each mixture

As indicated in Figure 6.8, the retention of water where bagasse fiber was added is higher than the other ones. This may be due to the characteristics of bagasse fiber which has a high retention of water. This should be explored deeply since it may supply dry shrinkage avoiding the development of cracks.

6.5.2 Compressive strength test

Figure 6.9 shows the results of the compressive strength of shotcrete. The shotcrete specimens' strengths are 23.73, 22.88, 23.24, 23.94, 24.45, and 24.29 N/mm^2 for C, BF, VF, BS, BA, and FA, respectively.

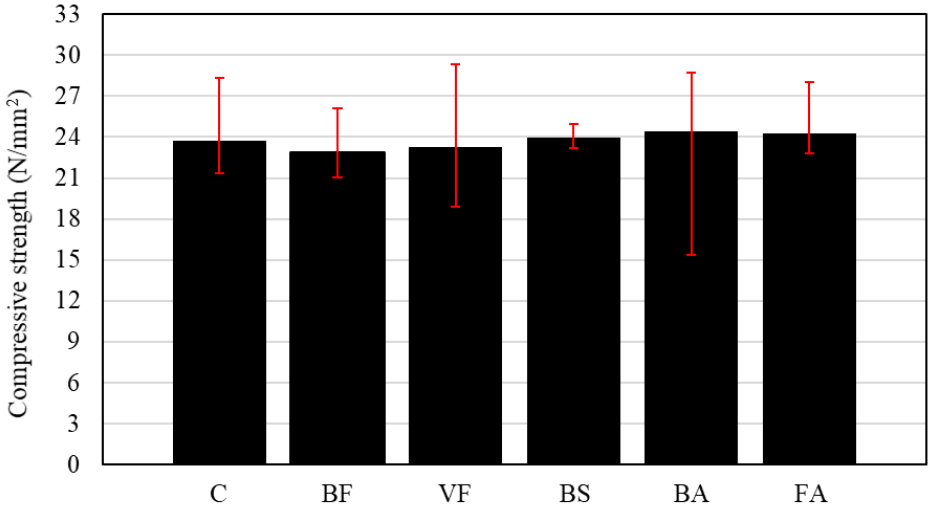

Figure 6.9 Compressive strength of shotcrete at 28 days

As shown in Figure 6.9, the strengths of shotcrete containing fibers were relatively smaller when compared to C. However, BS, BA, and FA, which bagasse sand, bagasse ash, and fly ash added to the composites, the compressive strength increased compared to the control mixture C.

6.5.3 Flexural strength test

Figure 6.10 demonstrates the results of flexural strength. According to Figure 6.10, the flexural strengths are 7.06, 6.93, 7.03, 8.32, and 7.50 N/mm^2 for BF, VF, BS, BA, and FA, respectively. These values exceeded the flexural strength of C, which reaches 6.69 N/mm^2.

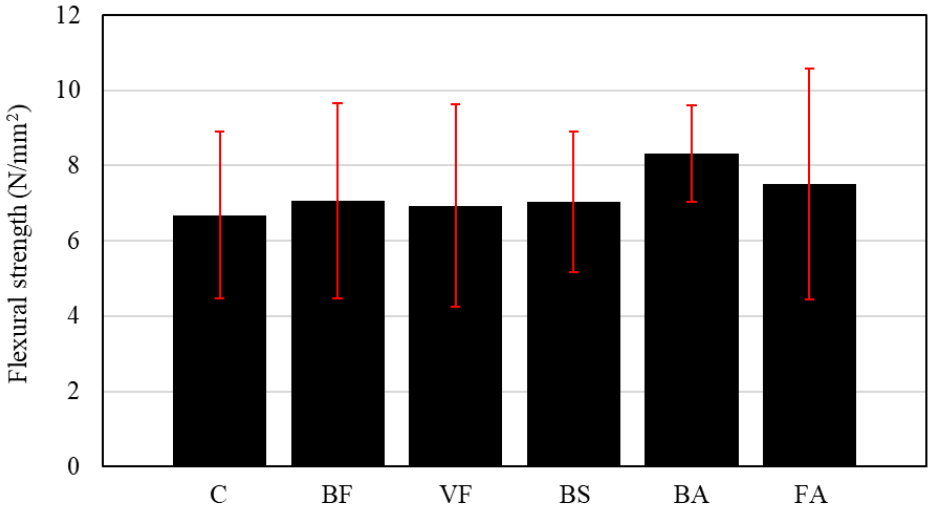

Figure 6.10 Flexural strength of shotcrete at 28 days

As explained in Chapter 4, the high flexural strengths in specimens with fibers' addition are caused

because they act as a stress transfer bridge. This contributes to minimizing crack propagation, controlling their openings, and possibly delaying the mortar's breakage.

6.5.4 Split tensile strength test

Figure 6.11 summarizes the average splitting tensile strength results of shotcrete. As shown in Figure 6.11, the splitting tensile strength is 3.75, 3.63, 3.65, 3.69, 3.78, and 3.84 N/mm^2 for C, BF, VF, BS, BA, and FA, respectively.

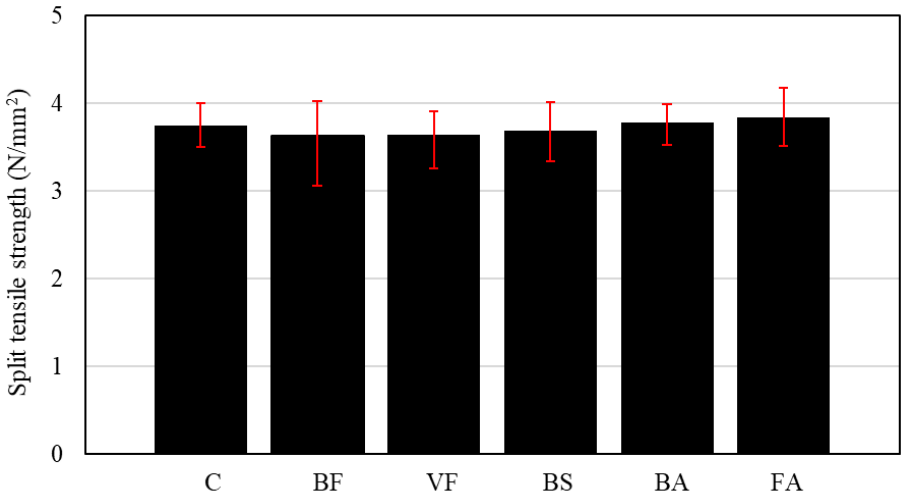

Figure 6.11 Split tensile strength of shotcrete at 28 days

6.5.5 Shrinkage strain measurements

Figure 6.12 shows the shrinkage strain derived from the length change measurement due to the drying shrinkage.

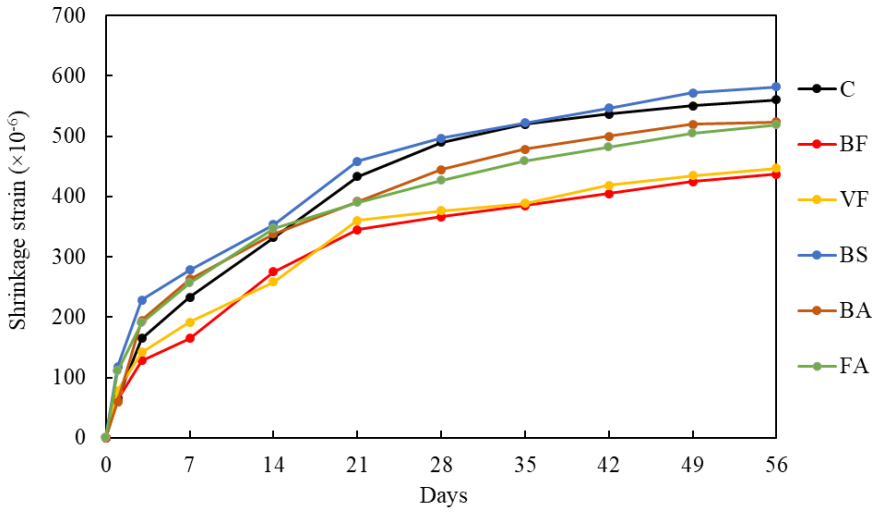

Figure 6.12 Shrinkage strain of shotcrete

According to Figure 6.12, the samples' shrinkage strain, regardless of the fiber type, is smaller than that of the control mixture. For BS, where fiber was not added to the mixture, the shrinkage strain is slightly higher than C. This may be because that an amount of bagasse sand may be reacted as a pozzolanic material, resulting in a high drying shrinkage strain due to the self-shrinkage. The same tendency could be seen in the cases of BA and FA. The drying shrinkage strain in these cases is higher than C in the early period. However, in these cases, the bagasse fiber suppressed the shrinkage after 14 days, and the shrinkage strain becomes smaller than that C.

6.5.6 Adhesion strength test

Figure 6.13 shows the mortar adhesion strength at 28 days of age. In all cases, the specimens broke at the concrete/shotcrete surface. From Figure 6.13, it possible to see that the adhesion strength at the age of 28 days of all mixtures is similar or higher than 2.0 N/mm^2, exceeding the adhesion strength standard of 1.5 N/mm^2[5].

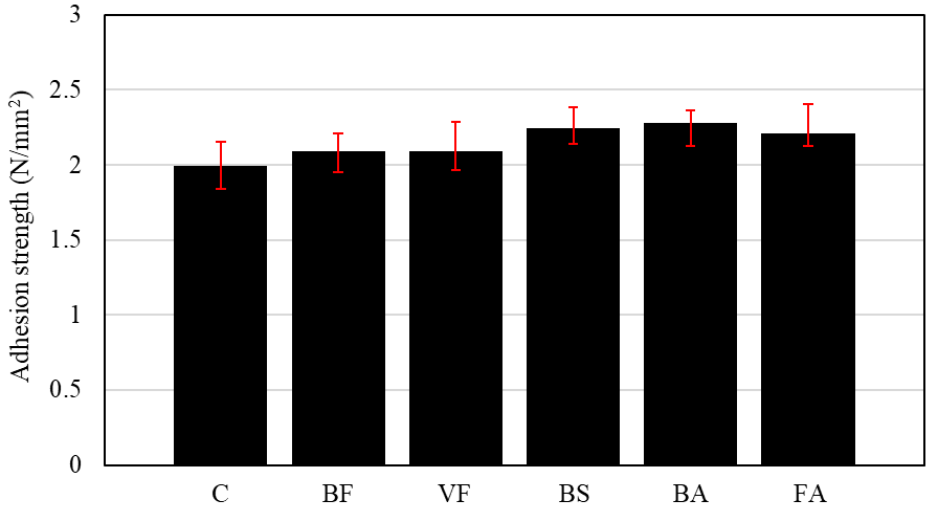

***Figure 6.13** Adhesion strength of shotcrete after 28 days of curing*

Besides, in BS, BA, and FA, the adhesion strength is higher than C. This may be due to increased shotcrete viscosity by adding ashes and bagasse sand in the mixture.

6.6 Conclusion of chapter

In this chapter, the mortar application with the addition of sugarcane residues as shotcrete was investigated. The results showed similarity to that shown in Chapter 4. Therefore, the shotcrete with the addition of sugarcane residues can be used to prevent surface weathering and erosion, and in some cases, to control small-scale rock falls. The main results are shown as follow:

1. The porosity rate of the specimens with the addition of bagasse fiber increased compared to the control mixture.
2. The compressive strength difference of all mixtures remained between ±1 N/mm^2.
3. The flexural strength of all mixtures exceeded the values of C, which reached 6.69 N/mm^2. In BA, the flexural strength was 8.32 N/mm^2.
4. The shrinkage strain of the specimens, regardless of the fiber type or residues, is smaller than that of the control mixture.
5. The adhesion strength at the age of 28 days of all mixtures is similar or higher than the value of 2.0 N/mm^2, exceeding the adhesion strength standard of 1.5 N/mm^2.

6.7 References

[1] Duncan C. Wyllie, Foundations on Rock: Engineering Practice, Second Edition, CRC Press, 1999.

[2] Ribeiro, B.; Uchiyama, T.; Tomiyama, J.; Yamamoto, T.; Yamashiki, Y., "An Environmental Assessment of Interlocking Concrete Blocks Mixed with Sugarcane Residues Produced in Okinawa," *Resources,* vol. 9, no. 93, 2020.

[3] Ribeiro, B., Yamashiki, Y. & Yamamoto, T, "A study on mechanical properties of mortar with sugarcane bagasse fiber and bagasse ash," *Journal of Material Cycles and Waste Management,* 2020.

[4] Marc Jolin, J.-D. Lemay, N. Ginouse, B. Bissonnette and É. Blouin-Dallaire, "The effect of spraying on fiber content and shotcrete properties," *Shotcrete for Underground Support XII,* 2015.

[5] NEXCO (Nippon Expressway Company), Structure Construction Management Guidelines, 2019.

7 DURABILITY OF CONCRETE WITH ADDITION OF SUGARCANE RESIDUES

7.1 Introduction

In an era where reducing the environmental load is necessary for a sustainable society, new policies and ideas are being implemented to emphasize maintaining a concrete structure useful as long as possible. Commonly, the physical life of a reinforced concrete (RC) structure is based on the steel bars' corrosion embedded in concrete. When these reinforcements corrode, the resulting rust occupies a greater volume than the steel, creating tensile stresses in the concrete. The consequences are cracking, delamination, and spalling the concrete. The deterioration of RC structures can be caused by chloride attack, carbonation, and other factors[1, 2].

In a high alkali environment, such as concrete, the steel bar can react with oxygen to form a thin layer on its surface, protecting it from corrosion. Unfortunately, concrete is a permeable material, allowing the ingress of chlorides from deicing salts or marine atmospheres, and allowing gases, mainly CO_2, to neutralize the pore solution, making the concrete an appropriate environment for embedded steel bar corrosion.

When the concrete becomes carbonated around the steel bar, the steel bar loses its corrosion protection function. The carbonation of concrete is when atmospheric carbon dioxide reacts with the cement hydration products to form calcium carbonate. This phenomenon's importance is related to reducing the concrete alkalinity to a pH near 8[3]. Since the steel bars in RC are protected from corrosion by the highly alkaline environment inside the concrete (pH ≈ 13), with the carbonation, this protection ceases and the steel bars corrode[4]. The primary carbonation reaction is that of calcium hydroxide, described by:

$$CO_2(g \rightarrow aq) + Ca(OH)_2(s \rightarrow aq) \rightarrow CaCO_3(aq \rightarrow s) + H_2O$$

In the chloride attack, regardless of the concrete alkalinity, the steel bar's passive film is destroyed when the chloride concentration near the steel bar surface reaches the critical value. There are three possibilities of occurrence of Cl^- in concrete[5]:

- chemically bounded with tricalcium aluminate (C_3A), forming calcium chloroaluminate or Friedel's salt ($C_3A.CaCl_2.10H_2O$);
- absorbed on the surface of the pores; and

・Cl^- as free ions.

The free chlorides are the ions that are more worrisome due to their increased mobility through the pores, reaching the steel bar in a short period. When this occurs, they can destroy the passive oxide film of the steel bar in concrete.

Generally, structures attacked by chloride are viewed around the sea since the seawater contains approximately 3.4% of NaCl and is slightly alkaline (pH 8), being a good electrolyte, which can cause corrosion of the steel bar. However, chloride attack can also be seen in structures built in snowy weather, in which agents as sodium chloride and calcium chloride are used as anti-freezing in roads[6]. Also, chloride may penetrate concrete during the manufacture by using water with salts and fine aggregates from the sea without adequate salt removal[7].

Although the mechanism of destruction of the passive oxide film is not yet fully understood due to the complexities in examining the process, the chloride presence at the steel-concrete interface, whatever its origin, is known to have an easy ability to destroy the passive oxide film[8]. However, according to the American Concrete Institute (ACI), the chloride ions become incorporated at localized weak spots in the thicker films, creating defects and allowing easy ionic transport. In sub-monolayer passivity, the chloride ions may compete with the hydroxyl ions for locations of high activity on the metal surface, preventing these reactive sites from becoming passivated[9]. In either case, with the passive film's breakdown, the steel bar reacts with H_2O and O_2, and active corrosion can occur at these breakdown locations. After corrosion initiates, it proceeds autocatalytically, resulting in a decrement of the reinforced concrete structure's performance.

A certain amount of chloride ions in relation to the concentration of hydroxyls promote the corrosion of steel. As cited by Alonso[10], Hausmann and Gouda were the first to identify the mean value of the Cl^-/OH^- ratio, which is around 0.6 in solutions simulating the concrete pore solution. According to the Japan Society of Civil Engineers, steel bars' corrosion in concrete starts when the chloride ion concentration at the steel bars' vicinity reaches 1.2 kg/m^3[11]. However, recently, it was established that this value could vary depending on the type of cement used and the water-cement ratio, being different calculation formulas proposed[12].

In both cases, carbonation and chloride attack, the steel bar reacts with oxygen and water, corroding the steel bars, resulting in a reduction of the reinforcement's cross-section area, which decreases the structure's performance.

Chapter 5 investigated the reduction in the heat of hydration, the thermal expansion resistance, and the fresh and mechanical properties of the concrete with sugarcane residues in massive concrete. The result showed that, by adding 2.0% of bagasse fiber and 5.0% of pozzolanic material to the concrete, the heat of hydration was reduced. The strain due to the thermal expansion was smaller than the control mixture. Moreover, the compressive, flexural, and split tensile strength increased in comparison to the control mixture. However, little is known about how the concrete added with bagasse fibers and bagasse ash can be affected by the carbonation and the chloride ion penetration.

In this chapter, the mechanical properties of the sugarcane residues in concrete were studied. The fibers and ashes concrete specimens were prepared, and strength tests, such as compressive and flexural strength tests, were performed. The velocity of carbonation and the velocity and concentration of chloride ions penetrating the concrete were investigated.

7.2 Research design and methodology

7.2.1 Flow chart of the experimental approach

Figure 7.1 shows the overall flow of this chapter.

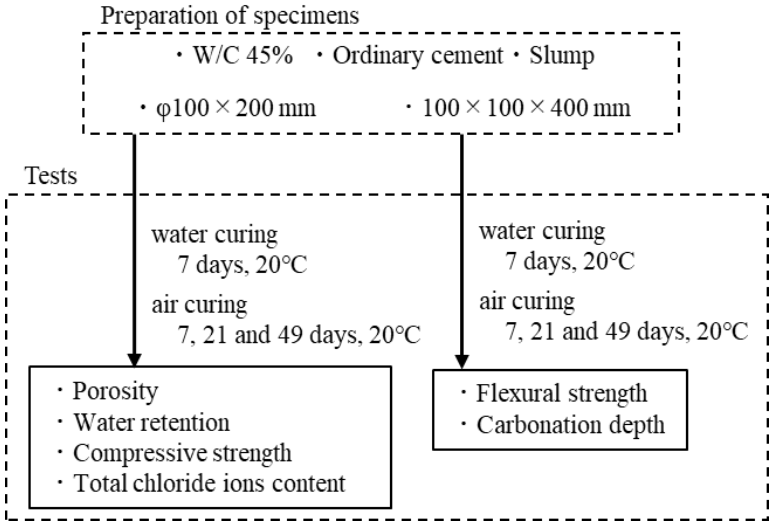

Figure 7.1 Overall flow of this research

As shown in the flow chart of research in Figure 7.1, after the specimens' preparation, the strength tests were performed to determine the mechanical properties of concrete added with sugarcane residues. Also, samples were prepared to investigate the resistance to the carbonation and chloride ion ingress in the cementitious composite sugarcane residues.

7.2.2 Materials

The preliminary trials applied to sugarcane bagasse residues were the same as described in previous studies[13, 14]. The properties of the PVA fibers and sugarcane bagasse residues are given in Table 7.1.

Table 7.1 Properties of the sugarcane bagasse residues

Properties	PVA Fiber (VF)	Bagasse Fiber (BF)	Bagasse Ash (BA)	Bagasse Sand (BS)
Density (g/cm^3)	1.09	0.71	2.1	1.29
Length (mm)	18.0	17.9 (average)	—	—
Diameter (mm)	0.2	0.56 (average)	—	—
Aspect Ratio	90	32	—	—
Tensile strength (N/mm^2)	975	132	—	—

The specimens were made using ordinary Portland cement (C), and all aggregates used in this study were collected from Okinawa Prefecture, Japan. The two types of fine aggregates, sea sand (S_1) and crushed sand (S_2), were acquired from Arakawaoki and Motobu, respectively, and the coarse aggregates (G) were acquired from Motobu. The maximum size of the coarse aggregate is 20 mm. For the comparisons, a commercially available PVA fiber (VF; density: 1.10 g/cm^3; length: 18 mm; diameter: 0.2 mm; aspect ratio: 90) for concrete and fly ash (FA) grade II was used. The physical properties of cement and aggregates materials are given in Table 7.2.

Table 7.2 Physical properties of cement and aggregates

Properties	Materials				
	C	S_1	S_2	G	FA
Density (g/cm^3)	3.16	2.61	2.67	2.61	2.33
Total alkali content (%)	0.46	—	—	—	—
Specific surface area (cm^2/g)	3320	–	–	–	6981
Loss on ignition (%)	2.2	–	–	–	1.4

For the concrete mixture, two kinds of admixtures were used in this study to improve the workability of concrete. The properties of the water-reducing agent (WRA) and air-entraining agent (AEA) are shown in Table 7.3.

Table 7.3 Properties of admixtures

Admixtures	Main components	Color	Density (20°C, g/cm^3)	Total alkali content (%)	Cl^- content (%)
WRA (No.70)	Complexes of lignin sulfonic acid compound and polyol	Dark brown	1.23-1.27	1	0.03
AEA (303A)	Alkyl ether type anionic surfactant	Light yellow	1.02-1.06	1.1	0.01

7.2.3 Concrete mixture

The mix proportions of the concrete are shown in Table 7.4. Mixture C was prepared in the laboratory, with a water to binder ratio (W/C) of 45%. Mixture C represents the control specimens and contains no sugarcane residue materials. In BF samples, the mixture was prepared with a bagasse fiber volume ratio of 2.0% compared to the total fine aggregate volume. A concrete specimen using PVA fibers was made with the fiber volume ratio of 2.0% to total fine aggregate volume to compare the bagasse fibers' performance. Besides, samples were prepared using bagasse sand (BS), bagasse ash (BA), and fly ash (FA). The volume ratio of the bagasse sand, bagasse ash, and fly ash was 5.0% when compared to the fine aggregate volume. For BA and FA, the specimens were prepared with the same volume of fibers as BF2, and the bagasse ash and fly ash acted as a binder. Thus, the W/B becomes 43% and 41%, respectively.

Table 7.4 Mix proportions

Composites	Fiber (Vol. %)	W/B (%)	Unit (kg/m^3)											
			C	W	S1	S2	G	BS	BA	FA	VF	BF	WRA	AEA
C	—	45	389	175	440	450	950	—	—	—	—	—	1.17	0.0125
BF2	2.0				431	441		—	—	—	—	14		
VF2	2.0							—	—	—	7	—		
BS5	—				418	427		28	—	—	—	—		
BA	2.0	43			392	401		—	22	—	—	14		
FA	2.0	41						—	—	39	—			

7.2.4 Preparation of concrete specimens

All the concrete mixtures were mixed using a twin-shaft compulsory mixer. First, the coarse aggregate, cement/ashes, and fine aggregate were mixed for 30 seconds. Then, the specified amount of water/fiber was added and mixed for 30 more seconds. After that, the mixer was stopped for 90 seconds. While the mixer was stopped, during the first 30 seconds, the concrete that had adhered to the paddle was scraped off with a spatula and put at the center of the mixer. After the pause, the mortar was mixed for 90 seconds. Before casting, the slump flow (JIS A 1150) was conducted on the

concrete mixture to determine its workability.

For each concrete mixture, specimens of φ100 × 200 mm were cast to determine the compressive strength (JIS A 1108), porosity rate test, and chloride penetration test. Furthermore, specimens of 100 × 100 × 400 mm were prepared to determine the flexural strength (JIS A 1106) and accelerated carbonation test (JIS A 1153). Three specimens were assayed in each test.

After the casting, all specimens were cured in the laboratory at ambient temperature for 24 hours. The specimens were then de-molded and cured underwater at 20°C for 7 days. Subsequently, the specimens were cured in the air at a room temperature of 20°C until the respective tests.

7.2.5 Accelerated carbonation test

After the curing period (7 days underwater and 7 days in air), the accelerated carbonation test was conducted using the 100 × 100 × 400 mm concrete specimens. The temperature and relative humidity settings were 20 ± 2°C and 60 ± 5%, respectively. The accelerated carbonation test duration was 14 and 42 days; that is, the age of concrete was 28 and 56 days, respectively. The measurement of carbonation depth was following JIS A 1152. The schematic representation of the carbonation depth test is shown in Figure 7.2.

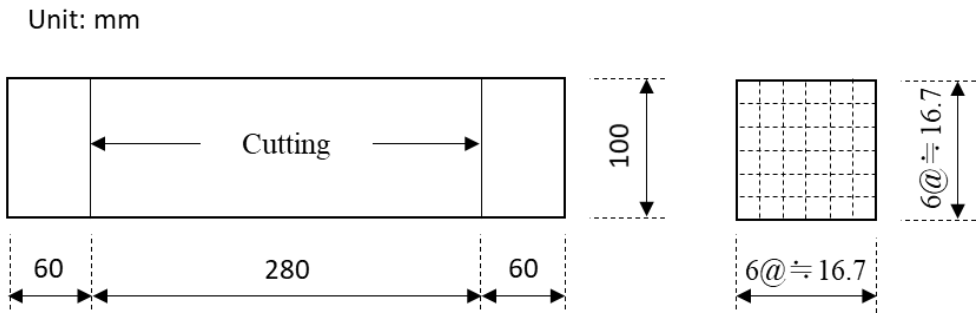

Figure 7.2 Schematic representation of the carbonation depth test

As shown in Figure 7.2, the specimens were cut at 60 mm from both ends of the specimen. After spraying a 1% phenolphthalein solution on the cut surface, the distance from the concrete surface to the colored area was measured with a caliper. The number of measurement points was set at 5 points divided into six parts on one surface, a total of 40 points (5 points × 4 surfaces × 2 cuts) in one specimen. The value of carbonation depth is the average of the three specimens' carbonation depths, a total of 120 points.

7.2.6 Chloride penetration test

Figure 7.3 shows the schematic representation of the chloride penetration test. As shown in Figure 7.3, right after the curing (7 days underwater and 7 days in air), the specimens prepared for the chloride penetration test were immersed in a 10% aqueous NaCl solution at room temperature of 20°C. The specimens' lateral side was coated with epoxy to make the saltwater permeate in one direction only. After 14 and 42 days of immersion, that is, an age of concrete of 28 and 56 days, respectively, the specimens were cut in each 1 cm from the exposed surface, and the total chloride ions content was measured based on JIS A 1154.

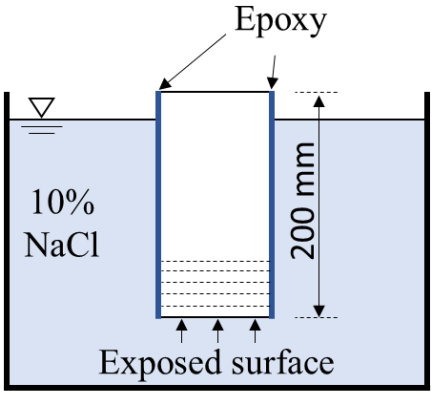

Figure 7.3 Schematic representation of the chloride penetration test

7.3 Results and discussions

First, the results of the fresh and hardened concrete properties are presented and examined. Afterward, the durability, chloride ion content, and carbonation depth, of concrete are debated.

7.3.1 Fresh Concrete

Figure 7.4 shows the results of the slump test. As shown in Figure 7.4, the slump values are smaller in mixtures where the fibers were added compared to the control mixture. The slump of C is 7.2 cm, and BS is 6.7 cm, while for BF, VF, BA, and FA, the ones where the fraction volume of fiber was 2% in comparison to the total volume of fine aggregate, the slump reduced to 6.5, 5.1, 5.7, and 5.4 cm, respectively. These slump value variations between non-fiber reinforced concrete and fiber reinforced concrete can be explained due to the formation of a bridge network of fibers into the concrete that restrained the deformation of the fresh concrete during the test.

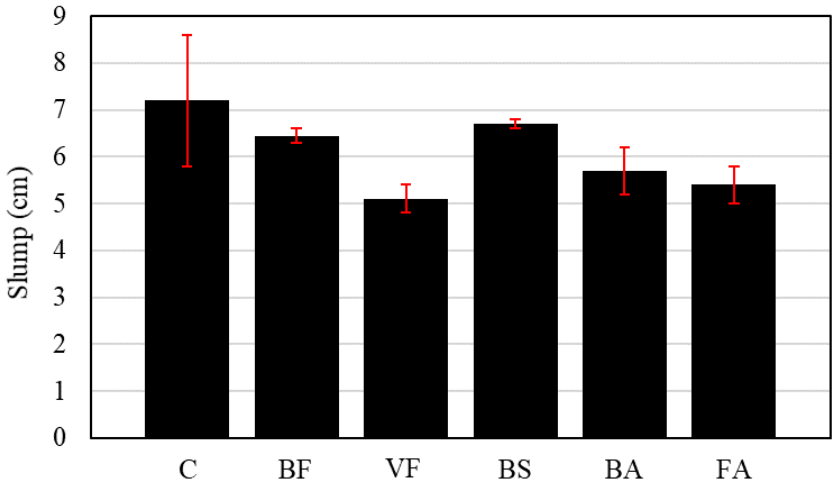

Figure 7.4 Slump test results

For VF, the slump value is smaller. This may be attributed to PVA fiber's diameter, which is approximately three times smaller than that of bagasse fiber. As a result, the number of PVA fibers is higher than the bagasse fiber specimens, resulting in a smaller deformation during the slump test.

In the cases of BA and FA, with the addition of ashes and the increase in the binder amount, the viscosity of concrete increased, resulting in a decrease in the slump compared to BF. The same behavior could be seen in BS since the bagasse sand particles are between 0.149 and 2 mm, smaller than the fine aggregates.

7.3.2 Compressive Strength

Figure 7.5 shows the compressive strength of each concrete mixture after 28 and 56 days of curing. At 28 days, the results obtained were 44.93, 44.16, 45.94, 50.02, 47.05, and 46.54 N/mm^2 and at 56 days were 46.57, 47.67, 47.50, 51.37, 49.03, and 49.48 N/mm^2 for C, BF, VF, BS, BA, and FA, respectively. After 28 days of curing, the addition of 2% of bagasse fiber, the compressive strength briefly decreases, probably due to the increase in the porosity of the concrete and soluble sugars in the fibers, which may retard the cement hydration. However, at 56 days, the compressive strength of BF becomes higher than that of the control composite C and similar to VF strength. This result may indicate that the cement hydration is affected in an early time only and tend not to affect the hydration in the long term.

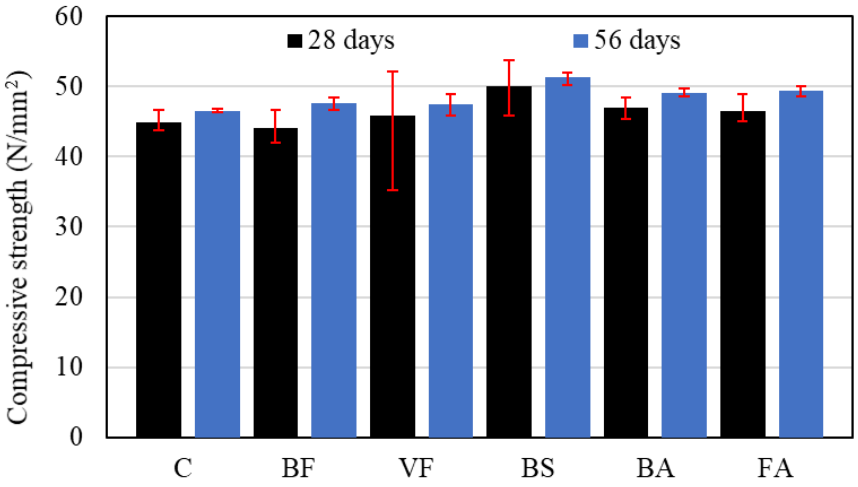

Figure 7.5 Compressive strength of each concrete mixture after 28 and 56 days of curing

For VF, the compressive strength is higher in comparison to C at 28 and 56 days. However, the strength variation is higher than the other samples. This variation may be due to the facility of the PVA fibers agglomerate during the mixing. The number of fibers in VF was higher because the PVA fiber diameter is smaller than bagasse fiber.

When the ashes were added into the mixture, the compressive strength was higher, except when BA and FA are compared to BS. This may be because, in the case of BS, the bagasse fiber was not used. Thus, without the use of the fibers, the compressive strength is not affected. On the other hand, the bagasse sand may collaborate to fill the concrete's pores, increasing its strength.

7.3.3 Flexural Strength

Figure 7.6 demonstrates the flexural strength test results of each concrete mixture after 28 and 56 days of curing. From Figure 7.6, it is possible to see that the flexural strength was 3.04, 3.48, 3.75, 3.16, 3.70, and 3.71 N/mm^2 after 28 days of curing and 3.56, 3.87, 3.89, 3.68, 3.93, and 3.91 N/mm^2 after 56 days of curing for C, BF, VF, BS, BA, and FA, respectively.

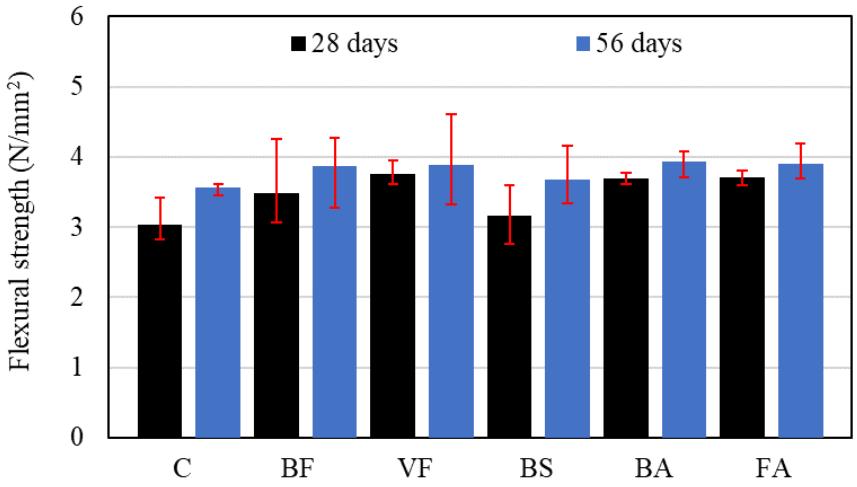

Figure 7.6 Flexural strength of each concrete mixture after 28 and 56 days of curing

As shown in Figure 7.6, when the fibers are mixed in the composite, the flexural strength increases compared to the control composite C. It is known that conventional concrete (composite C in this study) exhibits brittle collapse when the developed tensile stress exceeds the limited strength of concrete under tension. However, the composites that fibers were added demonstrate a pseudo-ductile tensile response and enhanced energy dissipations capacities relative to composite C's brittle behavior.

The same tendency of the compressive strength, at 28 days, the flexural strength of BF is smaller than VF. However, after 56 days of curing, BF's flexural strength becomes similar to the flexural strength of VF. Since fibrous concrete's cracking requires debonding and pull-out of the randomly distributed fibers in the concrete mass, PVA fibers may have been debonded and pulled-out, and the crosslinking effect may not be effectively exhibited.

7.3.4 Carbonation depth

Figure 7.7 shows the depth of carbonation of each concrete mixture after 14 and 42 days of exposing the concrete to the accelerated carbonation testing. As shown in Figure 7.7, the carbonation depth for C is 0.34 and 2.40 mm at 14 and 42 days, respectively. For BF, the carbonation depth decreases to 0.26 and 2.24 mm at 14 and 42 days, respectively. When the concrete pore is filled with water, the carbon dioxide has to dissolve and diffuse through water. The diffusion in a liquid is about 10000 times slower than in air; consequently, the carbonation tends to be slow. However, when the concrete becomes dry, and voids are not filled with water, the carbon dioxide penetrates them, neutralizing the saturated liquid phase of calcium hydroxide and other hydrated compounds of the cement matrix. For C, the drying process could be faster than BF, resulting in a smaller carbonation

resistance. This may be explained by the high amount of water that the fibers can retain. As reported in previous research, the water retention ratio of specimens added with bagasse fibers tends to be higher than C[13].

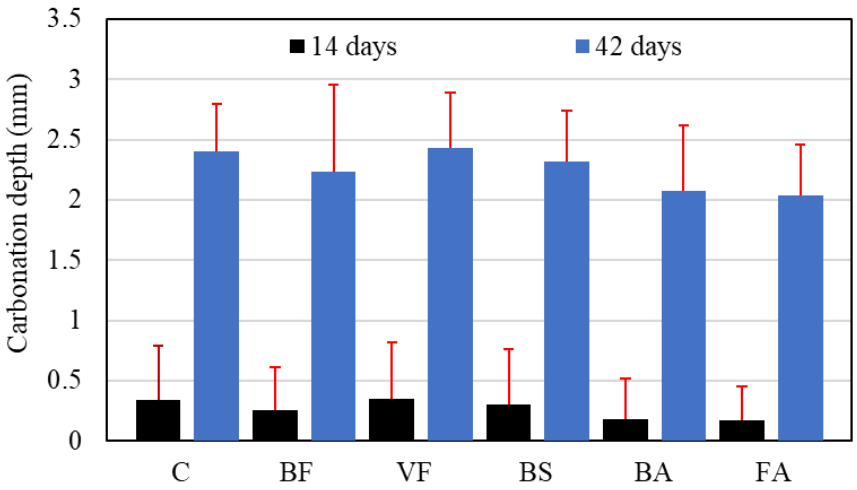

Figure 7.7 Carbonation depth of each concrete mixture after 14 and 42 days of exposure to the accelerated carbonation testing

For VF, the carbonation depth at 14 and 42 days is 0.35 and 2.43 mm, respectively, showing a slight increase compared to C. A possible explanation for this is that fine bubbles of air may have been clumping together while the concrete mixes and eventually turning into empty spaces. These empty spaces may have been facilitated the penetration of carbon dioxide, increasing the carbonation depth.

As shown in Figure 7.7, the carbonation depth of BS is 0.30 and 2.32 mm at 14 and 42 days, respectively. When the bagasse sand is added into the mixture, the carbonation resistance tends to increase compared to C. Since the bagasse sand particles are smaller than 2 mm, they may fill the concrete pores, avoiding the penetration of carbon dioxide. The same was observed in BA and FA, where the carbonation depth after 14 and 42 days is 0.18 and 2.07 mm, and 0.17 and 2.04 mm, respectively. However, in BA and FA, the carbonation depth is smaller than that BS, once the water retention ratio is higher than BS, where bagasse fibers are added in the concrete.

7.3.5 Total chloride ions content

Figure 7.8 and Figure 7.9 show the total chloride ions content in concrete after 14 and 42 days of immersion in a 10% aqueous solution of NaCl.

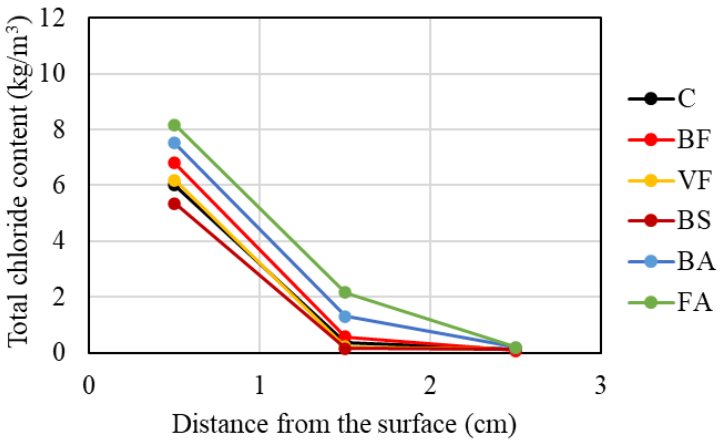

Figure 7.8 Total chloride ions content in concrete after 14 days of immersion in a 10% aqueous solution of NaCl

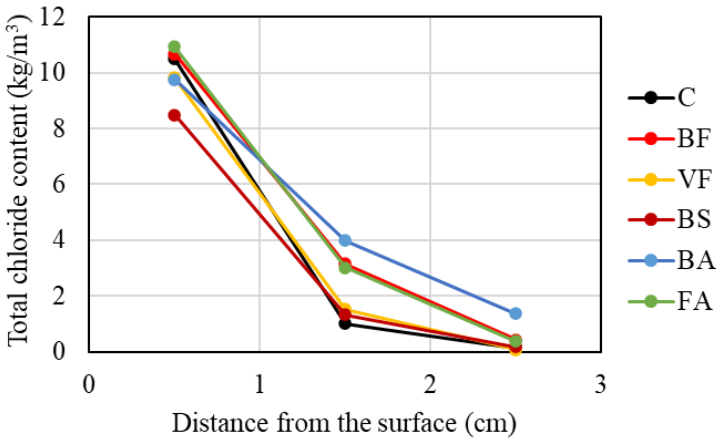

Figure 7.9 Total chloride ions content in concrete after 42 days of immersion in a 10% aqueous solution of NaCl

As shown in Figure 7.8 and Figure 7.9, the total chloride ions content in the specimens where bagasse fiber was added into the mixture is higher. This may be due to bagasse fiber's ability to absorb water, facilitating the penetration of chlorides into the composite. A previous study demonstrated that whi le fibers' presence increased the coefficient of chloride diffusion based on total chlorides, there was a decrease in the coefficient related to free chlorides. The authors concluded that fibers appear to bind the chlorides and inhibit their transport through concrete[15]. Since the present research did not investigate the free chloride content, a future investigation should clarify the mechanism and discuss countermeasures against chloride penetration.

7.4 Conclusion of chapter

This study revealed that the concrete with the addition of bagasse fibers was not severely affected by carbonation. Instead, the carbonation of the concrete added with bagasse fibers was slightly

smaller than that of the control mixture.

1. The slump of the control mixture case is 7.2 cm, and of bagasse sand mix is 6.7 cm. In contrast, in the samples of bagasse fiber, PVA fiber, bagasse ash, and fly ash, where the fiber's fraction volume was 2% compared to the total volume of fine aggregate, the slump was reduced to 6.5, 5.1, 5.7, and 5.4 cm, respectively.
2. The compressive strength at 28 days was 44.93, 44.16, 45.94, 50.02, 47.05, and 46.54 $N/mm^{2,}$ and at 56 days was 46.57, 47.67, 47.50, 51.37, 49.03, and 49.48 N/mm^2 for control mixture, bagasse fiber, PVA fiber, bagasse sand, bagasse ash, and fly ash, respectively.
3. The flexural strength was 3.04, 3.48, 3.75, 3.16, 3.70, and 3.71 N/mm^2 after 28 days of curing and 3.56, 3.87, 3.89, 3.68, 3.93, and 3.91 N/mm^2 after 56 days of curing for control mixture, bagasse fiber, PVA fiber, bagasse sand, bagasse ash, and fly ash, respectively.
4. The carbonation depth for the control mixture is 0.34 and 2.40 mm at 14 and 42 days, respectively, while for BF, the carbonation depth decreases to 0.26 and 2.24 mm at 14 and 42 days, respectively. For the specimens containing bagasse sand, bagasse ash, and fly ash added to the mixture, the depth of carbonation decreased to 0.30 and 2.32 mm, 0.18 and 2.07 mm, and 0.17 and 2.04 mm after 14 and 42 days, respectively.
5. The total chloride ions content where bagasse fiber was added in the mixture was higher than the other cases.

7.5 References

[1] S.A. Ghahari, A.M. Ramezanianpour, A.A. Ramezanianpour and M. Esmaeili, "An Accelerated Test Method of Simultaneous Carbonation and Chloride Ion Ingress: Durability of Silica Fume Concrete in Severe Environments," *Advances in Materials Science and Engineering,* 2016.

[2] M.Anwar and Dina A.Emarah, "Resistance of concrete containing ternary cementitious blends to chloride attack and carbonation," *Journal of Materials Research and Technology,* vol. 9, no. 3, pp. 3198-3207, 2020.

[3] F. Pacheco Torgal, S. Miraldo, J.A. Labrincha, J. De Brito, "An overview on concrete carbonation in the context of eco-efficient construction: Evaluation, use of SCMs and/or RAC," *Construction and Building Materials,* vol. 36, pp. 141-150, 2012.

[4] M.A. Peter, A. Muntean, S.A. Meier, M. Böhm, "Competition of several carbonation reactions in concrete: A parametric study," *Cement and Concrete Research,* vol. 38, no. 12, pp. 1385-1393, 2008.

[5] Oswaldo Cascudo, O controle da corrosão de armaduras em concreto : inspeção e técnicas

eletroquímicas (in portuguese), São Paulo: Pini, 1997.

[6] S.W. Dean, "Natural Atmospheres: Corrosion," in *Encyclopedia of Materials: Science and Technology*, Elsevier, 2011, pp. 5930-5938.

[7] Jianzhuang Xiao, Chengbing Qiang, Antonio Nanni, Kaijian Zhang, "Use of sea-sand and seawater in concrete construction: Current status and future opportunities," *Construction and Building Materials,* vol. 155, pp. 1101-1111, 2017.

[8] Hossein DorMohammadi, Qin Pang, Pratik Murkute, Líney Árnadóttir & O. Burkan Isgor, "Investigation of chloride-induced depassivation of iron in alkaline media by reactive force field molecular dynamics," *npj Mater Degrad,* vol. 3, no. 19, 2019.

[9] American Concrete Institute Committee 222, "Protection of Metals in Concrete Against Corrosion (ACI 222R-01)," 2001.

[10] C Alonso, C Andrade, M Castellote, P Castro, "Chloride threshold values to depassivate reinforcing bars embedded in a standardized OPC mortar," *Cement and Concrete Research,* vol. 30, no. 7, pp. 1047-1055, 2000.

[11] Japan Society of Civil Engineers, Standard Specifications for Concrete Structures - Design, 2008.

[12] Japan Society of Civil Engineers, Standard Specifications for Concrete Structures - Design, 2017.

[13] Ribeiro, Bruno; Yamamoto, Takashi; Yamashiki, Yosuke., "A Study on the Reduction in Hydration Heat and Thermal Strain of Concrete with Addition of Sugarcane Bagasse Fiber," *Materials,* vol. 13, no. 13, 2020.

[14] Ribeiro, B., Yamashiki, Y. & Yamamoto, T, "A study on mechanical properties of mortar with sugarcane bagasse fiber and bagasse ash," *Journal of Material Cycles and Waste Management,* 2020.

[15] M. Sappakittipakorn and N. Banthia, "Corrosion of Rebar and Role of Fiber Reinforced Concrete," *Journal of Testing and Evaluation,* vol. 40, no. 1, pp. 127-136, 2012.

8 DEVELOPMENT OF INTERLOCKING CONCRETE BLOCKS WITH ADDED SUGARCANE RESIDUES

8.1 Introduction

The infrastructure of a region usually depends on its availability of natural resources like sand and gravel. However, exhaustive mining leads to vegetation loss, loss of water retaining strata, lower groundwater table, and disturbance in the existing ecosystem. For these reasons, several regions adopted mining restrictions, which reduced suitable aggregates' availability at shorter haul distances. Consequently, aggregates' transportation from longer distances to construction sites increased their cost, increasing the total cost of construction[1].

The use of local aggregates for concrete is desirable not only to decrease costs but also to reduce environmental impact since more extended transportation emits more greenhouse gases. Nonetheless, the resource base's limitation does not allow several regions to produce their aggregates or suffer due to the shortage of options. Also, for islands with small land areas, it is imperative to conduct eco-friendly production activities from the viewpoints of waste reduction, resource-saving, and prevention of global warming.

Recently, the application of agro-residues in concrete has gained interest due to the high amount available worldwide. Among several agro-residues, there is the bagasse, which is a residue of sugarcane[2]. Usually, the bagasse is used as a primary fuel source in sugar/ethanol mills[3]. As a result, residual products composed of sand, ash[4, 5, 6, 7, 8], and non-burned bagasse are generated from the boilers. The sugarcane residues are generated in large quantities and create a severe disposal problem for the ethanol-sugar industry, affecting the environment and public health[9].

The bagasse ash is rich in silica and has a potential for pozzolanic reactivity and filler effect in concrete and mortar mixtures[10]. For this reason, to improve the quality of the burned residues collected from the boiler, a re-burning treatment process is applied[11, 12]. However, the re-burning treatment may be an unsustainable process due to the additional CO_2 emissions, no being an ecologically friendly approach.

In some studies, it was observed that the addition of polypropylene and steel fibers improves the mechanical properties of concrete[13, 14, 15]. It is known that plain concrete under tension exhibits brittle failure with initial cracking when there is no reinforcement[16]. However, the use of fibers in concrete as non-conventional mass reinforcement has been proved a promising alternative since it primarily enhances the inherent deficiencies of concrete, such as the weak tensile strength and the

limited deformation capacity in the presence of cracking[17]. This because cracking and, eventually, tensile failure of fiber reinforced concrete requires a debonding and pulling of the randomly distributed fibers in the concrete[13, 18].

Considering the results of the studies mentioned above, the bagasse fiber in cement composites may also improve concrete's mechanical properties. Previous studies reported that natural fiber reinforced cement composites have a high potential for replacing standard fiber materials due to their high performance in mechanical properties and their low cost[19, 20, 21, 22]. Therefore, the use of sugarcane residues in their original form - that is, in the state that the residues are generated out of mills or boilers - be a way to make both the civil engineering industry and the sugar/ethanol industry more sustainable[23].

In a previous study[23], sugarcane residues were classified into three different categories by the process of sieving: bagasse fiber, bagasse sand, and bagasse ash. These residues were utilized to prepare mortar specimens and to investigate the mechanical properties of mortars. The study revealed that mortar added with 2% of bagasse fiber showed a higher percentage of water retention when compared to the mortar specimens without fiber due to the high amount of bagasse fiber. However, the fibers used in this research passed through a 4.76 mm sieve and remained in a 2 mm sieve, leaving bagasse bigger than 4.76 mm to be cut or used in another way.

Recently, the phenomenon of the Urban Heat Islands (UHI) became a significant issue. The large proportion of artificial surfaces, such as concrete, absorbs and store more heat than natural vegetation, increasing the temperature in urban areas[24]. Several measures have been developed to mitigate UHI. These measures include cooler pavements' design by increasing the albedo of surfaces and making them more reflective, permeable, porous, and water retentive[25].

Since the sugarcane bagasse fiber is known for its high-water retention and water absorption characteristics, there is a possibility to take these advantages and use bagasse fiber bigger than 4.76 mm as concrete aggregates for the production of sidewalk blocks since they do not require high strength resistance. This study, therefore, uses sugarcane residues in their original form to prepare interlocking concrete blocks and investigate the flexural strength of these blocks. Besides, assessing the performance on the temperature decrease of sidewalk pavement material containing sugarcane residues was performed.

8.2 Research design and methodology

8.2.1 Materials

The surface layer of all interlocking concrete blocks was made using white Portland cement (WPC) and quartz sand (QS). In the case of the base layer of all interlocking concrete blocks, ordinary Portland cement (C), coarse aggregate FM: 5.00 (G), and fine aggregate FM: 3.05 (S) were used. Tap water (W) and the chemical admixture CA (MasterMatrix 200, 1.03-1.07 g/cm^3) for immediate demolding products (air entrainment type) were used in both layers for the preparation of the interlocking concrete blocks.

Figure 8.1 shows a diagram of the aggregate production process using sugarcane residues, and Figure 8.2 shows the categorized residual materials used in this study. The sugarcane residues (raw bagasse and burned residues) were acquired from a sugar mill in Okinawa Prefecture, Japan. The raw bagasse was dipped in water at 30°C for 30 minutes and then dried in the open air. This process is intended to reduce the residual sugar content of the bagasse and eliminate impurities [20, 26, 27]. Afterward, the residues were classified by the sieving process. The raw bagasse that passed through a 9.52 mm sieve and remained in a 4.75 mm sieve was classified as a large bagasse fiber (BFL), while the raw bagasse that passed through a 4.75 mm sieve and remained in a 2.36 mm sieve was classified as a small bagasse fiber (BFS). The burned residues that passed through a 1.18 mm sieve and remained in a 0.297 mm sieve were classified as bagasse sand (BS). The physical properties of the materials are given in Table 8.1.

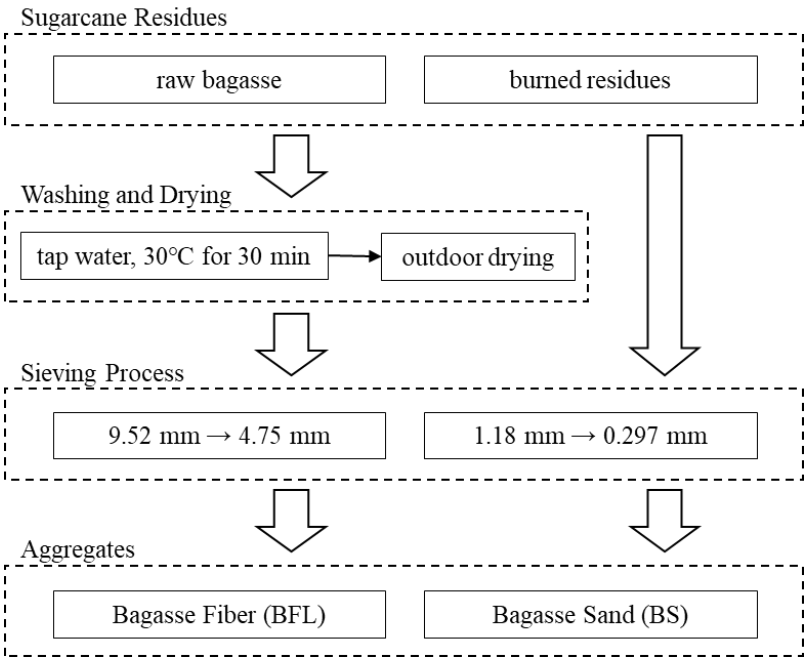

Figure 8.1 Diagram of the aggregate production process

BFS BFL BS

Figure 8.2 Sugarcane residual material

Table 8.1 Physical properties of cement and aggregates

Properties	Materials							
	Surface layer		Base layer					
	WPC	QS	C	G	S	BFL	BFS	BS
Density (g/cm^3)	3.05	2.60	3.16	2.68	2.68	0.49	0.49	1.29
Total alkali content (%)	0.1	—	0.56	—	—	—	—	—
Specific surface area (cm^2/g)	3440	—	3280	—	—	—	—	—
Loss on ignition (%)	2.79	—	2.26	—	—	—	—	—

8.2.2 Concrete mixture

The mix proportions of the surface and the base layer of interlocking concrete blocks are shown in Table 8.2. The surface layer's composite is the mixture with water to cement ratio (W/C) of 25.0%. The surface layer mixture was the same for all blocks. In the base layer case, composite C is the mixture with a W/C of 14.7%. Composite C represents the standard interlocking concrete blocks and contains no sugarcane residues materials. In the case of BFL blocks, three mixtures were prepared with non-burned residues volume ratios of 1, 2, and 5% compared to the total amount of aggregates. In order to compare the influence of the bagasse fiber size in the interlocking concrete blocks, blocks using BFS were prepared with a volume ratio of 2% compared to the total amount of aggregates. Moreover, the interlocking concrete blocks using bagasse sand (BS) were prepared. In this case, the BFL volume ratio is 2%, and the BS volume ratio is 5%, for a total of sugarcane residues ratio of 7% compared to the total amount of aggregates. All residues materials were replaced in place of the aggregates in the same proportions.

Table 8.2 Mix proportions of the surface and base layer of specimens

Layer	Composites	Residues Type	Residues (Vol. %)	W/C	Unit (kg/m^3)									
					WPC	QS	C	W	G	S	BFL	BFS	BS	CA
Surface	—	—	—	0.25	582.6	1721.7	—	145.6	—	—	—	—	—	1.2
Base	C	—	—	0.15	—	—	436.1	64.0	1068.0	1068.0	—	—	—	1.1
	BFL1	Bagasse Fiber	1		—	—			1057.3	1057.3	3.9	—	—	1.1
	BFL2	Bagasse Fiber	2		—	—			1046.6	1046.6	7.8	—	—	1.1
	BFL5	Bagasse Fiber	5		—	—			1014.6	1014.6	19.5	—	—	1.1
	BFS2	Bagasse Fiber	2		—	—			1046.6	1046.6	—	7.8	—	1.1
	BS	Bagasse Fiber	2		—	—			993.2	993.2	7.8	—	51.4	1.1
		Bagasse Sand	5		—	—								

8.2.3 Preparation of blocks

The surface layer concrete was prepared using an oscillating type mixer (OM-70NB8). First, the cement and the quartz sand were placed into the mixer and dry mixed for 20 seconds at low speed (rotation speed: 120 ± 5 rpm). After that, the mixer speed was changed to high speed (rotation speed: 216 ± 5 rpm), and the dry mixing continued for 30 seconds. The water and admixture were then placed into the mixer and mixed for 20 seconds at low speed (rotation speed: 120 ± 5 rpm) and 50 seconds at high speed (rotation speed: 216 ± 5 rpm).

In the base layer concrete, the cement and sand were placed into the mixer and dry mixed for 20 seconds at low speed (rotation speed: 120 ± 5 rpm) and for another 30 seconds at high speed (rotation speed: 216 ± 5 rpm). Later, the residues, water, and admixture were placed into the mixer and mixed for another 30 seconds at low speed (rotation speed: 120 ± 5 rpm) and 60 seconds at high speed (rotation speed: 216 ± 5 rpm). All mixtures were mixed in an oscillating type mixer (OM-350NB8).

The mixture of the base layer of interlocking concrete blocks was cast in formwork of 98 × 198 × 60 mm, pressed (about 2682.5 kgf), and vibrated (50 Hz, 4000 rpm) for about 1 second. Right after, the mixture of the surface layer of interlocking concrete blocks specimens was cast on the base layer mixture in the formwork, pressed (about 3756.0 kgf), and vibrated (55 Hz, 4500 rpm) for additional 4 seconds. Then, the specimens were de-molded, placed in a room, and cured for 1, 3, 5, 7, 10, 14, and 28 days. The outline of the samples is shown in Figure 8.3.

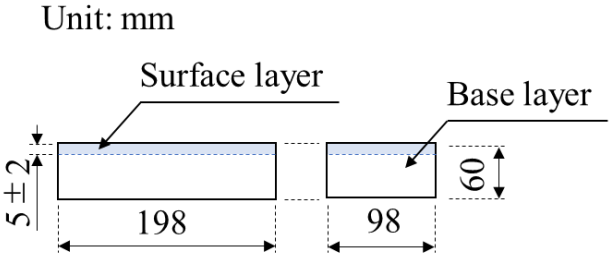

Figure 8.3 Outline of specimens

8.2.4 Flexural strength test

A flexural strength test was performed to determine the flexural strength of the blocks according to JIS A 5371 at 1, 3, 5, 7, 10, 14, and 28 days. The flexural strength was calculated using the following equation:

$$\sigma = \frac{3LF}{2bd^2}$$

Where:

σ: flexural strength (N/mm^2);

L: span (mm);

F: maximum load (N);

b: width (mm); and

d: thickness (mm).

The blocks were placed on equipment with the surface layer facing up, as shown in Figure 8.4.

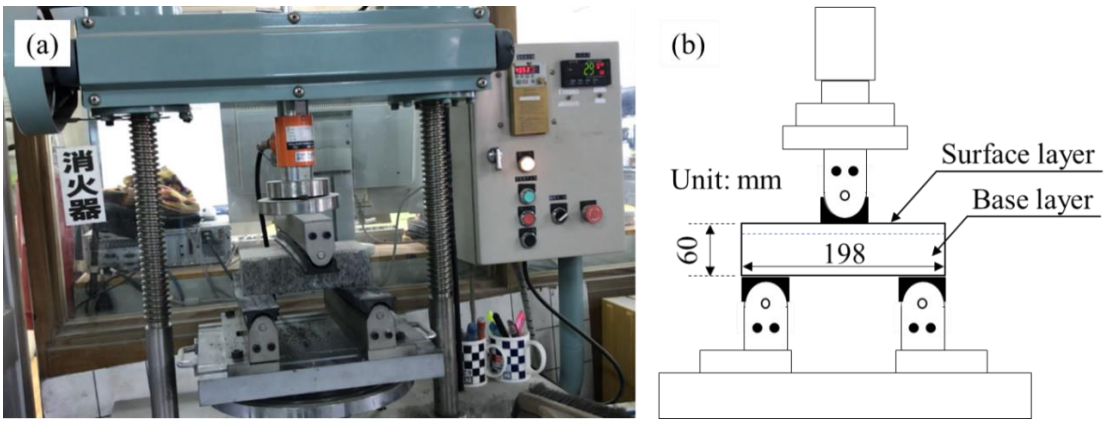

Figure 8.4 Overview of the test rig (a) and details of the placement of the block in the rig(b)

8.2.5 Surface temperatures measurement

The interlocking concrete blocks' surface temperature was measured to evaluate the mitigation effects of urban heat islands. Three blocks of each mixture were soaked in water for 24 hours. After that, the blocks were removed from the water and placed horizontally on a net for 30 minutes in order to remove the excess water on the blocks' surface. Afterward, as shown in Figure 8.5, each mixture's blocks were put on a formwork made by polyethylene foam to avoid influences from undesired sides and expose just one side. Right after the placement, the blocks were exposed to solar radiation for 7 hours. The blocks' surface temperature was measured every 15 minutes during the solar radiation exposure using a non-contact digital infrared thermometer and a thermography camera. This measurement was realized on April 22, 2020, with an ambient temperature between 24 and 28°C, with humidity between 52 and 77%.

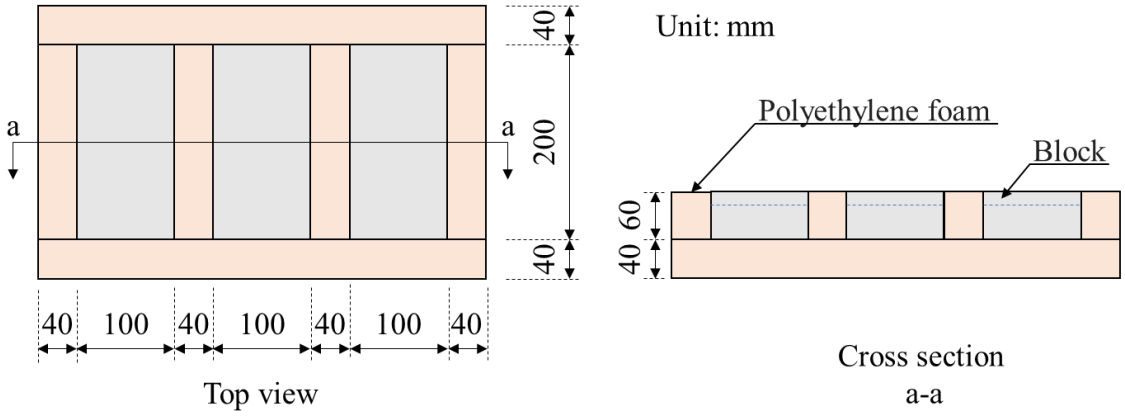

Figure 8.5 Polyethylene foam form

The surface temperature measurement was measured at both surfaces of the blocks. One block with the surface layer facing up and two blocks with the base layer facing up. The effect of sugarcane residues on the mitigation of surface temperature of blocks can be directly evaluated with the base layer facing up.

The interlocking concrete blocks used to measure the surface temperatures were also used to determine the water retention content and water evaporation rate. After the blocks of each mixture were soaked in water for 24 hours, removed from the water, and placed horizontally on a net for about 30 minutes, the blocks were weighted as wet mass (M1). At the end of 7 hours of exposure to solar radiation, the weight of the blocks was measured (M2) again to calculate the water evaporation rate. After measuring M2, the blocks were completely dried in a drying furnace at 105°C until they attained a substantially constant mass. Afterward, the blocks were stored, cooled to room temperature, and then their weights (M3) as absolute dry mass were measured. The equation used in

the calculation of water evaporation rate is the following:

$$\boldsymbol{ER_w = \frac{M_1 - M_2}{M_1 - M_3} \times 100}$$

Where:

ER_w: water evaporation rate (%);

M_1: wet mass of block (g);

M_2: mass of block right after 7 hours of exposure to solar radiation (g); and

M_3: absolute dry mass of block (g).

The water retention content was calculated using the following equation:

$$\boldsymbol{RC_w = \frac{M_1 - M_3}{V}}$$

Where:

RC_w: water retention content (g/cm^3)

V: volume of block (cm^3)

8.3 Results and discussions

8.3.1 Flexural strength test

Figure 8.6 shows the flexural strength test results after 1, 3, 5, 7, 10, 14, and 28 days of curing. According to JIS A 5371, the interlocking concrete blocks with a flexural strength above or equal to 3 N/mm^2 could be used as pavement for pedestrians restricted to light vehicle traffic. When the flexural strength is above or equal to 5 N/mm^2, the restriction is extended to heavy vehicle traffic.

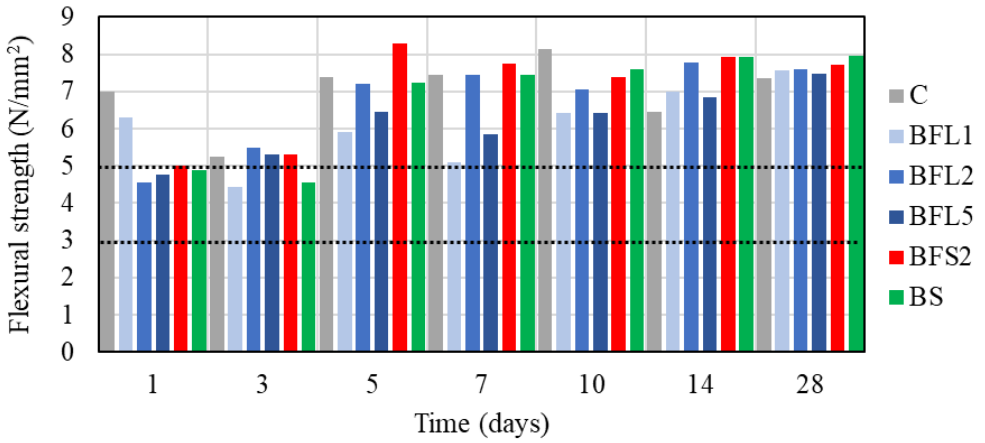

Figure 8.6 Flexural strength of each mixture at 1, 3, 5, 7, 10, 14, and 28 days

As shown in Figure 8.6, all mixtures' flexural strength exceeded the requiring standard for pavement for pedestrians restricted to light vehicle traffic. However, in the cases where the sugarcane residues were added into the mixture, the flexural strength is smaller than C and could not achieve 5 N/mm^2 after one day of curing. The probable explanation is that the presence of some water-soluble sugars may have retarded the setting of concrete[28].

In order to verify the presence of sugar, 4 g of bagasse fiber was cut, and 40 mL of H_2O was added; subsequently, this mixture was allowed to stand for about 2 hours. Later, it was centrifuged at 8000 rpm at 20°C for 30 minutes. Then, 10 ml supernatant was lyophilized and dissolved in 1 ml of acetonitrile/water (CH_3CN/H_2O=75/25). This solution was used as a sample to analyze the reducing sugar. Thereafter, 0.2 ml of sample, 0.4 ml of reagent A ($NaCO_3$ (40g/L), Glycine (16g/L), $CuSO_4 \cdot 5H_2O$ (0.45g/L)) and 0.4 ml of reagent B (neocuproine hydrochloride (0.15g/100ml)) were mixed. The mixture was heated at 100°C for 12 minutes and rapidly cooled. 1 ml of H_2O was added, and the absorbance at 450 nm was measured. From the calibration curve prepared with glucose, the reducing sugar content of the sample was determined as a glucose equivalent.

The result indicates that the reducing sugar content was 1.49 mg/g, confirming the presence of water-soluble sugars that affected the hardening and hydration of cement. However, as shown in Figure 8.6, the flexural strength of blocks added with residues tends to increase with time, and after ten days of curing, all blocks satisfied the standard of 5 N/mm^2.

After 14 days, the flexural strength was 6.46, 7.00, 7.78, 6.84, 7.92, and 7.93 N/mm^2; after 28 days, the flexural strength was 7.36, 7.58, 7.60, 7.47, 7.72, and 7.96 N/mm^2 for C, BFL1, BFL2, BFL5, BFS2, and BS, respectively. From these results, it can be said that the higher the amount of fiber added, the higher is the flexural strength acquired. These high flexural strengths are caused by the

fiber networks, which act as a stress transfer bridge. The fiber network reinforces the blocks against the crack propagation, controlling their openings and possibly delaying the blocks' breakage. However, in the case of BFL5, the flexural strength was not proportional, resulting in a flexural strength smaller than the case BFL1. When a high amount of fibers is added to the blocks, the fibers may not effectively transfer the stress to the other cross-sections of the blocks. This may be due to the voids between the fiber and the matrix, as can be seen in Figure 8.7, and due to the fiber clusters together, which may affect the transmission of stress.

Figure 8.7 Voids between the fiber and the matrix (cross-section)

It is also possible to see from Figure 8.6 that the flexural strength of BFS2 is higher than BFL2. In other words, when thin fibers are added to the mixture, the flexural strength tends to be higher than when thick fibers are added to the mixture. Since the sieving process classified the bagasse fibers, the BFS tends to be more uniform, distributing uniformly into the mixture. In BFL, the fibers tend to cluster easier, which probably hinders their distribution into the matrix. However, in the case of BS, the flexural strength after 14 days exceeds all cases. Although the fibers used in BS are the BFL, the bagasse sand tends to fill the small pores of the blocks in which the blocks become denser than compared to the case of BFL2.

8.3.2 Water retention content

Figure 8.8 shows the water retention content of interlocking concrete blocks. According to "Manual for Interlocking Blocks Pavement Design and Construction" published by the Japan Interlocking Blocks Pavement Engineering Association (JIPEA), the water retentivity of the "water-retentive type" interlocking blocks has to be greater or equal to 0.15 g/cm^3.

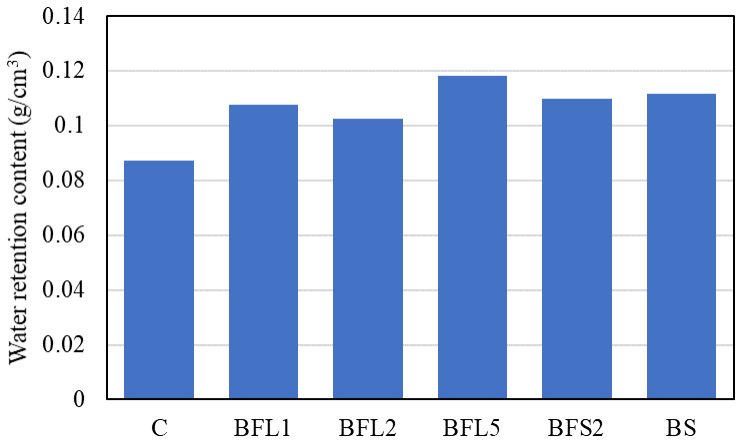

Figure 8.8 Water retention content

Although this study's purpose was not to achieve the standards of "water-retentive type" interlocking blocks, it is possible to see from Figure 8.8 that the water retention content increased with the addition of the sugarcane residues. In BFL5, the water retention content achieved a value of 0.118 g/cm^3, while the water retention content of the control composite C was just 0.087 g/cm^3. This increase may be due to the bagasse fibers having an excellent water-holding capacity and the possible significant amount of voids between the fiber and the matrix. The advantage of retaining a higher amount of water in concrete blocks pavement is that it can prevent the rise in temperature of the road surface by removing heat by the evaporation of moisture[29].

8.3.3 Surface temperatures measurement and water evaporation rate

Figure 8.9 and Figure 8.10 show the surface temperature measurement of the interlocking blocks when the surface layer and base layer are facing up, respectively. Figure 8.11 illustrates the water evaporation rate ER_w of the interlocking blocks.

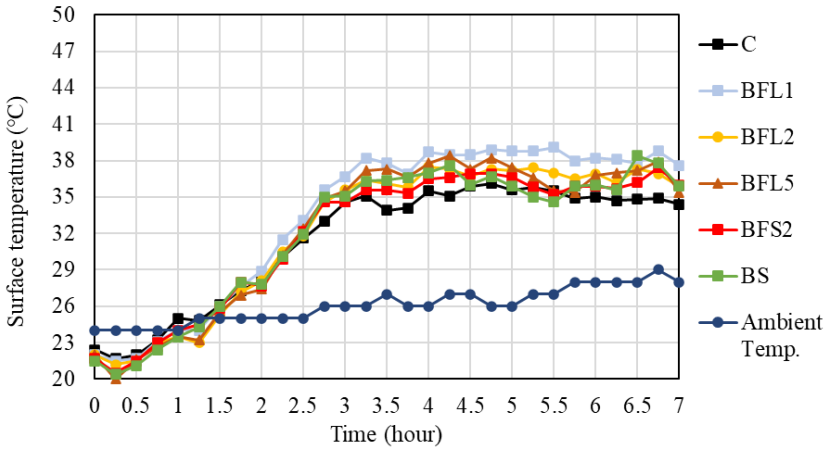

Figure 8.9 Surface temperature of the interlocking blocks (surface layer)

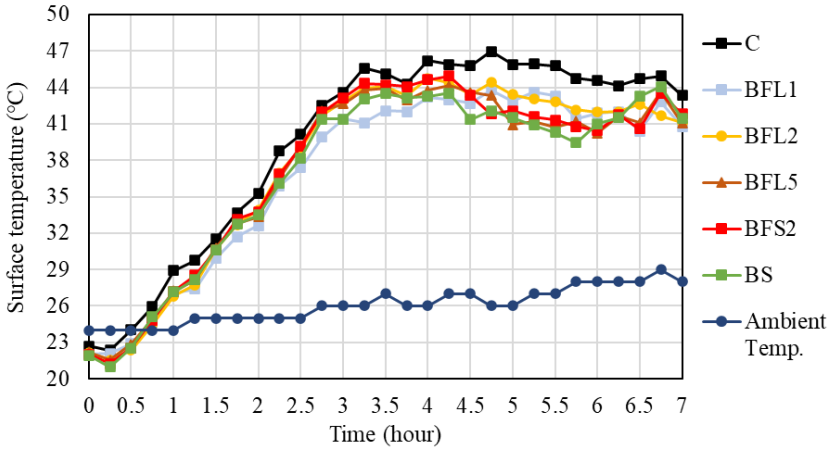

Figure 8.10 Surface temperature of the interlocking blocks (base layer)

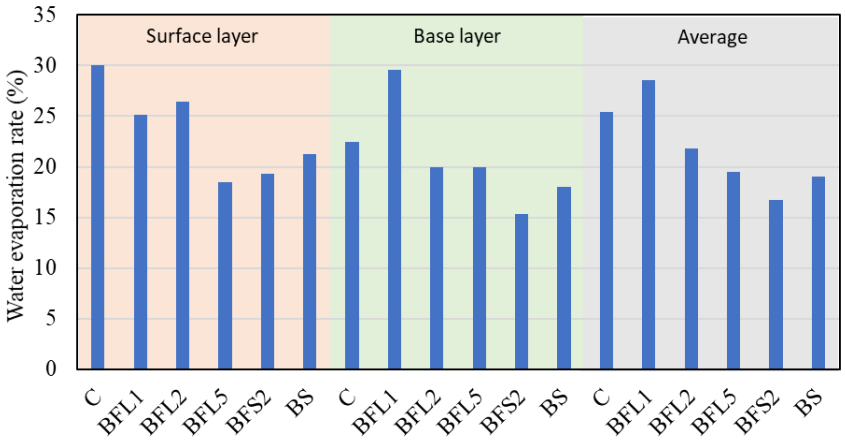

Figure 8.11 Water evaporation rate

The averages of the surface temperatures of the surface layer for C, BFL1, BFL2, BFL5, BFS2, and BS were 31.4, 33.4, 32.3, 32.3, 31.9, and 32.0°C, respectively. The average surface temperatures were 39.4, 37.0, 37.6, 37.3, 37.5, and 37.0°C. The average temperatures of the surface layers were lower than the temperatures of the base layers. This difference is due to the surface color: the surface layer was prepared using a white Portland cement, and consequently, the surface color became white - which can reflect much more solar radiation than a grey color (base layer). The average surface temperatures of both layers for C, BFL1, BFL2, BFL5, BFS2, and BS were 35.4, 35.2, 35.0, 34.8, 34.7, and 34.5°C, respectively.

Figure 8.9 shows that mix C has a lower temperature than the other samples. However, it can be seen in Figure 8.11 that the water evaporation rate in the case of C is higher in comparison to other cases. A smaller water retention content and higher water evaporation may result in a higher elevation on surface temperature on the hottest days. It is possible to see in Figure 8.10 that when the base layer is faced up, and the surface color is grey, the surface temperature of C is higher than

the other cases, as well as its evaporation rate (Figure 8.11) is higher than the other cases, excepting BFL1.

Figure 8.12 illustrates the relationship between the surface temperature and the water evaporation rate. It is possible to see in Figure 8.12 that, in the cases of C and BFL1, the surface temperatures and the water evaporation rates are higher in comparison to the other cases. From these results, it can be concluded that the surface temperature of the blocks may be reduced by the addition of a certain amount of sugarcane residues into the interlocking concrete blocks and may mitigate the urban heat island. Also, reducing the surface temperature with added sugarcane residues into the blocks may be expected for a more extended period since the water evaporation rate is lower than C. However, other factors such as density, wind effect, and ambient humidity should be investigated to clarify the whole mechanism.

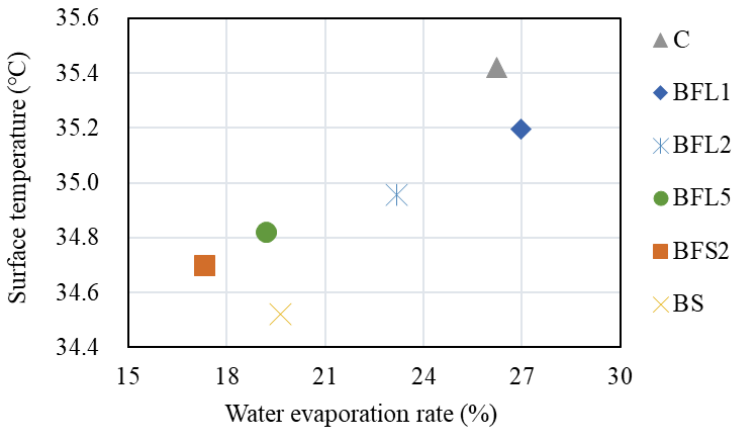

Figure 8.12 Relation between the surface temperature and the water evaporation rate

8.4 Conclusion of chapter

Sugarcane residues in their original form were used to prepare interlocking concrete blocks. The flexural strength slightly increases due to the effect of the fibers network. Besides, since the sugarcane bagasse fiber has a good water retention characteristic, the interlocking concrete blocks surface's surface was reduced, with smaller water evaporation. The results obtained in this study can be summarized as:

1. The flexural strength was 6.46, 7.00, 7.78, 6.84, 7.92, and 7.93 N/mm^2 after 14 days of curing and 7.36, 7.58, 7.60, 7.47, 7.72, and 7.96 N/mm^2 after 28 days of curing for C, BFL1, BFL2, BFL5, BFS2, and BS, respectively. These values meet the requirement stipulated by JIS A 5371 of 5 N/mm^2, which may be used as pavement for pedestrians and heavy vehicle traffic.
2. The water retention content increases with the addition of the sugarcane residues. In BFL5,

which were prepared with a volume ratio of 5% of bagasse fibers (4.75-9.52 mm) 5% compared to the total amount of aggregates, the water retention content achieved a value of 0.118 g/cm^3. In contrast, the water retention content of the control composite C was 0.087 g/cm^3.

3. The average surface temperature of both surface and base layers for C, BFL1, BFL2, BFL5, BFS2, and BS were 35.4, 35.2, 35.0, 34.8, 34.7, and 34.5°C, respectively.
4. In C and BFL1 cases, the surface temperatures and the water evaporation rates are higher in comparison to the other cases, in which the amount of residue was higher.

8.5 References

[1] Jayvant Choudhary, Brind Kumar, Ankit Gupta, "Utilization of solid waste materials as alternative fillers in asphalt mixes: A review," *Construction and Building Materials,* vol. 234, 2020.

[2] Jnyanendra Kumar Prusty, Sanjaya Kumar Patro, S.S. Basarkar, "Concrete using agro-waste as fine aggregate for sustainable built environment – A review," *International Journal of Sustainable Built Environment,* vol. 5, no. 2, pp. 312-333, 2016.

[3] Silvio Rainho Teixeira; Amanda Arenales; Agda Eunice de Souza; Renata da Silva Magalhães; Angel Fidel Vilche Peña; Davi Aquino; Rosane Freire, "Sugarcane bagasse: applications for energy production and ceramic materials," *The Journal of Solid Waste Technology and Management,* pp. 229-238, 2015.

[4] Almir Sales; Sofia Araújo Lima, "Use of Brazilian sugarcane bagasse ash in concrete as sand replacement," *Waste Management,* vol. 30, p. 1114–1122, 2010.

[5] Fernando C.R. Almeida; Almir Sales; Juliana P. Moretti; Paulo C.D. Mendes, "Sugarcane bagasse ash sand (SBAS): Brazilian agroindustrial by-product," *Construction and Building Materials,* vol. 82, pp. 31-38, 2015.

[6] J.F. Martirena Hernández; B. Middendorf, M. Gehrke; H. Budelmann, "Use of wastes of the sugar industry as pozzolana in lime-pozzolana binders: study of the reaction," *Cement and Concrete Research,* vol. 28, no. 11, pp. 1525-1536, 1998.

[7] Nuntachai Chusilp; Chai Jaturapitakkul; Kraiwood Kiattikomol, "Effects of LOI of ground bagasse ash on the compressive strength and sulfate resistance of mortars," *Construction and Building Materials,* vol. 23, p. 3523–3531, 2009.

[8] K. Umamaheswaran; Vidya S. Batra, "Physico-chemical characterisation of Indian biomass ashes," *Fuel,* vol. 87, p. 628–638, 2008.

[9] Suzimara Rovani, Jonnatan J. Santos, Paola Corio and Denise A. Fungaro, "An Alternative and Simple Method for the Preparation of Bare Silica Nanoparticles Using Sugarcane Waste

Ash, an Abundant and Despised Residue in the Brazilian Industry," *Journal of the Brazilian Chemical Society,* vol. 30, pp. 1524-1533, 2019.

[10] E. CÂMARA; R. C. A. PINTO; J. C. ROCHA, "Setting process on mortars containing sugarcane bagasse ash," *Ibracon Structures and Materials Journal,* vol. 9, no. 4, pp. 617-642, 2016.

[11] M.A. Tantawy; A.M. El-Roudi; A.A. Salem, "Immobilization of Cr(VI) in bagasse ash blended cement pastes," *Construction and Building Materials,* vol. 30, pp. 218-223, 2012.

[12] G.C. Cordeiro; R.D. Toledo Filho; E.M.R. Fairbairn, "Effect of calcination temperature on the pozzolanic activity of sugar cane bagasse ash," *Construction and Building Materials,* vol. 23, pp. 3301-3303, 2009.

[13] C.E. Chalioris, E.F. Sfiri, "Shear Performance of Steel Fibrous Concrete Beams," *Procedia Engineering,* vol. 14, pp. 2064-2068, 2011.

[14] H.T. Wang, L.C. Wang, "Experimental study on static and dynamic mechanical properties of steel fiber reinforced lightweight aggregate concrete," *Construction and Building Materials,* vol. 38, pp. 1146-1151, 2013.

[15] İlker Bekir Topçu, Mehmet Canbaz, "Effect of different fibers on the mechanical properties of concrete containing fly ash," *Construction and Building Materials,* vol. 21, no. 7, pp. 1486-1491, 2007.

[16] Seung-Won Choi, Jongkwon Choi, and Seong-Cheol Lee, "Probabilistic Analysis for Strain-Hardening Behavior of High-Performance Fiber-Reinforced Concrete," *Materials,* vol. 12, no. 15, 2019.

[17] Constantin E. Chalioris, "Analytical approach for the evaluation of minimum fibre factor required for steel fibrous concrete beams under combined shear and flexure," *Construction and Building Materials,* vol. 43, pp. 317-336, 2013.

[18] Violetta K. Kytinou, Constantin E. Chalioris and Chris G. Karayannis, "Analysis of Residual Flexural Stiffness of Steel Fiber-Reinforced Concrete Beams with Steel Reinforcement," *Materials,* vol. 13, no. 12, 2020.

[19] Noor Zawati Zakaria, Mohd Zailan Sulieman, Roslan Talib, "Turning Natural Fiber Reinforced Cement Composite as Innovative Alternative Sustainable Construction Material A Review Paper," *International Journal of Advanced Engineering, Management and Science (IJAEMS),* vol. 1, no. 8, pp. 24-31, 2015.

[20] Ferreira, Carla Regina; Tavares, Sheron Stephany; Ferreira, Bruno Henrique Moreira; Fernandes, Amanda Martins; Fonseca, Sara Jane Gomes; Oliveira, Carlos Augusto de Souza; Teixeira, Ricardo Luiz Perez; Gouveia, Leonardo Lúcio de Araújo, "Comparative

study about mechanical properties of strutural standard concrete and concrete with addition of vegetable fibers," *Materials Research,* vol. 20, no. 2, pp. 102-107, 2017.

[21] Rosamaria Codispoti, Daniel V. Oliveira, Renato S. Olivito, Paulo B. Lourenço, Raul Fangueiro, "Mechanical performance of natural fiber-reinforced composites for the strengthening of masonry," *Composites Part B: Engineering,* vol. 77, pp. 74-83, 2015.

[22] Ribeiro, Bruno; Yamamoto, Takashi; Yamashiki, Yosuke., "A Study on the Reduction in Hydration Heat and Thermal Strain of Concrete with Addition of Sugarcane Bagasse Fiber," *Materials,* vol. 13, no. 13, 2020.

[23] Ribeiro, B., Yamashiki, Y. & Yamamoto, T, "A study on mechanical properties of mortar with sugarcane bagasse fiber and bagasse ash," *Journal of Material Cycles and Waste Management,* 2020.

[24] Sushobhan Sen, Jeffery Roesler, Benjamin Ruddell and Ariane Middel, "Cool Pavement Strategies for Urban Heat Island Mitigation in Suburban Phoenix, Arizona," *Sustainability,* vol. 11, 2019.

[25] Mohajerani, A. Bakaric, J. and Jeffrey-Bailey, "The Urban Heat Island Effect, its Causes, and Mitigation, with Reference to the Thermal Properties of Asphalt Concrete," *Journal of Environmental Management,* vol. 197, pp. 522-538, 2017.

[26] Matheus Roberto Cabral; Juliano Fiorelli; Holmer Savastano Junior; Robert Lagacé; Stéphane Godbout; Joahnn H. Palacios, "Study of the potential use of the sugarcane bagasse in cement-panels," *10th International Conference on Composite Science and Technology,* 2015.

[27] Marie-Ange Arsène; A. Okwo; Ketty Bilba; A. B. O. Soboyejo; W. O. Soboyejo, "Chemically and thermally treated vegetable fibers for reinforcement of cement-based composites," *Materials and Manufacturing Processes,* vol. 22, no. 2, pp. 214-227, 2007.

[28] K Bilba, M-A Arsene, A Ouensanga, "Sugar cane bagasse fibre reinforced cement composites. Part I. Influence of the botanical components of bagasse on the setting of bagasse/cement composite," *Cement and Concrete Composites,* vol. 25, no. 1, pp. 91-96, 2003.

[29] A. KARASAWA, K. TORIIMINAMI, N. EZUMI, K. KAMAYA, "Evaluation of performance of water-retentive concrete block pavements," *8th International Conference on Concrete Block Paving,* 2006.

9 AN ENVIRONMENTAL AND COST ASSESSMENT OF CONCRETE WITH ADDITION OF SUGARCANE RESIDUES

9.1 Introduction

The transportation of aggregates from longer distances to construction sites increases the total cost of construction[1, 2] and impacts the environment with greenhouse gas emissions due to long-distance transportation.

Okinawa Prefecture is one of the 47 prefectures of Japan, located in the southwest of the country. Since Okinawa Prefecture consists of a series of small islands, the concrete aggregates are generally crushed stone and sea sand due to the lack of adequate places to obtain ordinary river aggregates[3]. Also, the mining/collection of the aggregates is concentrated on the main island of Okinawa, where the capital city Naha is located. Therefore, the aggregates are transported from the main to smaller islands by vessels. Figure 9.1 illustrates the prices per m^3 of the fine aggregates, which are available online or published monthly in a magazine[4, 5], and the location of sugar factories in Okinawa Prefecture[6].

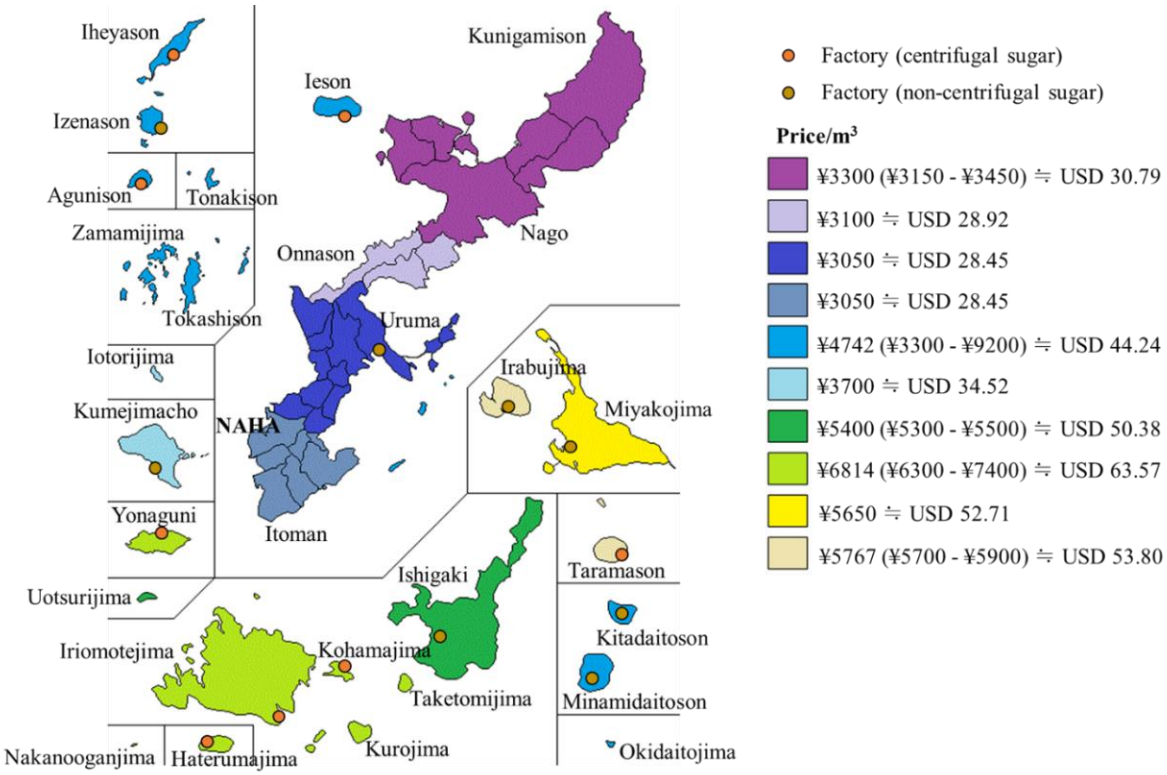

Figure 9.1 Price of the fine aggregates and location of sugar factories in Okinawa Prefecture

The use of sugarcane residues as construction aggregates provides a more sustainable alternative to

the construction industry and the sugar/ethanol industry[7]. Local sugarcane residues as aggregates for concrete, especially for islands with small land areas, are desirable since they can reduce the environmental load and decrease transportation greenhouse gas emissions. Besides, the development of more construction material options is critical since a country's policies may repeatedly change. The Japanese government announced that it aims to reduce coal-fired power generation by about 90% by 2030[8]. This can dramatically reduce fly ash production in all of Japan, and consequently, it may impact the use of fly ash as aggregates. Therefore, this study aims to assess the environmental impacts and costs reduction of the utilization of sugarcane residues as concrete aggregates in the production of interlocking concrete blocks by vising structures of prevention or mitigation of natural disasters.

9.2 Environmental Assessment

9.2.1 Goal and scope

This study aims to make an environmental assessment comparison between interlocking blocks with sugarcane residues and conventional interlocking concrete blocks. However, except for aggregates where the proportions were modified (see Table 8.2), materials such as cement, water, and chemical admixtures were excluded from the research scope and the mixing process that was carried out under the same conditions for all mixtures. The scope of recycling interlocking concrete blocks removed after their useful life as pavement was also excluded from the analysis. Usually, the leading destination of recycled mortar and concrete is the construction of pavement[9]. This study assumed that the interlocking blocks used here could be recycled to pavements materials.

Based on the above, the study has focused only on sugarcane residues and conventional aggregates. It has set the scope of the investigation to the raw materials, manufacturing, and transportation processes.

9.2.2 System boundaries of scenarios

Three scenarios were considered on the main island of Okinawa. Figure 9.2 shows the system boundaries on the main island of Okinawa.

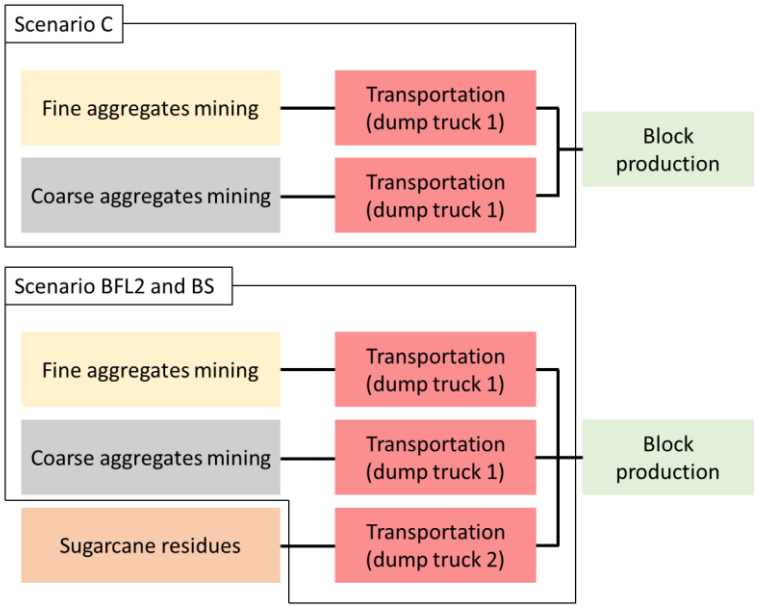

Figure 9.2 System boundaries on the main island of Okinawa

As seen in Figure 9.2, scenario C considers the conventional interlocking concrete blocks' environmental assessment in which sugarcane residues were not used. Scenario BFL2 and BS consider the environmental assessment of the interlocking concrete blocks with sugarcane residues. The mix proportion of the blocks used in each scenario is shown in Table 8.2.

Also, similar scenarios were applied on two other islands: Minamidaito and Yonaguni. In these cases, there is a more complex way of transportation. Figure 9.3 and Figure 9.4 show the system boundaries in the cases of Minamidaito and Yonaguni, respectively. It was assumed that the blocks were prepared near each island's main port to avoid other transportation. Also, the sugarcane residues are produced on the same island where the interlocking concrete blocks were supposedly produced (see Figure 9.1). Therefore, the residues do not need vessel transportation.

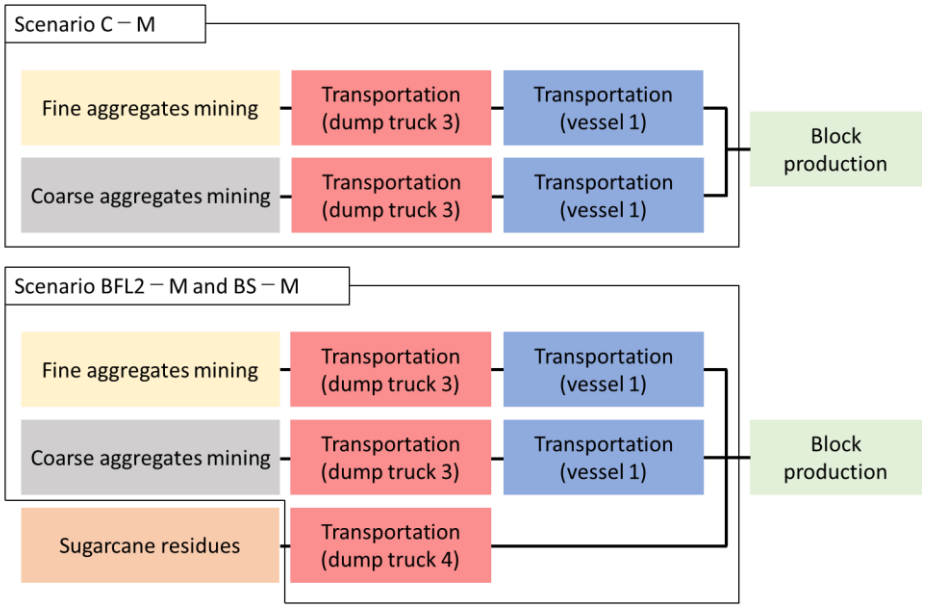

Figure 9.3 System boundaries on Minamidaito

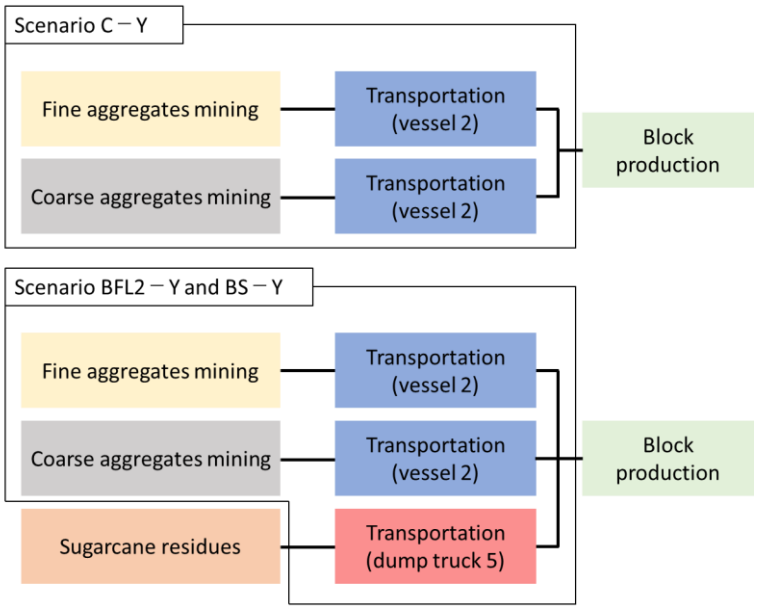

Figure 9.4 System boundaries on Yonaguni

The environmental load in all scenarios was calculated. However, since the bagasse residues are a waste of mining/collection, it was not considered. The functional unit of the assessment assumes 1000 liters of concrete.

9.2.3 Inventory

The environmental assessment analysis includes emissions associated with aggregate manufacturing and transportation. The environmental load associated with aggregate manufacturing and transportation is shown in Table 9.1. The truck and vessel presumed for the aggregates' transportation,

including the residues materials, were a 10-ton dump truck with a diesel engine and a 500-ton capacity vessel.

Table 9.1 Environmental load associated with aggregate manufacturing and transportation [10, 11]

	Unit (*)	Carbon dioxide (kg-CO_2/*)	Sulfur oxide (kg-SOx/*)	Nitrogen oxide (kg-NOx/*)	Dust and soot (kg-PM/*)
Fine aggregate	kg/t	3.7	0.00860	0.00586	0.00199
Coarse aggregate	kg/t	2.9	0.00607	0.00415	0.00141
Dump truck	km•t	0.117	0.0000901	0.000875	0.0000735
Vessel	km•t	0.162	0.00280	0.00470	0.0000721

The equation used to calculate the total environmental load is shown as follow:

$$\boldsymbol{EL} = \sum_{\boldsymbol{M_E}} [(\boldsymbol{A_S} \times \boldsymbol{E_S}) + (\boldsymbol{A_G} \times \boldsymbol{E_G})] + \sum_{\boldsymbol{T_E}} [(\boldsymbol{T_S} \times \boldsymbol{E_t}) + (\boldsymbol{T_G} \times \boldsymbol{E_t}) + (\boldsymbol{T_R} \times \boldsymbol{E_t})]$$

Where:

EL: total environment load (kg);

M_E: sum of emissions by aggregate (kg);

T_E: sum of emissions by aggregate transport (kg);

A_S: amount of fine aggregate (kg);

E_S: emissions by fine aggregate (kg/ton);

A_G: amount of coarse aggregate (kg);

E_G: emissions by coarse aggregate (kg/ton);

T_S: transport distance of fine aggregate (km);

T_G: transport distance of coarse aggregate (km);

T_R: transport distance of sugarcane residues (km); and

E_t: emissions by transport (kg/(km·ton)).

The distance from the mining/collection place of the aggregates and residues to the plant where the interlocking concrete blocks were prepared is shown in Table 9.2.

Table 9.2 Distance from mining/collection place to plant

Scenario	Transportation	Route	Distance (km)	
		From/To	Fine and coarse aggregate	Residues
Main Island	dump truck 1	Motobu/Uruma	51.4	—
	dump truck 2	Uruma/Uruma	—	9.5
Minamidaito	dump truck 3	Motobu/Naha	85.7	—
	dump truck 4	Minamidaito/Minamidaito	—	5.5
	vessel 1	Naha/Minamidaito	388	—
Yonaguni	dump truck 5	Yonaguni/Yonaguni	—	6.0
	vessel 2	Ishigaki/Yonaguni	131	—

9.3 Results and discussions

9.3.1 Environmental load associated with the production of interlocking concrete blocks

Figure 9.5, Figure 9.6, Figure 9.7, and Figure 9.8 show the amount of carbon dioxide, sulfur oxide, nitrogen oxide, and dust and soot emissions, respectively.

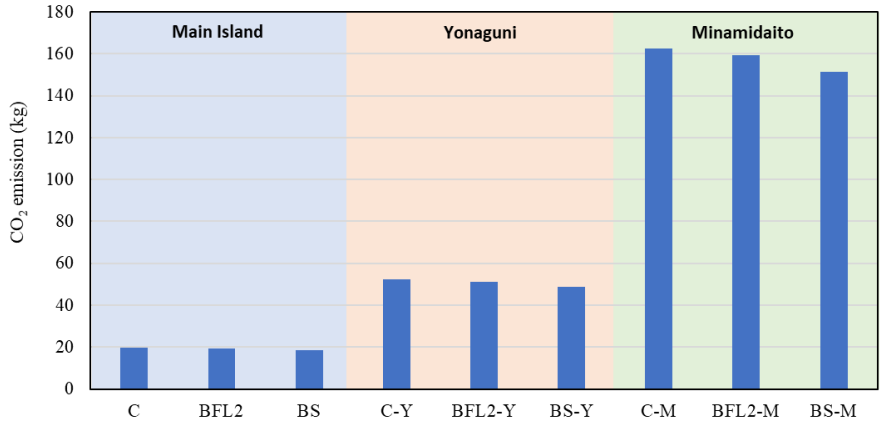

Figure 9.5 Carbon dioxide emissions

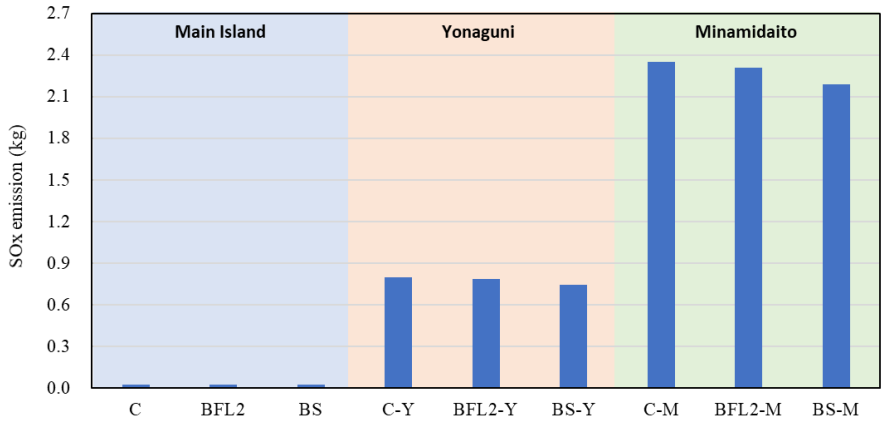

Figure 9.6 Sulfur oxide emissions

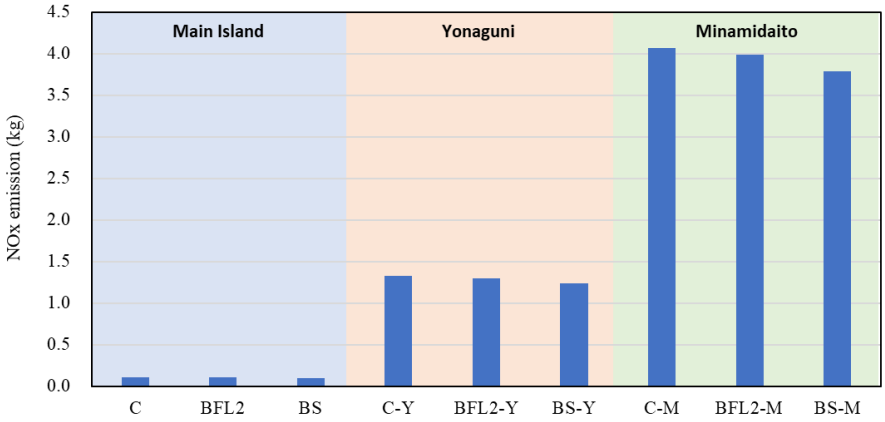

Figure 9.7 Nitrogen oxide emissions

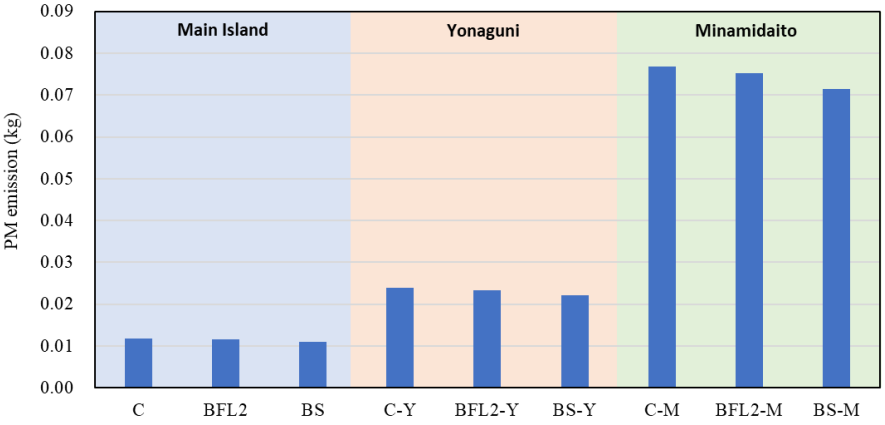

Figure 9.8 Dust and soot emissions

As Figure 9.5, Figure 9.6, Figure 9.7, and Figure 9.8 illustrate, the application of sugarcane residues can decrease the discharge of high-environmental-load substances into the air, water, and soil. A determining factor in the impact of concrete with sugarcane residues is the lower use of natural aggregates, which decrease the impacts from their extraction. In the BFL2 scenario, the percentage of substances decrease was around 1.96, 1.97, 1.94, and 1.95%, while in the BS scenario, in which the volume of the residues used in the mixture was 7%, it was around 6.67, 6.80, 6.54, and 6.65% compared to the C scenario for carbon dioxide, sulfur oxide, nitrogen oxide, and dust and soot emissions, respectively.

When the blocks are supposed to be made on Yonaguni and Minamidaito, the carbon dioxide, sulfur oxide, nitrogen oxide, and dust and soot emissions increase due to the long-distance transportation since the conventional aggregates come from other islands. However, in the scenarios in which the sugarcane residues were added into the mixture, the emissions were smaller than the standard interlocking concrete block. For BFL2-Y, the percentage of decrease of the substances was around

1.99, 2.00, 2.00, and 1.99%, while for BS-Y, it was 6.92, 7.00, 6.98, and 6.89% in comparison to the C-Y scenario; for BFL2-M, the percentage of decrease of the substances was around 2.00, 2.00, 2,00, and 2.00%, while for BS-M, it was 6.98, 7.00, 6.99, and 6.97% in comparison to the C-M scenario, for carbon dioxide, sulfur oxide, nitrogen oxide, and dust and soot emissions, respectively. These results are similar to the results obtained on the main island of Okinawa. However, the proportions of the environmental load were smaller than the main island results due to the need to transport the aggregates by vessels from other islands. In the case of Yonaguni, the aggregates are transported by vessels from the island of Ishigaki, which is located around 131 km from Yonaguni. For Minamidaito, the distance is around 388 km from the main island of Okinawa, where the aggregates were collected.

Although the environmental assessment analyses were performed simply, the results point out a consistent environmental benefit resulting from the replacement of conventional aggregates with sugarcane residues. This contribution of the decrease of the environment load may be more significant if the sugarcane residues are set to replace the fine aggregates. Besides, if we consider that sugarcane can sequestrate up to 0.66 ton of CO_2 per ha per year[12], and even that a part of bagasse is burned at the mill as fuel and generates CO_2, the carbon in sugarcane fiber came from CO_2 that was already present in the atmosphere[13], the addition of these residues in the preparation of interlocking blocks may be considered highly eco-friendly aggregates. The optimization of the concrete mixture and the durability of interlocking blocks should be investigated in detail to decrease the dependency of conventional aggregates from other islands, and consequently, the environmental load.

9.3.2 Cost analysis associated with the production of interlocking concrete blocks

A simple cost analysis was also carried out by setting the price for CO_2 reduction credits at ¥4500 (USD 59.71)/t·CO_2[14]. Figure 9.9 shows the cost reduction associated with the production of interlocking concrete blocks of each scenario.

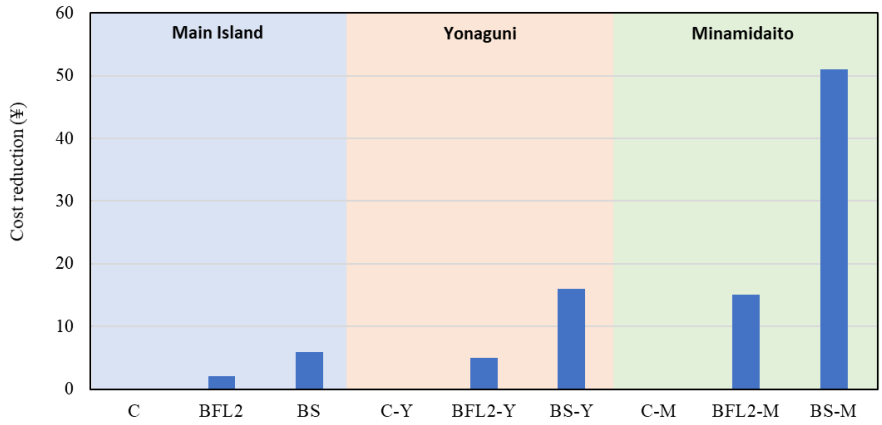

Figure 9.9 Cost reduction associated with the production of interlocking concrete blocks

For BFL2 and BS scenarios, on the main island, the concrete cost decreases to around ¥2 (USD 0.02) and ¥6 (USD 0.06), respectively, in comparison to C. In Yonaguni, the concrete cost decreases to around ¥5 (USD 0.05) and ¥16 (USD 0.15) for BFL2-Y and BS-Y, respectively, compared with C-Y. Lastly, in Minamidaito, the concrete cost of BFL2-M and BS-M decreases compared to C-M to around ¥15 (USD 0.14) and ¥51 (USD 0.48), respectively. These values reinforce that the use of local agro-residues, such as sugarcane residues, can favor the reduction of construction costs. However, some precautions must be taken not to undergo various production processes since it may increase the residues' production costs as aggregates.

9.4 Conclusion of chapter

In this chapter, the environmental load mitigation using sugarcane residues to replace a part of the aggregates and the cost analysis associated with interlocking concrete blocks' production were investigated. The environmental and cost assessment of three types of blocks prepared on three different islands in Okinawa Prefecture was performed. Although the environmental and cost assessment of the concrete with the addition of sugarcane residues was based on the production of interlocking concrete blocks, it can be expected that similar results from structures to prevent or mitigate natural disaster. The results obtained in this chapter can be summarized as:

1. The environmental load associated with the production of interlocking concrete blocks using sugarcane residues as aggregates was smaller than that of conventional aggregates, primarily due to the simplicity of residues acquisition.
2. When the blocks are supposed to be made on Yonaguni and Minamidaito, the carbon dioxide, sulfur oxide, nitrogen oxide, and dust and soot emissions increase due to long-distance transportation since the conventional aggregates come from other islands.

9.5 References

[1] Jayvant Choudhary, Brind Kumar, Ankit Gupta, "Utilization of solid waste materials as alternative fillers in asphalt mixes: A review," *Construction and Building Materials,* vol. 234, 2020.

[2] Flora Faleschini, Mariano Angelo Zanini, Carlo Pellegrino, Stefano Pasinato, "Sustainable management and supply of natural and recycled aggregates in a medium-size integrated plant," *Waste Managemen,* vol. 49, pp. 146-155, 2016.

[3] Hiroshi Seki and Nobuaki Otsuki, "Properties of aggregates in Okinawa for use of concrete materials (in Japanese)," *Technical Note of the Port and Harbour Research Institute, Ministry of Transportation, Japan,* vol. 240, 1976.

[4] Okinawa Prefectural Civil Engineering Construction Department, Detailed Design Unit Price List (in Japanese), October 2019.

[5] Keizai Chosa Kai, Sekisan Shiryo January 2020 Issue (in Japanese).

[6] Okinawa Prefectural Government, "Prefecture sugar production related organizations," Okinawa Prefectural Government, [Online]. Available: (https://www.pref.okinawa.jp/site/norin/togyo/documents/bunmitu.pdf)(https://www.pref.okinawa.jp/site/norin/togyo/documents/ganmitsutou.pdf). [Accessed 27 June 2020].

[7] Ribeiro, B., Yamashiki, Y. & Yamamoto, T, "A study on mechanical properties of mortar with sugarcane bagasse fiber and bagasse ash," *Journal of Material Cycles and Waste Management,* 2020.

[8] NHK World Japan, "Japan to cut coal-fired power generation by 90%," NHK World Japan, 2 July 2020. [Online]. Available: https://www3.nhk.or.jp/nhkworld/en/news/20200702_19/. [Accessed 3 July 2020].

[9] Jorge de Brito & Ricardo Robles, "Recycled aggregate concrete (RAC) methodology for estimating its long-term properties," *Indian Journal of Engineering and Materials Sciences,* vol. 17, pp. 449-462, 2010.

[10] Kawai Kenji, "Environmental load evaluation of concrete ① Environmental load related to concrete (translated by the author) (in Japanese)," *Concrete journal,* vol. 50, no. 6, pp. 554-561, 2012.

[11] Japan Society of Civil Engineers, Concrete Engineering Series, vol. 62, 2004.

[12] Jeffrey F. Parr, Leigh A. Sullivan, "Sugarcane the champion crop at carbon sequestration," *Australian Canegrower,* pp. 14-15, 2007.

[13] C. David Cooper, Introduction to Environmental Engineering, Waveland Press, 2014.

[14] Toshi H. Arimura & Tatsuya Abe, "The impact of the Tokyo emissions trading scheme on office buildings: what factor contributed to the emission reduction?," *Environmental Economics and Policy Studies,* 2020.

10 GENERAL CONCLUSIONS

For industry use, the bagasse residues must be classified and well characterized. This research aimed to propose an easy and accessible method of classification of sugarcane residues and investigate the application of the classified residues. The development of environmentally friendly mortar and concrete for preventive structures against natural disasters was then studied. The related conclusions are summarized in the following.

In chapter 3, "**Classification of the Sugarcane Residues and Their Characteristics,**" an easy and accessible classification method of the sugarcane residues was proposed. The residues were classified into three categories: bagasse fiber, sand, and ash. Tests to obtain the physical and mechanical properties of the bagasse fiber were made. Besides, the chemical components of the bagasse ash were investigated. The main results obtained in this chapter are:

1. Approximately 14% of the non-burned residues acquired from the mill can be added to mortar or concrete without any extra processing.
2. 1.36 mg/g of reducing sugar was detected in raw bagasse. This value increased when the raw bagasse was dipped in water at 30°C for 30 minutes to 1.49 mg/g. However, when the washed bagasse is alkali-treated, the reducing sugar content decreased to 1.05 mg/g.
3. The tensile strength of the fibers was 132 N/mm^2.
4. 79% of the total weight of the burned bagasse was smaller than 2.36 mm. From this total, around 5% of the total weight was smaller than 0.15 mm.
5. The chemical analysis showed that the sum of major oxides, SiO_2, Al_2O_3, and Fe_2O_3, was approximately 79%, 9% more than the required chemical composition of natural pozzolans according to ASTM C 618.
6. Although the bagasse ash (burned bagasse smaller than 0.15 mm) has an angular and irregular particle, the results indicate that BA conforms to the requirements prescribed standard (JIS A 6201) of fly ash type 2.

In chapter 4, "**A Study on Mechanical Properties of Mortar with Sugarcane Bagasse Fiber and Bagasse Ash,**" the categorized sugarcane residues were added in mortar to evaluate the physical and mechanical properties of mortar. The results obtained in this chapter can be summarized as:

1. The water retention ratio was higher when 2% of bagasse fiber was added compared to other cases due to the high percentage of fibers used, which can retain a high amount of water.
2. Despite the slight decrease in compressive strength, with the addition of fiber, the specimens'

ductility increased compared to the control specimen. However, when 5% of fly ash with 2% of bagasse fiber and when 5% of bagasse ash with 2% of bagasse fiber were added, the compressive strength exceeded the control specimen's compressive strength after 91 days.

3. The flexural strength of all-fiber mortar specimens exceeded the control specimen's value after 7, 28, and 91 days of curing.
4. With the addition of bagasse fiber, the drying shrinkage strain could be reduced to approximately the same level of the mixtures added with 2% of PVA fibers. After 49 days, when 2% of bagasse fiber was added, the drying shrinkage strain becomes smaller than the mixtures added with 2% of PVA fibers.
5. The adhesion strength at 28 days of all mortar mixtures is higher than 2.0 N/mm^2. These values exceed the adhesion standard strength of 1.5 N/mm^2.

In chapter 5, "**A Study on the Reduction in Hydration Heat and Thermal Strain of Concrete with Addition of Sugarcane Bagasse Fiber,**" the behavior of sugarcane residues in mass concrete structures, such as check dam and sabo structures, were evaluated. The most important results of this chapter are:

1. The slump decreased with the addition of the fiber amount compared to the control mixture. However, the amount of air increased as the amount of mixed fibers increased.
2. With the addition of the bagasse fiber, the heat of hydration of all mixtures was reduced. When 5% of the bagasse fiber was added, the peak temperature neared 48 °C, approximately 4.5 °C lower than the control mixture.
3. When the bagasse fiber was added, the peak temperature was reached later than the control mixture. When 2% of the bagasse fiber was added, the temperature peak was achieved 26 hours after the concrete placement, while the control mixture temperature peak was reached 4 hours earlier.
4. In the case of the control mixture, the strain rose to a value of approximately 55 μ, while, in the case of the mix in which 5% of bagasse fiber was added, the strain value was 30 μ, a difference of about 25 μ.
5. In the case where the bagasse fiber was added, the compressive strength decreased. However, the compressive strength increased when the ashes were added to the mixtures, thereby exceeding the control mixture.
6. The flexural strength of all concrete specimens with added fiber exceeded the value of the control specimen.
7. The split tensile strength increased when 2.0% of the fiber content was added to the mixture. On the other hand, with 5.0% of the fiber, the split tensile strength decreased.

Chapter 6, "**A Study on Mechanical Properties of Shotcrete with Addition of Sugarcane Residues,**" applies mortar with sugarcane residues such as shotcrete to protect and stabilize slopes from erosion and possible slides were investigated. The following are the main results obtained in this chapter:

1. The porosity rate of the specimens with the addition of bagasse fiber increased compared to the control mixture.
2. The compressive strength difference of all mixtures remained between ±1 N/mm^2.
3. The flexural strength of all mixtures exceeded the values of C, which reached 6.69 N/mm^2. In the case of BA, the flexural was 8.32 N/mm^2.
4. The shrinkage strain of the specimens, regardless of the fiber type or residues, is smaller than that of the control mixture.

In chapter 7, "**Durability of Concrete with Addition of Sugarcane Residues,**" the durability of concrete with sugarcane residues was investigated by the resistance to the carbonation and chloride ion ingress velocity. The most significant results of this chapter are the following:

1. The slump of the control mixture case is 7.2 cm and in the bagasse sand case is 6.7 cm. In contrast, in the cases of bagasse fiber, PVA fiber, bagasse ash, and fly ash, which the fraction volume of the fiber was 2% in comparison to the total volume of fine aggregate, the slump reduced to 6.5, 5.1, 5.7, and 5.4 cm, respectively.
2. The compressive strength at 28 days was 44.93, 44.16, 45.94, 50.02, 47.05, and 46.54 N/mm^2, and at 56 days was 46.57, 47.67, 47.50, 51.37, 49.03, and 49.48 N/mm^2 for the control mixture, bagasse fiber, PVA fiber, bagasse sand, bagasse ash, and fly ash, respectively.
3. The flexural strength was 3.04, 3.48, 3.75, 3.16, 3.70, and 3.71 N/mm^2 after 28 days of curing and 3.56, 3.87, 3.89, 3.68, 3.93, and 3.91 N/mm^2 after 56 days of curing for the control mixture, bagasse fiber, PVA fiber, bagasse sand, bagasse ash, and fly ash, respectively.
4. The carbonation depth for the control mixture is 0.34 and 2.40 mm at 28 and 56 days, respectively, while in the case of BF, the carbonation depth decrease to 0.26 and 2.24 mm at 28 and 56 days of curing, respectively. When bagasse sand, bagasse ash, and fly ash are added to the mixture, the depth of carbonation decreased to 0.30 and 2.32 mm, 0.18 and 2.07 mm, and 0.17 and 2.04 mm after 28 and 56 days of curing, respectively.
5. The total chloride ions content where bagasse fiber was added in the mixture was higher than the other cases.

Chapters 8 and 9 are the author's work as a visiting foreign researcher at the University of Ryukyus, Okinawa Prefecture, Japan, during his Overseas Internship. In Chapter 8, "**Development of Interlocking Concrete Blocks with Added Sugarcane Residues,**" bagasse fibers that are relatively larger than the bagasse fibers defined in Chapter 3 were used to interlocking concrete blocks. In this chapter, the mechanical properties and temperature surface of the blocks with the addition of bagasse fiber were investigated. The results obtained in this chapter can be summarized as follows:

1. The flexural strength was 6.46, 7.00, 7.78, 6.84, 7.92, and 7.93 N/mm^2 after 14 days of curing and 7.36, 7.58, 7.60, 7.47, 7.72, and 7.96 N/mm^2 after 28 days of curing for C, BFL1, BFL2, BFL5, BFS2, and BS, respectively. These values meet the requirement stipulated by JIS A 5371 of 5 N/mm^2, which may be used as pavement for pedestrians and heavy vehicle traffic.
2. The water retention content increases with the addition of the sugarcane residue. In the case of BFL5, which was prepared with bagasse fibers (4.75-9.52 mm) with a volume ratio of 5% in comparison to the total amount of aggregate, the water retention content achieved a value of 0.118 g/cm^3. In contrast, the water retention content of the control composite C was 0.087 g/cm^3.
3. The averages of the surface temperature of the surface and base layer for C, BFL1, BFL2, BFL5, BFS2, and BS were 35.4, 35.2, 35.0, 34.8, 34.7, and 34.5 °C, respectively.
4. In the case of C, in which no sugarcane residue was used, and in the case of BFL1, in which a residue volume ratio of 1% in comparison to the total amount of aggregate was added in the blocks, the surface temperatures and the water evaporation rates are higher in comparison to the other cases, in which the amount of residue was higher.

In Chapter 9, "**An Environmental and Cost Assessment of Concrete with Addition of Sugarcane Residues,**" the environmental load mitigation by using sugarcane residues to replace a part of aggregates was investigated. The environmental assessment of three types of blocks prepared on three islands in Okinawa Prefecture was made. The most important results of this chapter can be summarized as follows:

1. The environmental load associated with the production of interlocking concrete blocks using sugarcane residues as aggregates was smaller than that of conventional aggregates, mainly due to the greater simplicity of acquisition of the residues.
2. In the scenarios where the blocks are supposed to be made on Yonaguni and Minamidaito, the carbon dioxide, sulfur oxide, nitrogen oxide, and dust and soot emissions increase due to long-distance transportation since the conventional aggregates come from other islands.

A fundamental concept for environmentally friendly construction material using sugarcane residues has been successfully established in this study, aiming for a practical application. Also, it has been proposed a straightforward classification of sugarcane residues and their use as materials as construction materials for disaster mitigation structures. The classified residues were proposed for mass concrete applications, such as check dams and sabo structures and shotcrete. Moreover, in order to the wide use of the residues and avoid new processing, unclassified residues were used as materials for interlocking concrete blocks.

The use of these residues decreases the load on the environment by replacing conventional aggregates and reduces the structures' cost. Furthermore, it has been found that the sugarcane bagasse fibers can be used as the prevention of cracks in disaster mitigation structures.

However, to achieve satisfactory performance in the service of concrete structures, complementary investigations should be conducted appropriately. In the follow-up survey from this research, the author wishes to evaluate the long-term durability of mortar and concrete with the addition of sugarcane residues.

Appendix

PROJECT BASED RESEARCH

Sugarcane Bagasse Concrete - Heading Towards Implementation

INTRODUCTION

The use of sugarcane residues as aggregates in concrete may reduce environmental problems, such as the reduction of mining of natural aggregates and the improper disposal of sugarcane residues. Therefore, this project proposes to spread the use of sugarcane bagasse concrete in Okinawa Prefecture, Japan, by interacting with the local community. Besides, a workshop was held to discuss the possibility of introducing a sustainable business from this work's results.

A FOLLOW-UP PROJECT

Overview

Based on the previous research, a follow-up project including community work and workshop was conducted with aims to:

1. let local people know the importance of using sugarcane residues for building a sustainable society,
2. transfer knowledge about the potential use of sugarcane residues as aggregate in concrete,
3. let local people realize various problems and consider countermeasures against UHI, and
4. discuss among the local government, institutions, and companies a sustainable way to continue the production of interlocking blocks with sugarcane residues and apply them in local communities.

This project is summarized in Figure 1. As shown in Figure 1, This project started by contacting the local government, companies, academic experts, local farmers, and citizens to invite them to collaborate with this project.

This project's aim was explained to the collaborators and volunteers, giving them a basic knowledge of the background of the sugarcane bagasse concrete. Also, the possible contributions to the environment, civil construction industry, sugar/ethanol industry, and farmers and government by using sugarcane residues were explained as well.

Following the overall explanation, preparation for the project's execution was begun by laying interlocking concrete blocks in a park together to the local community. The details, such as determining the location where the paver blocks were placed, dates, and the mix proportions of the

blocks, were decided together with the collaborators. The mix proportions of the block are described in Chapter 8.

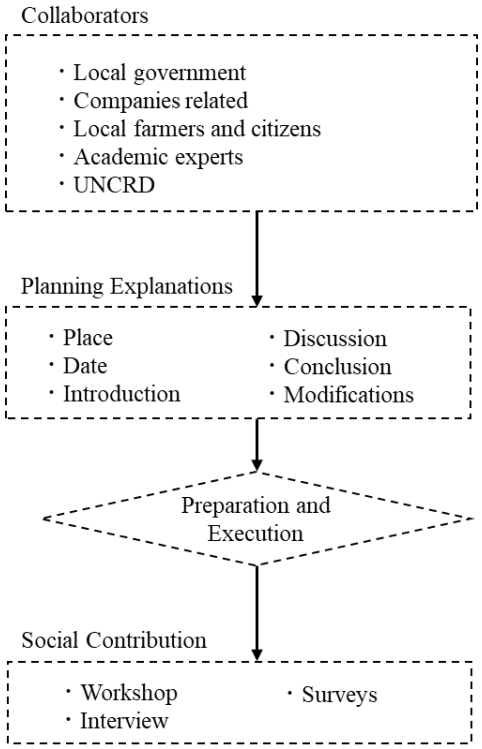

Figure 1 Overall flow of this PBR

Right after the execution of the work, evaluations about this project were made. It includes interviews and surveys about what the collaborators and volunteers thought about the interlocking concrete blocks with sugarcane residues and about this project in general.

Finally, all the processes, interviews, and surveys made in this study were summarized and presented in a workshop.

Community work

The interlocking concrete blocks with sugarcane residues were laid in a park on November 12th, in Nishihara Town, Okinawa Prefecture, at the Nishihara Athletic Park, shown in Figure 2. This location's choice was motivated due to the park's users slip on the wet grass since the location inclines approximately 30 degrees.

Figure 2 Construction site

After deciding where to lay the blocks, the work of digging the ground has begun. An area of 6.0 m^2 was dug approximately 8 cm deep, as shown in Figure 3.

Figure 3 Construction site after dug

The preparation of the blocks was the same as described in 8.2.3. A total of 15 volunteers were involved in this work.

Workshop

A workshop was held on December 7th in Nishihara Town, Okinawa Prefecture, at the University of the Ryukyus, Researcher Exchange Facility, from 13:00 until 16:30.

The workshop's objective is straightforward: to overcome barriers among stakeholders and different sustainable issues, including environmental, technological, and economic issues. This will be achieved by combining and advancing existing technologies for sustainable processing of sugarcane residue as construction aggregate, generating revenue.

Specifically, this workshop addressed the 3Rs (reduce, reuse, and recycle) ideals, sugar/alcohol and construction industry problems, and countermeasures that can be applied to achieve sustainable development in both industries. Furthermore, the workshop presented case studies and experiences from Okinawa Citizens' Recycling Movement of 3Rs projects; transferred knowledge about the potential use of sugarcane residues as aggregate in concrete; received feedback from users and Okinawa Prefectural government and local level authorities; exchanged views and good practices among participants, and identified possibilities and challenges for moving towards the implementation of sugarcane residues as concrete aggregate.

The detailed schedule of this workshop is shown in Figure 4.

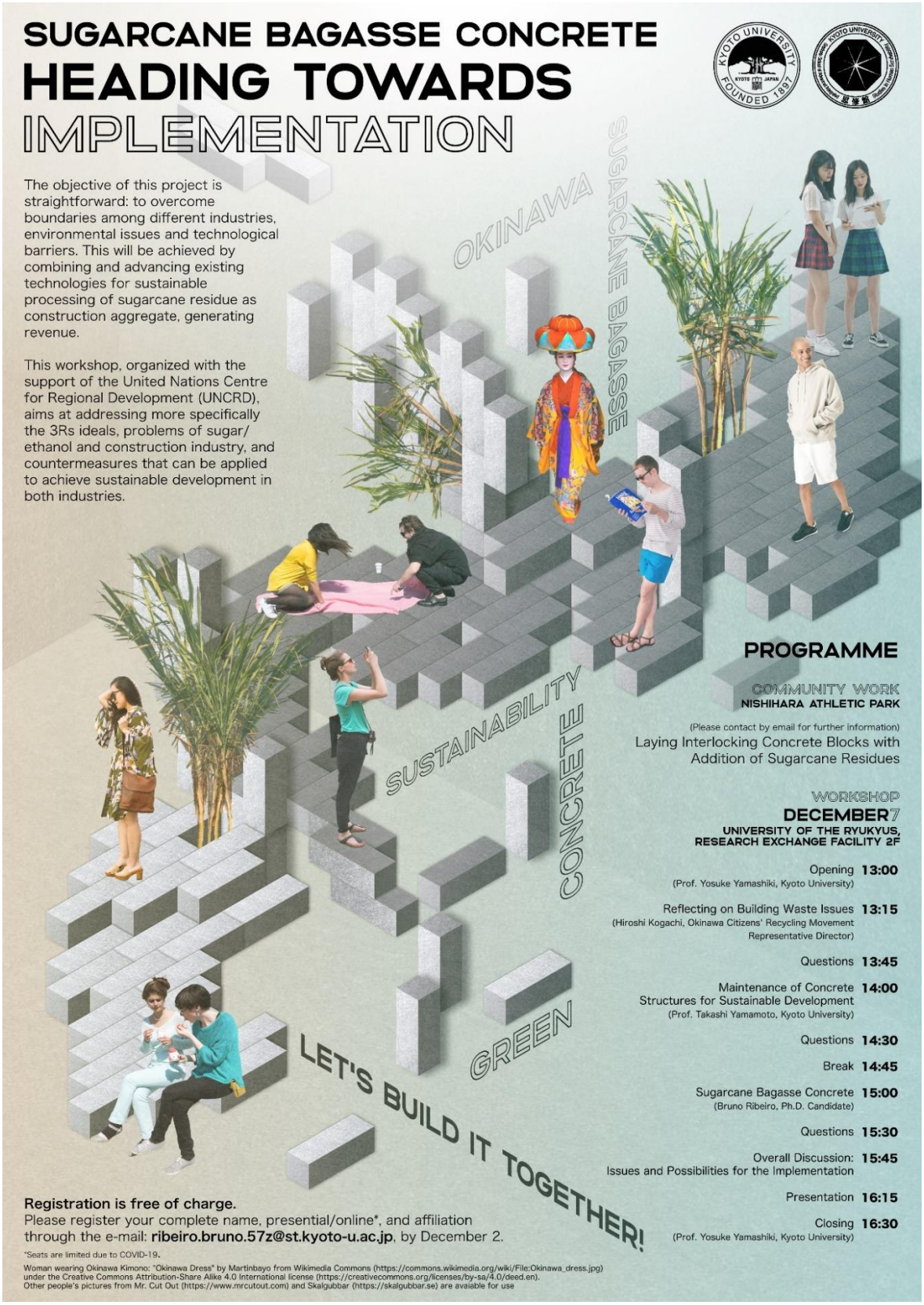

Figure 4 Poster of the workshop

ACHIEVEMENTS

Community work

The output of this project is shown in Figure 5.

Figure 5 Construction site after laying interlocking concrete blocks

In order to evaluate the slip resistance for pedestrians, the test described on JIPEA-TM-6 was applied. According to the "Manual for Interlocking Blocks Pavement Design and Construction" published by Japan Interlocking Blocks Pavement Engineering Association (JIPEA), the sliding resistance value (BPN value) has to be greater or equal to 40 BPN for pedestrian roads. The average BPN value acquired from this work was 61.7 BPN which indicates a fair value compared to the standard.

Workshop

Figure 6 shows a snapshot of the workshop.

Figure 6 Participants of the workshop

The total participants were 37, including people from the government, private companies including civil construction companies and sugar companies, academics, and local citizens. Overall, the goal

of the workshop was achieved: it was possible to raise awareness about the sugarcane residues and local resources; collaborators came up with new ideas for the use of sugarcane residues; also, how to make this business model sustainable was discussed among collaborators.

COLLABORATIVE APPROACH FOR COMMONS: TOWARD SUSTAINABLE AND RESILIENT SOCIETY

Sugarcane residue can contribute to a sustainable society in that it can be used as a construction material for its worldwide accessibility and because of its renewability. Besides, by using sugarcane residue as construction materials, conventional resources such as sand can be saved. This will result in the avoidance of landscape destruction. Moreover, the reduction of greenhouse gas emissions is another promising factor.

To face hurricanes, earthquakes, extreme heat, and flooding posed by climate change, less warm urban areas will do a far better job at maintaining habitable temperatures in the event of an extended power outage. As such, the buildings using sugarcane residue will emit far less carbon dioxide, which contributes to climate change, during normal operations.

It is to note, in addition to the previous research that identified the high-water retention and reduced surface temperature as a countermeasure for UHI when natural bagasse fibers are incorporated in concrete blocks for pavements, strategies to increase the resilience and adaptive capacity to use local materials and products should be taken into account. This is especially because the lack of precedents of the use of sugarcane residue concrete makes its implementation difficult. By introducing the knowledge and information to different stakeholders, it will be possible to increase resilience and facilitate the adaptation of sugarcane residue as construction material, even without precedents.

In conclusion, producing concrete secondary products, such as blocks with added sugarcane residues, and registering these products as local brands can be a step forward toward creating a resilient society. Besides, by combining this approach with local business, an innovative business model can be formed to produce a sustainable and resilient product with locally available materials, the creation of local brands, urban heat island mitigation, and environmental load reduction. To achieve this, it should involve the whole local community with "commons" that can cover overarching public interests, stakeholders, and generations; in the case of Okinawa Prefecture: sugarcane.